HAL
open science

Preparation and Properties of Bio-Based Polyurethane Foam Prepared from Modified Natural Rubber and Poly(ϵ-caprolactone)

Suwat Rattanapan

To cite this version:

Suwat Rattanapan. Preparation and Properties of Bio-Based Polyurethane Foam Prepared from Modified Natural Rubber and Poly(ϵ-caprolactone). Polymers. Le Mans Université; Prince of Songkla University, 2016. English. NNT : 2016LEMA1036 . tel-01476202

HAL Id: tel-01476202

https://theses.hal.science/tel-01476202

Submitted on 24 Feb 2017

HAL is a multi-disciplinary open access archive for the deposit and dissemination of scientific research documents, whether they are published or not. The documents may come from teaching and research institutions in France or abroad, or from public or private research centers.

L'archive ouverte pluridisciplinaire **HAL**, est destinée au dépôt et à la diffusion de documents scientifiques de niveau recherche, publiés ou non, émanant des établissements d'enseignement et de recherche français ou étrangers, des laboratoires publics ou privés.

UNIVERSITE BRETAGNE LOIRE

Université du Maine

Thèse de Doctorat

* (instructions page en annexe)

Suwat RATTANAPAN

Mémoire présenté en vue de l'obtention du
grade de Docteur de l'Université du Maine
sous le sous le sceau de l'Université Bretagne Loire

École doctorale : *3MPL*
Discipline : *Chimie des matériaux, CNU 33*
Spécialité : *Chimie des Physicochimie des polymères*
Unité de recherche : *IMMM, UMR CNRS 6283*
Soutenue le *27/06/2016*
Thèse N° :

Preparation and properties of bio-based polyurethane foam prepared from modified natural rubber and poly(ε-caprolactone)

JURY

Rapporteurs :	**Sophie BISTAC**, Professeur, University of Haute Alsace Mulhouse France **Anuwat SAETUNG**, Maitre de conférences, Prince of Songkla University
Examinateurs :	**Pranee PHINYOCHEEP,** Professeur, Mahidol University
Directeur de Thèse :	**Varaporn TANRATTANAKUL**, Professeur, Prince of Songkla University
Co-directeur de Thèse :	**Jean-François PILARD,** Professeur, Université du Maine
Co-encadrant :	**Pamela PASETTO**, Maitre de conférences, Université du Maine

Thesis Title Preparation and Properties of Bio-Based Polyurethane Foam Prepared from Modified Natural Rubber and Poly(ε-caprolactone)

Author Suwat Rattanapan

Major Program Polymer Science and Technology (Prince of Songkla University) and Chemistry and Physical Chemistry of Polymer (University of Maine)

Academic Year 2016

ABSTRACT

The aim of this research was to prepare a bio-based polyurethane foam (PUF) containing hydroxyl telechelic oligomers from natural rubber (HTNR) and waste tire crumbs (HTWT) and polycaprolactone diol (PCL) as soft segments. The studied parameters included type of polyols and molar ratio between HTNR/PCL and HTWT/PCL. The molecular weight of HTNR and HTWT derived from ^{1}H-NMR spectra were 1,800 and 1,400 g/mol, respectively. The molecular weight of PCL diol was 2000 g/mol. The effect of HTNR/PCL and HTWT/PCL molar ratio (1/0, 1/0.5, 1/1 and 0.5/1) on the foam formation rate and physical and chemical properties of the resulting PUF was investigated. The chemical structure of HTNR, HTWT and PUF were confirmed by FTIR and ^{1}H-NMR. PCL diol provided faster reaction, thus higher PCL diol content showed higher foam formation rate. The foam density slightly changed with the molar ratio whereas the specific tensile strength of all samples was in the same range. The average diameter of cell increased with increasing contents of PCL diol. The addition of PCL diol resulted in reduced elongation at break and compressive strength. The cellular structure observed by SEM micrographs of HTNR based foams showed an almost closed cell. The biodegradability was assessed according to a modified Sturm test. Low density polyethylene and sodium benzoate were used as a negative and positive control sample, respectively. PUF samples showed an induction time of 33 days in which the percentage of biodegradation was ~ 7-11%. The biodegradation of PUF containing only HTNR was 8.4% and 31.89% at 28 days and 60 days of testing respectively whereas the PUF containing 1/0.5 HTNR/PCL (by mole)

showed a higher biodegradation: 11.31% and 45.6% at 28 days and 60 days of testing respectively. The molar ratio of HTWT/PCL strongly affected the kinetic rate of foam formation and foam morphology. According to SEM micrographs, polyhedral closed cells were observed. The addition of the PCL diol increased the thermal degradation temperature of the PUF based on TGA results. A low kinetic rate provided PUF with a high density, small cell size and a broad cell size distribution. The biodegradation of PUF containing only HTWT was 31.2% and 51.3% at 28 days and 60 days of testing respectively whereas the PUF containing 1/0.5 HTWT/PCL diols (by mole) showed a higher biodegradation: 39.1% and 64.3% at 28 days and 60 days of testing respectively. The foam formation rate of HTWT based PUF was higher than the one of HTNR based PUF. All HTWT based PUF have a higher density than HTNR based PUF. The HTWT based PUF had an inferior cell size in comparison to HTNR based PUF. The cellular structure of HTNR based and HTWT based PUF were different, but all PUFs showed almost closed cells. The HTWT based PUF had a higher thermal degradation temperature and biodegradation properties than foams from HTNR.

Keywords: Bio-based polymer, bio-based polyurethane foam, biodegradable polymer, natural rubber, polycaprolactone, waste tire recycle, biodegradability

Titre de la Thèse Préparation et Caractérisation des Propriétés de Mousses Polyuréthane Biobasées Synthétisées à Partir du Caoutchouc Naturel Modifié et de la Poly(ε-caprolactone)

Auteur Suwat RATTANAPAN

Ecoles Doctorales Sciences et Technologie des Polymères (Prince of Songkla University) Chimie et Physicochimie des Polymères (Université du Maine)

Année Académique 2016

RESUME

L'objectif de ces travaux de recherche était de synthétiser de mousses polyuréthane (PUF) bio-basées à partir d'oligomères hydroxytéléchéliques issus du caoutchouc naturel (HTNR) ou à partir de poudrettes de pneus usagés (HTWT) et du diol de la polycaprolactone (PCL) comme segments soft. Les paramètres étudiés ont été le type de polyol et le rapport molaire entre HTNR/PCL et HTWT/PCL. La masse molaire de HTNR, HTWT et PCL étaient respectivement 1,800, 1400 et 2000 g/mol. L'effet du rapport molaire HTNR/PCL et HTWT/PCL (1/0, 1/0/5/, 1/1, et 0.5/1) sur la vitesse de formation des mousses et sur les propriétés chimiques et physiques a été étudié. Les structures chimiques de HTNR, HTWT et PUF ont été confirmées par FTIR et ^{1}H-RMN. Le diol de la PCL était le plus réactif donc augmentant le contenu de PCL-diol la vitesse de formation des mousses a augmenté. La densité des mousses a changé légèrement avec le rapport molaire cependant la résistance à la traction reste dans la même gamme. Le diamètre moyen des cellules a augmenté en fonction du contenu de PCL-diol et la tendance inverse a été observée pour l'allongement à la rupture et la résistance à la compression. L'observation au microscope électronique à balayage (MEB) a montré que les mousses basées sur les HTNR étaient alvéolées et fermées. La biodégradabilité a été évaluée selon le test de Sturm. Polyéthylène à baisse densité et benzoate de sodium ont été utilisés respectivement comme témoins négatif et positif. Les mousses ont montré une période d'induction de 33 jours dans lequel le pourcentage de dégradation était ~ 7-10%. La biodégradation de PUF contenant seulement HTNR a été 8.4% après 28 jours et 31.89% après 60 jours ; les

PUF contenants 1/0.5 HTNR/PCL ont montré un pourcentage supérieure : 11.31% après 28 jours et 45.6% après 60 jours. Le rapport molaire HTWT/PCL a influencé beaucoup la vitesse de formation des mousses et leur morphologie. Cellules fermées de forme polyédrique ont été observé par microscopie électronique à balayage. Les résultats de l'analyse thermogravimétrique ont montré que l'addition du diol de la PCL a augmenté la température de dégradation. Il a été observé qu'une basse vitesse de réaction génère des mousses à haute densité, petit diamètre de cellule et haute distribution des diamètres. La biodégradation des PUF contenant seulement HTWT a été 31.2% après 28 jours et 51.3% après 60 jours, tandis que les PUF contenant 1/0.5 HTWT/PCL ont montré une dégradation plus élevée : 39.1% après 28 jours et 64.3% après 60 jours. La vitesse de formation des mousses basées sur les HTWT était supérieure à celle des mousses basées sur les HTNR. Toutes les mousses basées sur les HTWT ont une densité supérieure et une taille de cellule inférieure à celles basées sur HTNR. La structure des cellules des mousses basées sur les HTNR ou HTWT était différente cependant toutes les mousses ont montré des cellules quasi complètement fermées. Les mousses basées sur les HTWT ont montré des propriétés thermiques et de biodégradation meilleures par rapport aux mousses basées sur les HTNR.

Mots clé : polymères bio-basés, mousse polyuréthane bio-basée, polymères biodégradables, caoutchouc naturel, polycaprolactone, recyclage pneumatiques usagés, biodégradabilité

ชื่อวิทยานิพนธ์ การเตรียมและสมบัติของโฟมพอลิยูรีเทนชีวภาพเตรียมจากยางธรรมชาติดัดแปรและพอลิคาโปรแลคโทน

ผู้เขียน นายสุวัฒน์ รัตนพันธ์

สาขา วิทยาศาสตร์และเทคโนโลยีพอลิเมอร์ (มหาวิทยาลัยสงขลานครินทร์) และ Chimie et physicochimie des Polymères (Université du Maine)

ปีการศึกษา 2559

บทคัดย่อ

วัตถุประสงค์ของงานวิจัยนี้ เพื่อทำการเตรียม โฟมพอลิยูรีเทนชีวภาพ (PUF) จากยางธรรมชาติดัดแปร ที่มีหมู่ปลายไฮดรอกซิล (HTNR) ยางคลัมบ์ดัดแปรที่มีหมู่ปลายไฮดรอกซิล (HTWT) และพอลิคาโปรแลคโทน (PCL) ศึกษาผลของชนิดพอลิออล และสัดส่วนโดยโมลระหว่าง HTNR/PCL และ HTWT/PCL ที่สัดส่วน 1/0, 1/0.5, 1/1 และ 0.5/1 โดยโมล น้ำหนักโมเลกุลของ HTNR, HTWT และ PCL ที่ใช้สำหรับงานวิจัยนี้ คำนวณจาก ^{1}H-NMR คือ 1,800, 1,400 และ 2,000 g/mol ตามลำดับ ลักษณะโครงสร้างทางเคมีของ HTNR, HTWT และ PUF สามารถวิเคราะห์และยืนยันด้วยเทคนิค FTIR และ ^{1}H-NMR รวมถึงทำการวัดอัตราการก่อโฟม (Foam formation rate) ทดสอบสมบัติทางกายภาพ ทางเคมี และสมบัติการย่อยสลายทางชีวภาพ พบว่าในกรณีของโฟมพอลิยูรีเทนจาก HTNR/PCL เมื่อใช้ PCL ในปริมาณที่มากขึ้นจะส่งผลให้อัตราการก่อโฟมเร็วขึ้น และขนาดของเซลโฟมมีขนาดใหญ่ขึ้นด้วย ในขณะที่ค่าความหนาแน่น และความต้านทานต่อแรงดึงจำเพาะมีการเปลี่ยนแปลงเล็กน้อย การเติม PCL ในส่วนผสมของโฟมยังส่งผลให้ความสามารถในการยืด ณ จุดขาด และความทนทานต่อการกดมีค่าลดลง การคืนตัวหลังการกดของโฟม PUF2 (สัดส่วนระหว่าง HTNR/PCL = 1/0.5) จะให้ค่าต่ำที่สุดคือ 40% ลักษณะของโฟมที่ได้จากการทดลองนี้โดยส่วนใหญ่จะเป็นแบบเซลปิด ความสามารถในการย่อยสลายทางชีวภาพของโฟม ทดสอบโดยใช้วิธี Sturm Test มี LDPE

เป็นตัวเปรียบเทียบเชิงลบ และใช้ Sodium benzoate เป็นตัวเปรียบเทียบเชิงบวก พบว่าโฟมเริ่มมีการย่อยสายเกิดขึ้นอย่างเห็นได้ชัดที่เวลา 33 วัน มีเปอร์เซ็นต์การย่อยสลายในช่วง 7-11 เปอร์เซ็นต์ เปอร์เซ็นต์การย่อยสลายของโฟมจาก HTNR (PUF1) อยู่ที่ระดับ 8.4 และ 31.89 เปอร์เซ็นต์ และเปอร์เซ็นต์การย่อยสลายของโฟมจาก HTNR/PCL (1/0.5) อยู่ที่ระดับ 11.31 และ 45.6 เปอร์เซ็นต์ ที่เวลาในการทดสอบ 28 และ 60 วัน ตามลำดับ กรณีของโฟมพอลิยูรีเทนจาก HTWT/PCL เมื่อใช้ PCL ในปริมาณที่มากขึ้นจะส่งผลให้ค่าความหนาแน่นสูงขึ้น ขนาดของเซลโฟมลดลงมีการกระจายของเซลในวงกว้างไม่สม่ำเสมอ เปอร์เซ็นต์การย่อยสลายทางชีวภาพของโฟมจาก HTWT (PUF5) อยู่ที่ระดับ 31.2 และ 51.3 เปอร์เซ็นต์ และเปอร์เซ็นต์การย่อยสลายของโฟมจาก HTWT/PCL (1/0.5) อยู่ที่ระดับ 39.1 และ 64.3 เปอร์เซ็นต์ ที่เวลาในการทดสอบ 28 และ 60 วัน ตามลำดับ เมื่อทำการเปรียบเทียบโฟมที่ได้จากการเตรียมโดยใช้พอลิออลหลักเป็น HTNR และ HTWT พบว่าโฟมจากพอลิออลหลัก HTWT ให้อัตราการก่อตัวของโฟมเร็วกว่า ขนาดของเซลโฟมเล็กกว่า ความหนาแน่น ความต้านทานต่อความร้อน และเปอร์เซ็นต์การย่อยสลายทางชีวภาพสูงกว่า เมื่อเทียบกับโฟมจากพอลิออลหลัก HTNR

คำสำคัญ: พอลิเมอร์ชีวภาพ โฟมพอลิยูรีเทนชีวภาพ พอลิเมอร์ย่อยสลายทางชีวภาพ ยางธรรมชาติ พอลิคาโปรแลคโทน และการย่อยสลายทางชีวภาพ

ACKNOWLEDGEMENTS

I would like to express my appreciation and gratitude to Associated Professor Dr. Varaporn TANRATTANAKUL who has been a wonderful advisor for giving me an opportunity to study Ph.D. Program and also her support and professional guidance during my Ph.D. period. I really thank to her enthusiasm for my research inspirations. Associate Professor Dr.Varaporn TANRATTANAKUL has been a delightful advisor, providing me with support, encouragement, patience and an endless source of ideas. I thank her for the countless hours that she has spending, discussing, reading and correcting with me, my manuscripts and my thesis.

I would also like to thank Professor Dr. Jean-François PILARD, my advisor, on condition that giving me an opportunity to do the research at Université du Main, France. His enthusiasm for research and his vision for the future have been an inspiration. He has given me support and his advices have greatly enhanced my research.

I am extremely grateful to Asst. Prof. Dr. Pamela PASETTO, my co-advisor, for spending her time to discuss the results of my experiments and finding the time to read and to correct my manuscripts and my thesis. Most importantly, I would like to thank her for her encouragement, patience and also much assistance in my personal life at Le Mans.

I am sincerely grateful to Graduate School, Prince of Songkla University and Rajamangala University of Technology Srivijaya for financial support. This work has been carried out under the collaboration between Prince of Songkla University and Université du Maine.

I am grateful to all the lecturers, technicians, office workers and all my friends at the Department of Material Science and Technology, Faculty of Science, Prince of Songkla University, also special for all members in VT group for their friendship, unlimited help and encouragement during my study period.

I would like to thank you all the lecturers, technicians and all friends in IMMM laboratory for their guidance and helpful in providing advice and also thank you all Thai students for their friendship, helpful and good atmosphere during my stay

in France. I would like to give special thanks to Krishna VENI BARATHA for her helpful and good atmosphere during my stay in Le Mans.

Finally, I would like to extend special thanks to my family for their financial support and endless encouragement. I dedicate this thesis to my family and all the teachers who have taught me since my childhood. I will never forget this time in my life and, most importantly, the people I met and who helped me to create, develop and complete this thesis.

To this end, I fully take all responsibility for any mistakes that may have occurred in this work.

Suwat Rattanapan

CONTENTS

	Page
ABSTRACTS	v
ACKNOWLEDGEMENTS	xi
CONTENTS	xiii
LIST OF TABLES	xviii
LIST OF FIGURES	xx
LIST OF ABBREVIATIONS	xxiv
CHAPTER 1 GENERAL INTRODUCTION	1
1.1 Background	1
1.2 Objectives	5
1.3 References	5
CHAPTER 2 LITERATURE REVIEW	8
2.1 Telechelic natural rubber	8
2.1.1 General information	8
2.1.2 Synthesis methods of telechelic polyisoprene	8
2.1.2.1 Oxidation in the presence of redox system	9
2.1.2.2 Oxidation by photochemical method	10
2.1.2.3 Oxidation at high temperature and high pressure	11
2.1.2.4 Cleavage by periodic acid or lead acetate	12
2.1.2.5 Metathesis degradation	14
2.2 Tires and waste tires	16
2.2.1 Tires production	16
2.2.2 Composition of tires	20
2.2.3 Waste tire recycling	21
2.2.3.1 Ambient grinding	22
2.2.3.2 Cryogenic grinding	22
2.2.3.3 Wet grinding	22
2.2.3.4 Extrusion	22
2.2.3.5 Abrasion	23

CONTENTS (continued)

Page

2.2.4 Characteristics of recovered rubber from waste tires 23

2.2.4.1 Shredded tires 23

2.2.4.2 Tire chips 23

2.2.4.3 Ground rubber 24

2.2.4.4 Crumb Rubber 24

2.2.5 Production and Specifications of Crumb Rubber 26

2.2.5.1 Ambient mechanical grinding Process 26

2.2.5.2 Cryogenic Grinding Process 27

2.2.5.3 Specifications 27

2.2.6 Uses of Crumb Rubber 28

2.3 Polycaprolactone 29

2.3.1 General physicochemical properties 29

2.3.2 Synthesis of Polycaprolactone 30

2.4 Polyurethane foams 31

2.4.1 Polyurethane foam chemistry 31

2.4.1.1 Gas-production Reaction (Blow Reaction) 31

2.4.1.2 Polymerization reaction (Gelation Reaction) 32

2.4.2 Type of polyurethane foams 33

2.4.2.1 Low density flexible foams 33

2.4.2.2 Low density rigid foams 34

2.4.2.3 High density flexible foams 34

2.4.3 Raw materials 35

2.4.3.1 Isocyanates 35

2.4.3.2 Polyols 37

2.4.3.3 Other additives 39

2.4.4 Polyurethane and polyurethane foams literature review 45

2.4.4.1 Polyurethane foams from petroleum-based polyol 45

2.4.4.2 Polyurethane foams from bio-based polyol 46

2.4.4.3 Polyurethane from NR and PCL based polyol 49

CONTENTS (continued)

Page

2.5 Biodegradation 53

2.5.1 General information 53

2.5.2 Biodegradation test 55

2.5.2.1 Modified Sturm test 56

2.5.2.2 Closed bottle test 57

2.5.2.3 Petri dish screen 57

2.5.2.4 Environmental chamber method 58

2.5.2.5 Soil burial test 58

2.5.3 Biodegradation of natural rubber 59

2.5.3.1 Natural rubber degrading bacteria 60

2.5.3.2 Natural rubber degrading fungi 61

2.5.3.3 Biodegradation process for reclaiming of rubber 61

2.5.4 Biodegradation of polycaprolacton 62

2.5.5 Biodegradation of polyurethane 63

2.5.6 The related publications 64

2.6 Characterizations 65

2.6.1 Mechanical properties 65

2.6.1.1 Tensile testing 65

2.6.1.2 Compression testing 67

2.6.2 Thermal gravimetric analysis (TGA) 68

2.6.3 Nuclear magnetic resonance spectroscopy (NMR) 69

2.6.4 Fourier transform infrared spectroscopy (FTIR) 70

2.6.5 Scanning electron microscope 71

2.6.6 Gel permeation chromatography (GPC) 72

2.7 References 74

CHAPTER 3 MATERIALS AND METHODOLOGY 85

3.1 Materials 85

3.2 Instruments 88

CONTENTS (continued)

Page

3.3 Methodology 88

3.3.1 Synthesis of telechelic oligomer (TNR) from natural rubber 89

3.3.1.1 Carbonyl telechelic natural rubber (CTNR) 89

3.3.1.2 Hydroxyl telechelic natural rubber (HTNR) 90

3.3.2 Synthesis of telechelic oligomers from waste tires 90

3.3.2.1 Carbonyl telechelic waste tires (CTWT) 90

3.3.2.2 Hydroxyl telechelic waste tires oligomers (HTWT) 91

3.3.3 Preparation of bio-based polyurethane foams from HTNR, HTWT and polycaprolactone diol (PCL) 92

3.3.4 Kinetic rate of bio-PUFs formation 94

3.3.5 Physical and mechanical properties 94

3.3.6 Characterizations 96

3.3.7 Biodegradation Tests 97

3.4 References 99

CHAPTER 4 RESULTS AND DISCUSSION 102

4.1 Preparation and properties of bio-based polyurethane foam (PUFs) from polycaprolactone diol (PCL) and natural rubber (NR) 102

4.1.1 Synthesis of carbonyl telechelic natural rubber (CTNR) 102

4.1.2 Synthesis of hydroxyl telechelic natural rubber (HTNR) 105

4.1.3 Synthesis and characterization of PUFs from HTNR and PCL 107

4.1.4 Physical properties of PUFs from HTNR and PCL 110

4.1.5 Morphology of PUFs from HTNR and PCL 112

4.1.6 Thermal properties of PUFs from HTNR and PCL 113

4.1.7 Mechanical properties of PUFs from HTNR and PCL 115

4.1.7.1 Tensile properties 115

4.1.7.2 Compression properties 117

4.1.8 Biodegradation of PUFs from HTNR and PCL 119

CONTENTS (continued)

Page

4.2 Preparation and properties of bio-based polyurethane foam (PUFs) from polycaprolactone diol (PCL) and waste tires (WT) 125

4.2.1 Composition of WT 125

4.2.2 Synthesis of carbonyl telechelic oligomers from waste tires (CTWT) 126

4.2.3 Synthesis of hydroxyl telechelic oligomers from waste tires (HTWT) 130

4.2.4 Synthesis and characterization of PUFs from HTWT and PCL 132

4.2.5 Physical properties of PUFs from HTWT and PCL 134

4.2.6 Morphology of PUFs from HTWT and PCL 137

4.2.7 Thermal properties of PUFs from HTWT and PCL 138

4.2.8 Biodegradation of PUFs from HTWT and PCL 140

4.3 References 143

CHAPTER 5 CONCLUSIONS 149

5.1 Preparation and properties of bio-based PUFs from PCL and NR 149

5.2 Preparation and properties of bio-based PUFs from PCL and WT 149

PERSPECTIVES 151

CURRICULUM VITAE 152

LIST OF TABLES

	Page
Table 2.1 Tires composition in the European Union	21
Table 2.2 Summary of material characteristics	25
Table 2.3 Crumb rubber specification	28
Table 2.4 The relation between the properties of polyols and applications of polyurethane polymer	39
Table 2.5 Tertiary amine catalysts and their application	40
Table 2.6 Organometallic catalysts and their application	41
Table 2.7 Chain extenders and cross linkers	44
Table 3.1 List of materials	85
Table 3.2 List of instruments	88
Table 3.3 Formulations of foams (Bio-PUFs) using HTNR and PCL as precursors	93
Table 3.4 Formulation of Bio-PUFs by using HTWT and PCL as precursors	93
Table 4.1 Chemical shift assignment of CTNR	103
Table 4.2 Wavenumber and functional groups of CTNR and HTNR	104
Table 4.3 Characteristics of carbonyl telechelic natural rubber (CTNR)	105
Table 4.4 Chemical shift assignment of HTNR	107
Table 4.5 Characteristics of hydroxyl telechelic natural rubber (HTNR)	107
Table 4.6 Wavenumber and functional groups of PUFs from HTNR, PCL and P-MDI	109
Table 4.7 Physical properties of PUFs from HTNR and PCL	110
Table 4.8 Thermal properties of PUFs from HTNR and PCL	113
Table 4.9 Tensile properties of PUFs from HTNR and PCL	115
Table 4.10 Compression properties of PUFs from HTNR and PCL	117
Table 4.11 Percentage of biodegradation of PUFs from HTNR and PC	119
Table 4.12 Chemical shift assignment of CTWT	127
Table 4.13 Wavenumber and functional groups of CTWT and HTWT	129
Table 4.14 Characteristics of carbonyl telechelic oligomers from waste tires (CTWT)	130

LIST OF TABLES (continued)

Page

Table 4.15 Chemical shift assignment of HTWT 131

Table 4.16 Characteristics of hydroxyl telechelic oligomers from waste tires (HTWT) 132

Table 4.17 Molecular weight of HTWT 132

Table 4.18 Physical properties of PUFs from HTWT and PCL 134

Table 4.19 Thermal properties of PUFs from HTWT and PCL 138

Table 4.20 Percentage biodegradation of PUFs from HTWT and PCL 140

LISTS OF FIGURES

	Page
Figure 2.1 Chemical structure of telechelic liquid natural rubber	8
Figure 2.2 Mechanism of the oxidizing cleavage of the natural rubber in latex phase by atmospheric oxygen in the presence of phenylhydrazine	10
Figure 2.3 Cleavage reaction of natural rubber in the presence of nitrobenzene under irradiation with ultraviolet light	10
Figure 2.4 The proposed mechanisms of cis-1,4-polyisoprene degradation reaction by hydrogen peroxide/UV radiation	11
Figure 2.5 The proposed degradation mechanisms of cis-1,4-polyisoprene by hydrogen peroxide at high temperature and high pressure	12
Figure 2.6 The degradation mechanisms of cis-1,4-polyisoprene and epoxidized cis-1,4-polyisoprene using H_5IO_6	13
Figure 2.7 Depolymerization mechanisms of 1,4-polybutadiene with diethyl 4-octene-1,8-dioate (a), bis(t-butyldimethysilyl)-3-hexene-1,6-diol diether (c), and 2-butene-1,4-diylbis(phthalimide) (e)	14
Figure 2.8 Metathesis alkenolysis of partially epoxidized polybutadiene	15
Figure 2.9 Structure produced for the metathetic depolymerization of hydroxyl telechelic cis-1,4-polyisoprene	15
Figure 2.10 Expected outputs of the degradation of waste tires by periodic acid	16
Figure 2.11 Expected outputs of the degradation of tire waste by metathesis	16
Figure 2.12 Tire functions	17
Figure 2.13 Tire construction	17
Figure 2.14 Tire production	18
Figure 2.15 scrap tire surface morphology comparison: (a) tire shred, (b) rubber chips, granulates, (e) buffing and (f) crumb rubber	26
Figure 2.16 Polymerization of ε-caprolactone by polycondensation and ring opening polymerization techniques	30

LIST OF FIGURES (continued)

Page

Figure 2.17 Morphology of flexible foam (a) and rigid foam (b) 34
Figure 2.18 Chemical structure of toluene diisocyanate (TDI) 36
Figure 2.19 General scheme for MDI production 36
Figure 2.20 Chemical structure of (a) 1,6-hexane diisocyanate (HDI), (b) isophorone diisocyanate (IPDI), (c) 1,5-napthalene diisocyanate (NDI), and (d) 1,4-phenylene diisocyanate (PDI) 37
Figure 2.21 Example of polyether and polyester polyols 37
Figure 2.22 Typical effects of silicone surfactant in a TDI-based slabstock foam 43
Figure 2.23 Structure of polyurethane foam prepared from bio-polyol 48
Figure 2.24 Synthesis of PCL diol and coupling reaction of PCL diols with PEG-Asp-PEG diols 51
Figure 2.25 Scheme of polymer degradation under aerobic and anaerobic conditions 54
Figure 2.26 Classification of the biodegradable polymers 55
Figure 2.27 Typical tensile specimen, showing a reduced gage section and enlarged shoulders (ASTM D 3574 Test E) 65
Figure 2.28 Stress-strain curves of (a) ductile, (b) semi-ductile and (c) brittle materials 66
Figure 2.29 TGA diagram of a thermobalance 68
Figure 2.30 Typical TGA and DTG curves 68
Figure 2.31 The basic arrangement of NMR spectrometer 69
Figure 2.32 A spinning nucleus can be regarded as a microscopic magnet 69
Figure 2.33 Schematic diagram of the optical layout of IR spectrometer 70
Figure 2.34 Stretching and bending vibrational modes for a CH2 group 71
Figure 2.35 Diagram of electron beam and specimens 72
Figure 2.36 Illustration of the separation of polymer molecules of different sizes 73
Figure 2.37 The general form of a calibration curve and chromatogram of different sizes of polymer 73

LIST OF FIGURES (continued)

Page

Figure 3.1 A schematic diagram of biodegradability testing system 99

Figure 4.1 ^{1}H-NMR spectrum of natural rubber (NR) 102

Figure 4.2 ^{1}H-NMR spectrum of CTNR 103

Figure 4.3 FTIR spectra of CTNR and HTNR 104

Figure 4.4 ^{1}H-NMR spectrum of HTNR 106

Figure 4.5 FTIR spectra of PUFs from HTNR and PCL 108

Figure 4.6 Chemical structure and reaction route of the PUF from HTNR and PCL 109

Figure 4.7 Kinetic characteristic of PUFs from HTNR and PCL 110

Figure 4.8 Density of PUFs from HTNR and PCL 111

Figure 4.9 Cell size of PUFs from HTNR and PCL 111

Figure 4.10 SEM micrographs of PUFs from HTNR and PCL 112

Figure 4.11 TGA curve of PUFs from HTNR and PCL 114

Figure 4.12 DTG curve of PUFs from HTNR and PCL 114

Figure 4.13 Tensile Strength of PUFs from HTNR and PCL 116

Figure 4.14 Specific tensile strength of PUFs from HTNR and PCL 116

Figure 4.15 Elongation at break of PUFs from HTNR and PCL 116

Figure 4.16 Compressive strength of PUFs from HTNR and PCL 117

Figure 4.17 Specific compressive strength of PUFs from HTNR and PCL 118

Figure 4.18 Compression set of PUFs from HTNR and PCL 118

Figure 4.19 Specific compression set of PUFs from HTNR and PCL 119

Figure 4.20 Percentage biodegradation of PUFs from HTNR and PCL 120

Figure 4.21 Colonies of total bacteria grown on Plate Count Agar of PUFs from HTNR/PCL (1/0.5 molar ratio) dilution 10^{-3}: before (a) and after (b) 60 days of biodegradation test 122

Figure 4.22 SEM micrographs of PUFs from HTNR/PCL (1/0.5 molar ratio) before (a) and after (b) 60 days of biodegradation test 123

Figure 4.23 FTIR spectra of PUFs from HTNR/PCL (1/0.5 molar ratio) 124

Figure 4.24 TGA and DTG curves of waste tires 125

Figure 4.25 ^{1}H-NMR spectrum of CTWT 126

LIST OF FIGURES (continued)

Page

Figure 4.26 FTIR spectra of CTWT and HTWT 128

Figure 4.27 ^{1}H-NMR spectrum of HTWT 130

Figure 4.28 Chemical structure and reaction route of the PUF from HTWT and PCL 133

Figure 4.29 FTIR spectra of PUFs from HTWT and PCL 134

Figure 4.30 Kinetic characteristic of PUFs from HTWT and PCL 135

Figure 4.31 Density of PUFs from HTWT and PCL 136

Figure 4.32 Cell size of PUFs from HTWT and PCL 136

Figure 4.33 SEM micrographs of PUFs from HTWT and PCL 137

Figure 4.34 TGA thermograms of PUFs from HTWT and PCL 139

Figure 4.35 DTG thermograms of PUFs from HTWT and PCL 139

Figure 4.36 Percentage biodegradation of PUFs from HTWT and PCL 141

Figure 4.37 FTIR spectra of PUFs from HTWT/PCL (1/0.5 molar ratio): before and after biodegradation test 142

Figure 4.38 Colonies of total bacteria grown on Plate Count Agar of PUFs from HTWT/PCL (1/0.5 molar ratio) dilution 10^{-3}: before (a) and after (b) 60 days of biodegradation test 143

LIST OF ABBREVIATIONS

CTNR	Carbonyl telechelic natural rubber
CTWT	Carbonyl telechelic waste tire
Đ	Dispersity
DABCO-33LV	Triethylene diamine
DABCO-T12	Dibutyltin dilaurate
DTG	Derivative thermogravimetric analysis
FTIR	Fourier transform infrared spectroscopy
GPC	Gel permeation chromatography
H_5IO_6	Periodic acid
HTNR	Hydroxyl telechelic natural rubber
HTWT	Hydroxyl telechelic waste tire
$\overline{M}n$	Number average molecular weight
$\overline{M}w$	Mass average molecular weight
$NaBH_4$	Sodium borohydride
NMR	Nuclear Magnetic Resonance
NR	Natural rubber
PB	Polybutadiene
PCL	Polycaprolactone
PI	Polyisoprene
P-MDI	Polymethylene polyphenylpolyisocyanate
PU	Polyurethane
PUF	Polyurethane foam
SEM	Scanning electron microscopy
TGA	Thermal gravimetric analysis
$ThCO_2$	Theoretical amount of CO_2
TLNR	Telechelic liquid natural rubber
WT	Waste tire

CHAPTER 1

GENERAL INTRODUCTION

1.1 Background

This thesis describes the research work carried out on the synthesis and characterization of biobased and biodegradable polyurethane foams prepared from polyols obtained from natural rubber or waste tires crumbs and polycaprolactone diol. The project was carried out between Prince of Songkla University and Université du Maine as it was in the framework of an international joint PhD program between Thailand and France.

Polyurethanes (PU) are playing a vital role in many industries because of their wide range of mechanical properties and their ability to be relatively easily machined and formed as plastics, foams and elastomers. PUs can be classified into flexible foams (~50%; furniture, mattresses, automotive seats), rigid foams (~30%; insulation and structural materials), as well as coatings, adhesives, sealants and elastomers (~20%; paints, binders, lacquers and elastomeric materials) [1]. Products in this family are chemically complex and may contain several different types of bonds, yet all have the polyurethane linkage in common. This linkage is formed from the reaction between the isocyanate and the hydroxyl group which gives urethane groups.

One type of polyurethane is polyurethane foams (PUFs). The production of PUF is well known. It includes two reactions. The first one is the reaction between isocyanate groups and hydroxyl groups, known as the gelling one, which forms the backbone urethane group. This reaction leads to the formation of a cross-linked polymer if polyols with several hydroxyl groups are used. A side reaction of a urethane group with an isocyanate group can take place to form an allophanate group, and it represents another possible way to further cross-link the polymer. The second one is the reaction between isocyanate group and water (known as the blowing agent) which forms the carbamic acid, which decomposes to give an amine and carbon dioxide gas in the form of bubbles. Next, the formed amine group reacts with another isocyanate group to give a disubstituted urea. Another secondary reaction

involves the formation of biuret linkages which could lead to the formation of covalent cross-linking. The correct balance between these reactions is required since it controls the foam stability and allows the generation of foams with tailored physical properties.

Polyols currently used in the production of polyurethanes are petrochemicals, being generally derived from propylene or ethylene oxides. Polyester polyols and polyether polyols are the most common polyols used in the polyurethane production. For flexible foams, polyester or polyether polyols with molecular weights greater than 2,500 g/mol are generally used. For semi-rigid foams, polyester or polyether polyols with molecular weights of 2,000-6,000 g/mol are generally used, while for rigid foams, shorter chain polyols with molecular weights of 200 to 4,000 g/mol are generally used. There is a very wide variety of polyester and polyether polyols available for use, with particular polyols being used to engineer and produce a particular PUF having desired properties, particular final toughness, durability, density, flexibility, compression set, modulus, and hardness. Generally, high molecular weight polyols and low functionality polyols tend to produce more flexible foams than do low molecular weight polyols and high functionality polyols. In order to eliminate the need to produce, store and use different polyols, it would be advantageous to have a single, versatile, renewable component capable of being used to create final polyurethane foams of widely varying qualities [2].

Use of petrochemicals such as polyester or polyether polyols is disadvantageous for a variety of reasons. As petrochemicals are ultimately derived from petroleum, they are nonrenewable resources. The production of a polyol requires a great deal of energy, as oil must be drilled, extracted from the ground, transported to refineries, refined, and processed to yield the polyol [3]. This method increases the number of steps of polyols production and consequently creates pollution which affects the environment.

Factors such as the price and availability of petroleum, and society concerns over global climate change continue to create increasing market pressure on the industry and domestic use of petrochemicals. Many industrial suppliers of basic chemicals are looking for alternative, sustainable sources of raw materials. In the polyurethanes industry, suppliers of polyols have been utilizing natural raw materials for many years in conjunction with petrochemical raw materials. Recently, the

polyurethanes industry has moved toward a greater replacement of petrochemical content with renewable resources [4-7].

Rubber is a hydrocarbon polymer, used for the manufacture of a number of commercial, industrial and household products. One type of rubber is natural rubber (NR). NR is an interesting material for chemical modification as it is a renewable resource, abundantly natural material, especially in Thailand. Natural rubber consists of *cis* 1,4 carbon- carbon double bonds on the polymeric backbone, which can be chemically modified to generate new polymeric materials. Chain cleavages of natural rubber by photochemical, oxidative and metathesis methods have generated telechelic liquid natural rubber precursors (TLNR). Such liquid natural rubber containing hydroxyl end functional groups (HTNR) has been used as a polyol for the synthesis of polyurethane films and foams [8-10]. Due to the non-polarity of HTNR, there is no hydrogen bonding between the soft and the hard segments resulting in a lower tensile strength, modulus and water resistance than PU containing polar polyols [11]. Polyurethane prepared using HTNR as a precursor has a low rate degradation due to its high resistance to biological attack and its hydrophobicity [12]. Moreover, there is a very wide variety of products containing NR available for use. The largest amounts of NR based products are tires. Tires are composed of various rubbers such as NR, butyl rubber (BR), styrene rubber (SBR) in different mixtures and compositions [13]. Once a tire has been permanently removed from a vehicle without the possibility of being returned to the road, it is defined as ‘waste tire’.

Waste tires (WT) are an interesting and cheap material for preparing WT-based telechelic oligomers. For several years, WT have been considered to be “black pollution” as they are produced in large quantities by industrialized nations, however the methods for their disposal are somewhat limited. Due to this problem, developing convenient methods for the disposal of WT is an ongoing area of research. Waste tires contain vulcanized rubber in addition to the rubberized fabric, along with reinforcing textile cords, steel or fabric belts, and steel-wire reinforcing beads. With different natural and synthetic rubbers and rubber formulations, other components in the tire include: stearic acid, zinc oxide, accelerators, carbon black, extender oil and sulfur. Moreover, tires are resistant to physical, chemical, and biological degradation.

Recently, telechelic oligomers have been synthesized from WT [9,14]. The periodic acid has been used for the oxidative cleavage of NR to give carbonyl telechelic NR (CTNR) [8-10,12,14-17]. Hence, the application of this method was adapted to the synthesis of oligomers from WT. Average molecular weight analysis of the degraded WT indicated that the periodic acid quantity can be used to control the number of carbon- carbon double bonds statistically cleaved. The liquid rubber showed ketone and aldehyde groups at the chain ends. Degradation studies of waste tires were also carried out by this oxidative cleavage using periodic acid, to achieve carbonyl telechelic oligomers from waste tires (CTWT). The CTWT reacted with sodium borohydride to achieve hydroxyl telechelic waste tires oligomers (HTWT) [9,14].

Polycaprolactone (PCL) is a semicrystalline aliphatic polyester derived from a ring opening polymerization of ε-caprolactone. It has a relatively low melting point of 60 °C. It is completely biodegradable by microorganisms (including some phytopathogens) in marine, sewage sludge, soil and compost ecosystem. PCL is degraded in at least two stages. The first stage involves non enzymatic hydrolytic ester cleavage, autocatalyzed by carbon end groups of the polymer chains. When the molecular weight is reduced to 5,000g/mol, the second stage starts with a slowing down of the rate of chain scission and the beginning of weight loss because of the diffusion of oligomeric species from the bulk. The polymer becomes prone to fragmentation and either enzymatic surface erosion or phagocytosis contributes to the absorption process [18]. Assuming that an addition of PCL segment in the HTNR and the HTWT –based PUFs makes possible their biodegradation, PUFs containing HTNR, HTWT and PCL as a soft segment have been synthesized during this research work.

To the best of our knowledge, there has been no previous report on the preparation of PUFs consisting of HTNR, HTWT and PCL as the soft segment. The present study investigated the influence of the molar ratio between HTNR/PCL and HTWT/PCL on foam formation, properties and biodegradation of bio-PUFs. A methodology to carry out biodegradation experiments using microorganisms from sewage water in a latex rubber factory (Top glove technology (Thailand). Co., Ltd.) was optimized and the promising results are described.

1.2 Objectives

1. Synthesis and characterization of hydroxyl oligomers from natural rubber (HTNR) and waste tire crumbs (HTWT).

2. Synthesis of bio-based polyurethane foams containing HTNR, HTWT and PCL diol as a soft segment.

3. Investigation of the mechanical and physical properties of the bio-based polyurethane foams.

4. Optimization of procedure to carry out biodegradation tests.

1.3 References

1. Dworakowska, S., Bogdał, D., Zaccheria, F. and Ravasio, N. 2014. The role of catalysis in the synthesis of polyurethane foams based on renewable raw materials. Catalysis Today. 223: 148-156.
2. Kurth, T.M., Kurth, R.A., Turner, R.B. and Kreifels, L.P. 2006. Oxylated vegetable-based polyol having increased functionality and urethane materials formed using the polyol: US Patents 7,084,230, Aug 1.
3. Acton, Q.A. 2013. Carbamates-advances in research and application-Chapter 9 urethane. Scholarly editions: USA.
4. Abdel Hakim, A.A., Nassar, M., Emam, A. and Sultan, M. 2011. Preparation and characterization of rigid polyurethane foam prepared from sugar-cane bagasse polyol. Materials Chemistry and Physics. 129(1-2): 301-307.
5. Babb, D.A. 2011. Polyurethanes from renewable resources. Advances in Polymer Science. 245: 315-360.
6. Tan, S., Abraham, T., Ference, D. and Macosko, C.W. 2011. Rigid polyurethane foams from a soybean oil-based Polyol. Polymer. 52(13): 2840-2846.
7. Tanaka, R., Hirose, S. and Hatakeyama, H. 2008. Preparation and characterization of polyurethane foams using a palm oil-based polyol. Bioresource Technology. 99(9): 3810-3816.

8. Kébir, N., Morandi, G., Campistron, I., Laguerre, A. and Pilard, J.-F. 2005. Synthesis of well defined amino telechelic cis-1,4-oligoisoprenes from carbonyl telechelic oligomers; first studies of their potentialities as polyurethane or polyurea materials precursors. Polymer. 46(18): 6844-6854.
9. Sadaka, F., Campistron, I., Laguerre, A. and Pilard, J.-F. 2012. Controlled chemical degradation of natural rubber using periodic acid: Application for recycling waste tyre rubber. Polymer Degradation and Stability. 97(5): 816-828.
10. Saetung, A., Rungvichaniwat, A., Campistron, I., Klinpituksa, P., Laguerre, A., Phinyocheep, P. and Pilard, J.-F. 2010. Controlled degradation of natural rubber and modification of the obtained telechelic oligoisoprenes: Preliminary study of their potentiality as polyurethane foam precursors. Journal of Applied Polymer Science. 117: 1279-1289.
11. Sun, X. and Ni, X. 2004. Block copolymer of trans-polyisoprene and urethane segment: Crystallization behavior and morphology. Journal of Applied Polymer Science. 94(6): 2286-2294.
12. Panwiriyarat, W., Tanrattanakul, V., Pilard, J.-F., Pasetto, P. and Khaokong, C. 2013. Preparation and properties of bio-based polyurethane containing polycaprolactone and natural rubber. J Polym Environ. 21(3): 807-815.
13. Kwon, E. and Castaldi, M.J. 2008. Investigation of Mechanisms of Polycyclic Aromatic Hydrocarbons (PAHs) Initiated from the Thermal Degradation of Styrene Butadiene Rubber (SBR) in N2 Atmosphere. Environmental Science & Technology. 42(6): 2175-2180.
14. Tran, T.K.N., Pilard, J.-F. and Pasetto, P. 2015. Recycling waste tires: Generation of functional oligomers and description of their use in the synthesis of polyurethane foams. Journal of Applied Polymer Science. 132(1): 1-11.
15. Panwiriyarat, W., Tanrattanakul, V., Pilard, J.-F., Pasetto, P. and Khaokong, C. 2013. Effect of the diisocyanate structure and the molecular weight of diols on bio-based polyurethanes. Journal of Applied Polymer Science. 130: 453-462.

16. Panwiriyarat, W., Tanrattanakul, V., Pilard, J.-F., Pasetto, P. and Khaokong, C. 2013. Physical and thermal properties of polyurethane from isophorone diisocyanate, natural rubber and poly(ε-caprolactone) with high NCO:OH content. Advanced Science Letters. 19(3): 1016-1020.
17. Panwiriyarat, W., Tanrattanakul, V., Pilard, J.-F. and Khaokong, C. 2011. Synthesis and characterization of block copolymer from natural rubber, toluene-2,4-diisocyanate and poly(ε-caprolactone) diol - based polyurethane. Materials Science Forum. 695: 316-319.
18. Leja, K. and Lewandowicz, G. 2010. Polymer biodegradation and biodegradable polymers – a review. Polish Journal of Environmental Studies. 19: 255-266.

CHAPTER 2

LITERATURE REVIEW

2.1 Telechelic natural rubber

2.1.1 General information

The term 'telechelic' was proposed originally by Uraneck *et al*. [1] for low molecular weight polymers bearing two functional end groups. Nowadays, this term is also applied to oligomers having two or more functional end groups [2]. Telechelic liquid natural rubber (TLNR) can be defined as a low molecular weight oligomer having number average molecular weight approximately 500-10000 g/mol and containing reactive functional end groups that can be used in further chain extension and cross-linking. TLNR still consists of isoprene units as shown in Figure 2.1, the basic structure of natural rubber (NR). The main difference from NR is that TLNR has reactive groups at the chain end which can be the same or different. Although research on the production of TLNR began in the early 1970s, commercial TLNR is still not widely available. Most TLNR used in research are prepared especially in the laboratory [2].

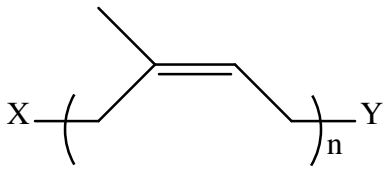

Figure 2.1 Chemical structure of telechelic liquid natural rubber [2].

2.1.2 Synthesis methods of telechelic polyisoprene

Basically, the methods involve controlled degradation or depolymerization of the NR backbone via oxidation chain scissions by either chemical or photochemical routes. The methods can be classified into 5 main categories.

2.1.2.1 Oxidation in the presence of redox system

This method utilizes an appropriate mixture of oxidizing and reducing agents (a redox couple). The redox couple can cleave polymer chains with the concomitant introduction of reactive terminal groups on the resulting oligomers. Thus, an oxidizing agent such as an organic peroxide, hydrogen peroxide, atmospheric oxygen or ferric chloride-oxygen, coupled with a reducing agent such as an aromatic hydrazine or sulphanilic acid were employed to depolymerize NR to yield TLNR bearing phenylhydrazone, carbonyl or hydroxyl terminal groups, depending on the type of redox system employed. The depolymerization reaction can be carried out either in an organic solvent or directly in the latex phase. Of these approaches, depolymerization of NR in the latex phase using phenylhydrazine as a reducing agent and atmospheric oxygen as an oxidizing agent is more favoured owing to it being economically viable on an industrial scale, and hence it was studied in detail. A reaction mechanism of controlled degradation of NR in the latex form by combination of phenylhydrazine and atmospheric oxygen yielding CTNR was proposed and is shown in Figure 2.2. However, the proposed mechanism has yet to be confirmed and needs more experimental evidence. An early investigation of the mechanism of depolymerization of NR using dimethyl-4,8-dodecadiene and squalene as model compounds for polyisoprene, shows that the phenyl radical may be involved in more than one stage of the reaction [2].

Tangpakdee *et al.* [3] have studied an oxidative degradation reaction of deproteinized natural rubber using different initiators, AIBN, potassium persulfate ($K_2S_2O_8$) and benzoyl peroxide in the presence of a carbonyl product such as acetone formaldehyde or propanal. They demonstrated that $K_2S_2O_8$/propanal system is most effective for NR degradation at 60 °C. The mechanism that they proposed is the oxidation of chain by radical initiator followed by the reaction of propanal with aldehyde end group. The obtained TLNR contained aldehyde and ketone groups.

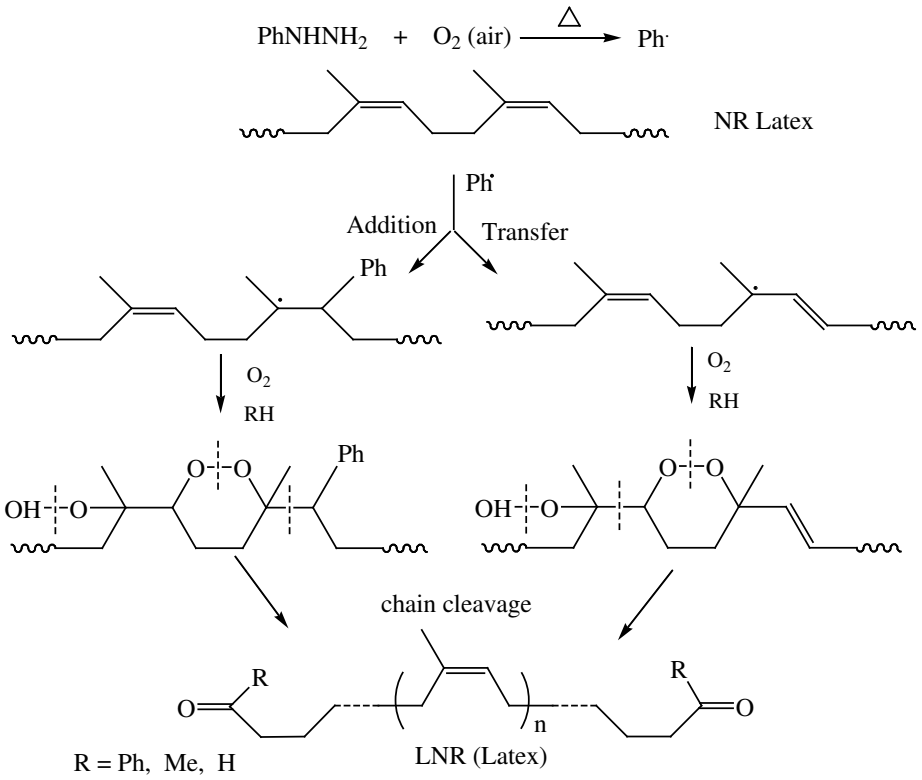

Figure 2.2 Mechanism of the oxidizing cleavage of the natural rubber in latex phase by atmospheric oxygen in the presence of phenylhydrazine [2].

2.1.2.2 Oxidation by photochemical method

Controlled degradation of NR by photochemical chain scission to prepare LNR was first explored by Cunneen. NR was irradiated with UV light in presence of nitrobenzene as a photosentisizer to give carbonyl telechelic natural rubber (CTNR) having $\overline{M}n$ of about 3,000 g/mol. However, no detail about number average functionality was given. The reaction involved is suggested to be that shown in Figure 2.3, but no detailed mechanism was proposed and the oligomer obtained was not well characterized [4].

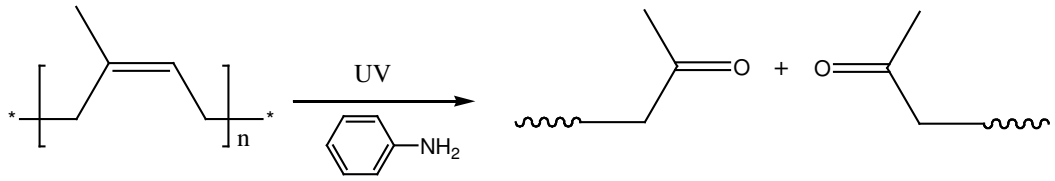

Figure 2.3 Cleavage reaction of natural rubber in the presence of nitrobenzene under irradiation with ultraviolet light [4].

Ravindran *et al.* [5] studied the preparation of hydroxyl telechelic natural rubber via photo-chemical degradation of natural rubber using hydrogen peroxide and irradiating with both a medium pressure mercury vapor lamp and direct sunlight. They reported that both resources have been efficient in the degradation and led to oligomers bearing hydroxyl end-groups, but their functionality was less than 2. Methyl alcohol was more suitable than THF solvent in large production of HTNR. However, side products were observed around 10% such as carbonyl and carboxylic compounds. The mechanism of this reaction is shown in Figure 2.4.

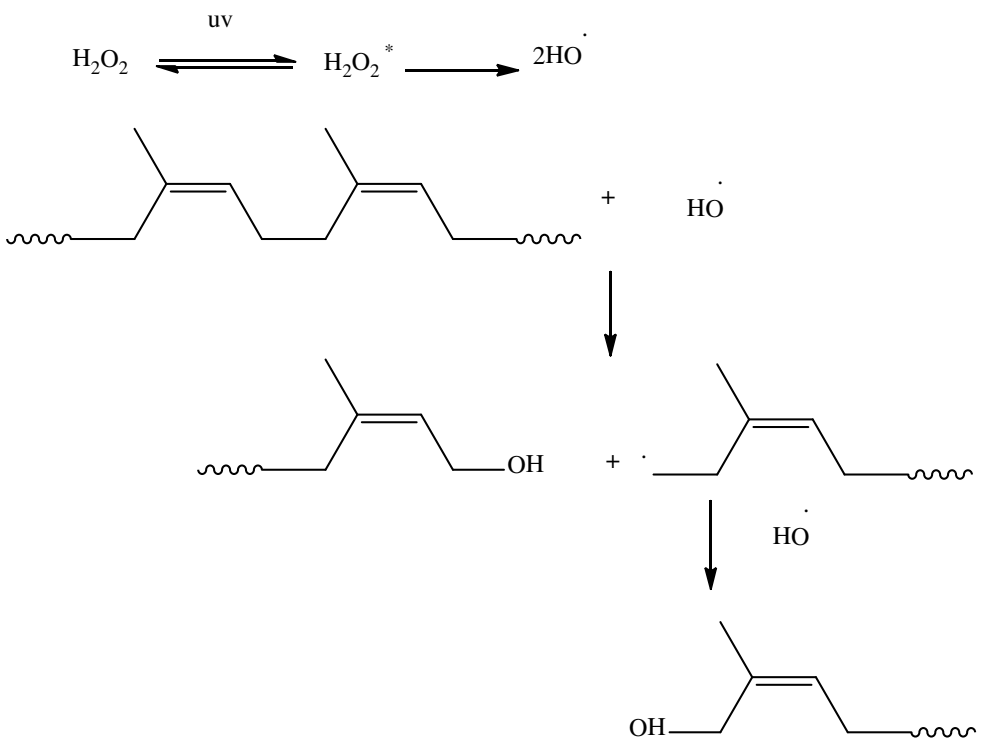

Figure 2.4 The proposed mechanisms of *cis*-1,4-polyisoprene degradation reaction by hydrogen peroxide/UV radiation [5].

2.1.2.3 Oxidation at high temperature and high pressure

In this method, masticated NR in toluene containing 30-40% hydrogen peroxide was heated at 150°C in a reactor at a pressure of 200-300 psi to yield HTNR having $\overline{M}n$ between 2,500 and 3,000 g/mol. Analytical data indicated that the efficiency of functionalization of HTNR by this method was low due to side reactions. Reaction mechanisms were proposed as shown in Figure 2.5 [6].

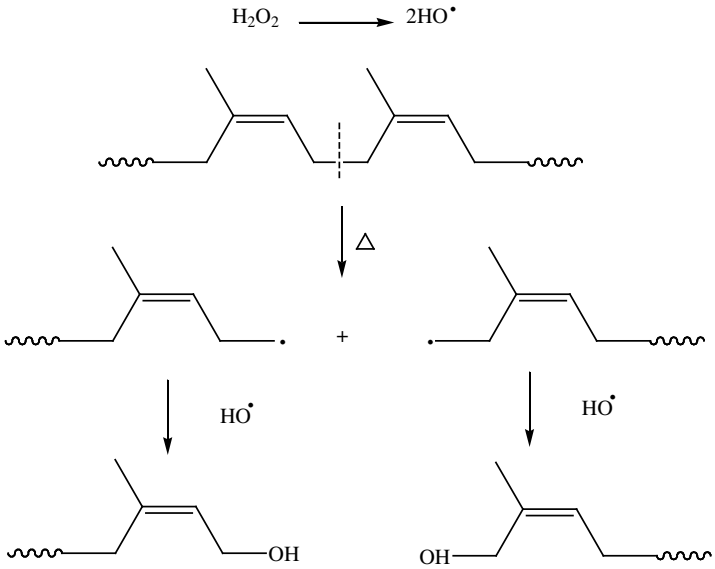

Figure 2.5 The proposed degradation mechanisms of *cis*-1,4-polyisoprene by hydrogen peroxide at high temperature and high pressure [6].

2.1.2.4 Cleavage by periodic acid or lead acetate

Lead tetraacetate, $Pb(OAc)_4$ and periodic acid (H_5IO_6) are interesting for degradation of polyisoprenic chain. Typically, both reagents cause cleavage of *vic*-glycols to yield carbonyl compounds. Burfield and Gan [7] found that $Pb(OAc)_4$ causes degradation of hydrolyzed epoxidized synthetic rubber faster than that of epoxidized synthetic rubber. Synthetic polyisoprene samples which presumably contain no 1,2-diols were also slowly degraded by $Pb(OAc)_4$. They also found that H_5IO_6 could be used to degrade NR and acid hydrolyzed NR. In the case of NR, it is believed that the chain degradation occurs in the presence of a few 1,2- diol units in the molecular chain. H_5IO_6 was also used by Reyx and Campistron to prepare telechelic liquid natural rubber [8]. They found that epoxide content of starting rubber decreased from 25% to 8% after degradation reaction. The NMR spectrum showed the presence of aldehyde and ketone moieties, residual oxiranes, and secondary furanic and cyclic structures.

Mauler *et al.* [9] found that degradation of *cis*-1,4-polyisoprene by using H_5IO_6/ ultrasonic radiation (sonochemical) was more efficient than the use of radiation or chemical degradation alone. The presence of ultrasound irradiation accelerated the chemical degradation process leading to lower molecular weight

products. The degradation of deproteinized epoxidized NR using H_5IO_6 was studied by Phinyocheep *et al.* [10]. The epoxidation of the deproteinized NR was carried out in a latex phase using performic acid formed by an *in situ* reaction between hydrogen peroxide and formic acid. The epoxidized NR was then degraded by H_5IO_6. In all ENR samples obtained, there was no observation of NMR signals corresponding to products of side reactions such as formation of diol and furan, as previously mentioned. After treatment with H_5IO_6, they still found epoxides and also the new signals of carbonyl and hydroxyl functional groups and the molecular weight decreased.

Gillier-Ritoit *et al.* [11] investigated chain degradation of polyisoprene (PI) and epoxidized polyisoprene using H_5IO_6 in organic solvents. Concerning the oligomers chain ends, the degraded PI gave ^{1}H-NMR characteristics similar to those of degraded epoxidized polyisoprene. The degraded rubber contained aldehyde and ketone terminal ends, but the reaction was slower in the case of epoxidized polyisoprene. They found that in the epoxidized polyisoprene, the H_5IO_6 cleavage of polymer chain occurred nearly instantaneously, while H_5IO_6 cleavage of double bonds of polyisoprene was a slower process. It appeared that two equivalents of H_5IO_6 were needed for cleavage of one equivalent of double bonds in polyisoprene. They proposed that the cleavage resulted from a two steps reaction. Firstly, H_5IO_6 reacted with a double bond to give an epoxide or α-glycol. Secondly, the epoxide or α-glycol was cleaved by reacting with the second molecule of H_5IO_6. They proposed the reaction pathway shown in Figure 2.6.

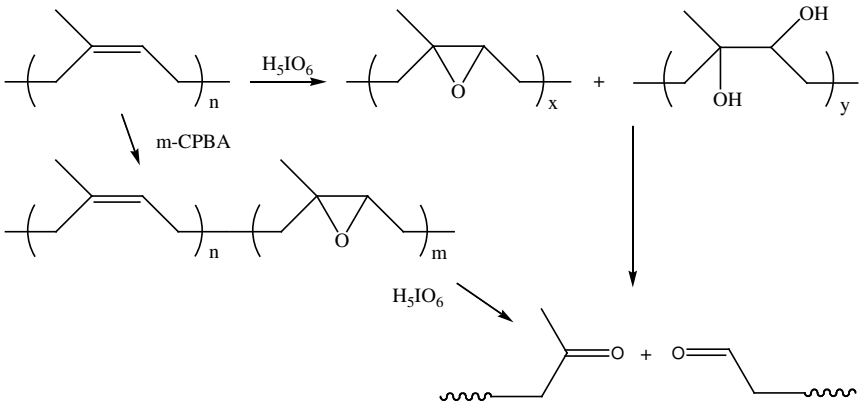

Figure 2.6 The degradation mechanisms of *cis*-1,4-polyisoprene and epoxidized *cis*-1,4-polyisoprene using H_5IO_6 [11].

2.1.2.5 Metathesis degradation

Depolymerization agents or chain transfer agents and catalysts, especially Lewis acid Schrock and Grubbs catalyst II, have been used in metathesis depolymerization of polyalkenamers including polydienes, resulting in oligomers and telechelic oligomers [12]. Use of Lewis acid catalyst such as $WCl_6/Sn(CH_3)_4$ can lead to side reactions. Therefore, Marmo and Wagener [13] reported the synthesis of mass-exact telechelic polybutadiene oligomers by metathesis degradation of *cis*-1,4-butadiene using allylsilane monoene and alkyldienes complex catalysts. They also synthesized the diester, disilyl ether and diamide telechelic polybutadiene oligomers via cyclic diene metathesis depolymerization. The characterization of obtained products showed that these telechelic macromolecules were perfectly difunctional. The mechanism described that in the first stage, the intermolecular cyclization of 1,4-polybutadiene takes place, then macrocyclic butadiene cross-metathesis proceeds with functionalized monoene to form linear difunctional telechelic oligomers as shown in Figure 2.7.

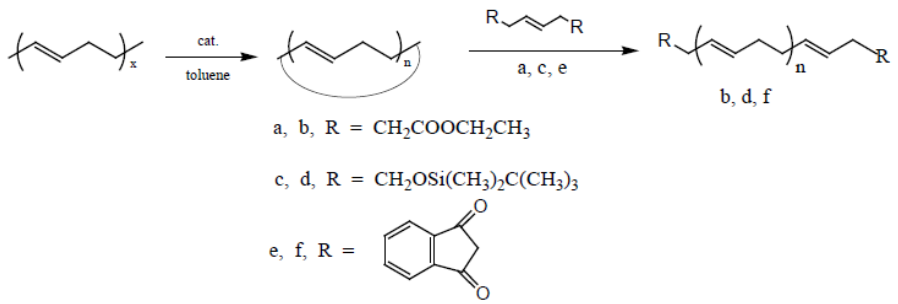

Figure 2.7 Depolymerization mechanisms of 1,4-polybutadiene with diethyl 4-octene-1,8-dioate (a), bis(*t*-butyldimethysilyl)-3-hexene-1,6-diol diether (c), and 2-butene-1,4-diylbis(phthalimide) (e) [13].

However, there is not much work using this technique in degradation of polyisoprene at the present time. Thanki *et al.* [12] performed metathetic alkenolysis of partially epoxidized *cis*-1,4-polybutadiene using Grubbs' ruthenium benzylidene compound as a catalyst and 4-octene as a depolymerizing agent, as shown in Figure 2.8. They found that when the molar ratio of monomer unit to catalyst decreased, yield of oligomer increased linearly.

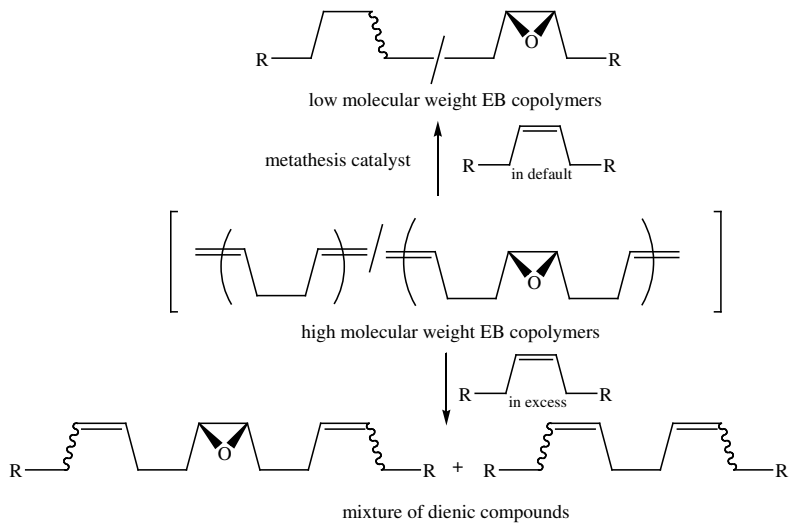

Figure 2.8 Metathesis alkenolysis of partially epoxidized polybutadiene [12].

Solanky *et al.* [14] developed a new approach for obtaining end-functionalized *cis*-1,4-oligoisoprene in a controlled manner through a metathesis methodology. Oligomers of molecular weight range 8,000-40,000 g/mol were obtained in high yield, while lower molecular weight was obtained in moderate yield. Moreover, they prepared telechelic polyisoprene with molecular weight 38,000 from deproteinized natural rubber in latex phase as shown in Figure 2.9.

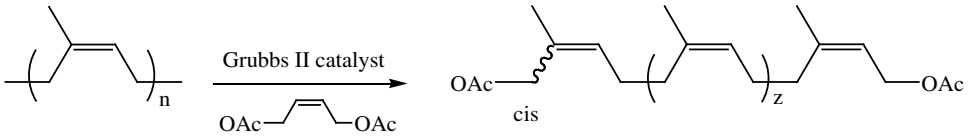

Figure 2.9 Structure produced for the metathetic depolymerization *cis*-1,4-polyisoprene [14].

Pilard *et al.* [15] prepared telechelic oligomers from waste tires by chemical oxidative and metathesis degradation. The chemical oxidative degradation of waste tires with periodic acid was explored. The influence of various parameters (temperature, time and amount of periodic acid) on the degradation reaction was studied. The adjustment of experimental parameters was used to optimize the reaction and high yields were obtained (80-85%), in a range of temperature from 15 to 40 °C. The products of this reaction are shown in Figure 2.10.

The second method was the metathesis degradation. The action of Grubbs II catalyst was exploited and *cis*-but-2-ene-1,4-diacetate was used as the transfer agent. The composition of waste tires including a mixture of polyisoprene and polybutadiene (PB), the products of this reaction are oligoisoprenes and oligobutadienes as shown in Figure 2.11

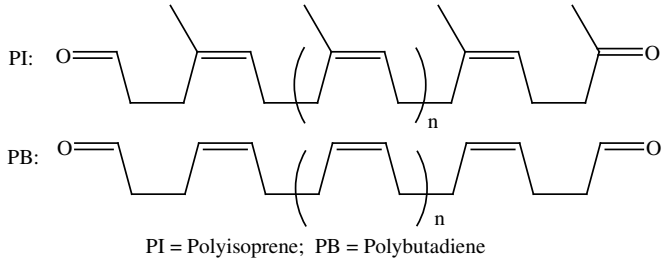

Figure 2.10 Expected outputs of the degradation of waste tires by periodic acid [15].

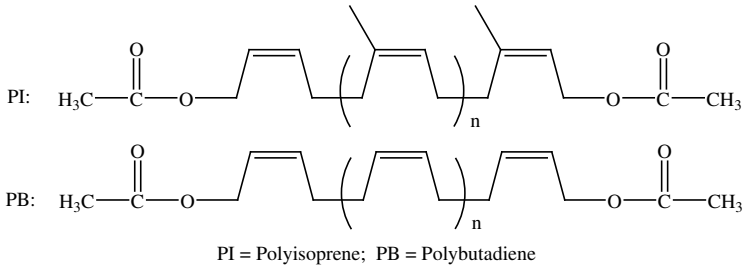

Figure 2.11 Expected outputs of the degradation of waste tires by metathesis [15].

2.2 Tires and waste tires

2.2.1 Tires production

Tires designed to last their shape and composition have evolved over the past decades. If we have to design and build a tire today, the compounder would find this to be a Herculean task. Figure 2.12, indicating tire functions, depicts the complex set of forces that act on a tire and that must be considered in its design and construction. The lateral direction means cornering and center of gravity control as it is tied to the performance of automobile and safety. The tire designer is constantly challenged to design a tire that will perform well when major complex, dynamic forces are involved in forward movement (such as stopping) and that will provide optimal safety in all kinds of weather and pavement conditions [16].

Figure 2.12 Tire functions [16].

The tire itself has evolved into a very complex mixture of polymer, textiles, and exotic steel components (this is illustrated in Figure 2.13, which depicts tire construction). This figure reflects many intricate parts that go into the makeup of today's modern tire.

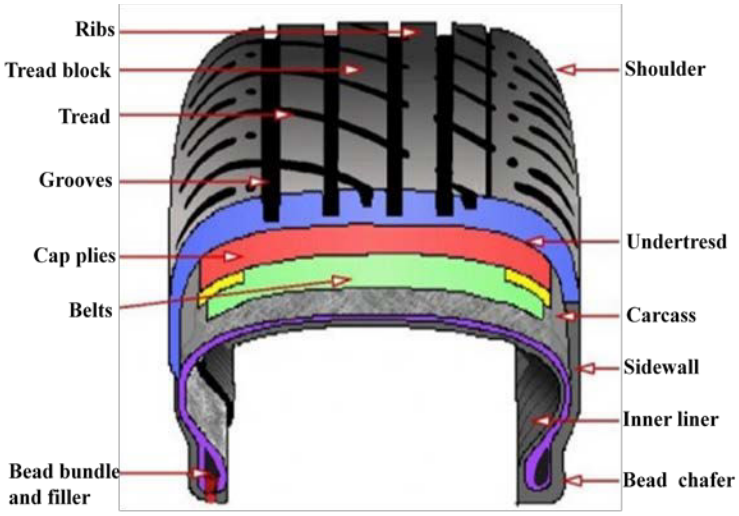

Figure 2.13 Tire construction [17].

Figure 2.14 represents how tire manufacturing has evolved into a very complex process.

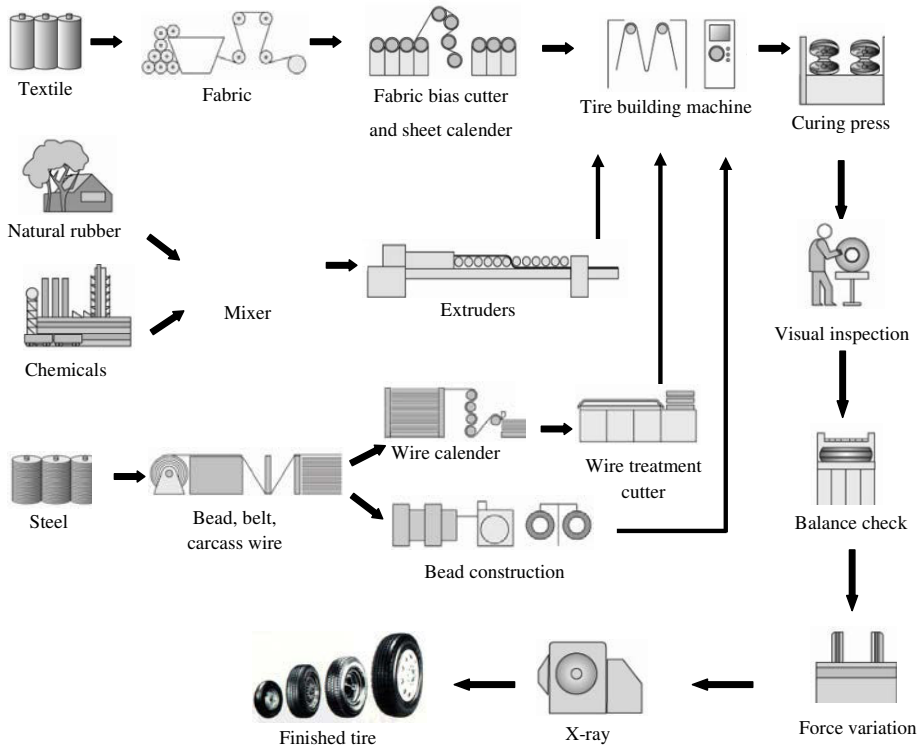

Figure 2.14 Tire production [18].

The tire production process begins with mixing basic rubbers with process oils, carbon black, antioxidants, accelerators and other chemicals such as vulcanizing agents, accelerators, plasticizers, and initiators, each of which contributes to a certain property of the compound. These ingredients are mixed in Banbury mixers operating at high temperature and pressure. Most often it is processed into carefully identified slabs that will be transported to breakdown mills [19]. The slabs of rubber produced are used to calender the body plies, chafers, cap plies or edge strips, steel belts, and all other fabric components used in the tire. Some manufacturers also use a steelastic machine to produce their fabric components. Slab stock is used for extruded components such as the sidewalls, treads, wedges and other solid rubber profiled components.

In the calendering process fabric cords and steel cords are coated with rubber stock. The rubber should be pressed between the individual twisted cord filaments which make up the steel belts. The body plies and reinforcing strips

incorporate polyester cord that is coated in an adhesive liquid. The cord is passed between large heated rolls of a calendering machine. A woven fabric is similarly prepared and calendered for the anti-chafing strips. Since rubber will not adhere to bare steel, the steel cord wires for the steel belts are coated with a very thin layer of brass. These brass coated, rubber encased steel cords (multi-strand cables) become the steel belts. The steel wire passes from the creel room on rollers through aligning combs into the calender where the wires are coated with a thin sheet of skim stock rubber. The rubber should also penetrate the steel cords for maximum adhesion. Both the polyester cords and steel cords are cut at specified angles and widths for use in tire building [20].

The extruder is often referred to as a “tuber” because it creates tube-like rubber components. The extruder functions by forcing rubber through dies of appropriate shape. The extruder consists of a screw, barrel or cylinder, head and die. A core or spider is used to form the hollow inside of tubing. Some tire components are formed by extrusion of uncured rubber, including beads, tread and sidewall components. Extruders are both hot and cold fed systems. Bead wire configurations fall into four primary categories: .037 weftless, .050 weftless, .050 single strand, and cable beads. The bead wire is plated with brass or bronze like the belt wire to provide high adhesion to the insulating rubber, which is usually pressed into and around the bead when it is drawn through an extruding die. Bead chaffer, which is rubber reinforcement around the bead wire, is also placed in the area of the beads to give strength and resilience during tire mounting. Tire tread incorporates several special rubber compounds which are simultaneously extruded to provide the appropriate dimensions for the specific tire. Typically, cement is applied to the underside of the tread where it contacts the steel belts or cap plies. This is commonly referred to as tread cement. It is then cut into the appropriate length for tire building. Cement is typically applied to both ends of the tread piece to obtain maximum adhesion. [20].

Component assembly and building, tire assembly can be a highly automated process. The tire assembly machine consists of a rotating drum, on which the components are assembled, and feeding devices to supply the tire builder with the components to assemble. The components of a tire include beads, plies, side walls and treads. After the components are assembled, the tire is often referred to as a “green tire”.

Tire builders and other workers in this area of the process are exposed to a number of repetitive motion operations. Components, often in heavy rolls, are placed onto the feeding portions of the assembly equipment. This may entail extensive lifting and handling of heavy rolls in a limited space. The nature of assembly also requires the tire builder to perform a series of similar or identical motions on each assembly. Tire builders utilize solvents, such as hexane, which allow the tread and plies of rubber to adhere. After being assembled, the green tire is sprayed with a solvent- or water-based material to keep it from adhering to the curing mould. These solvents potentially expose the spray operator, material handler and curing press operator. Nowadays, water-based materials are mostly used [18].

Curing press operators place green tires into the curing press or onto press loading equipment. Curing presses in operation in a variety of types, ages and degrees of automation. The press utilizes steam to heat or cure the green tire. Rubber curing or vulcanization transforms the tacky and pliable material to a non-tacky, less pliable, long-lasting state. When rubber is heated in curing or in earlier stages of the process, carcinogenic N-nitrosamines are formed therefore attempts should be made to limit N-nitrosamine exposure as much as feasible. In addition, dusts, gases, vapours and fumes contaminate the work environment when rubber is heated, cured or vulcanized [18].

2.2.2 Composition of tires

The basic component used to produce tires are synthetic and natural rubber, textile, steel and chemical additives. The proportions of these components depend on the specific characteristics of the tire. Generally, truck tires have larger natural rubber content than passenger car tires. Approximately, 80% of the weight of car tires and 75% of truck tires is rubber compound. The composition of the tires produced by different manufacturers is very similar [21]. Table 2.1 shows the material composition of passenger car and truck tires [22].

Natural rubber comes from the rubber tree plantations of *Hevea brasiliensis*. Synthetic elastomers are obtained from petroleum and coal requiring several stages to be produced. The most important chemical additive is zinc oxide which is used as an activator in the vulcanization process. Carbon black is added to

further improve the rubber properties, prevent oxidation and provide greater abrasion resistance. All components are finally mixed into internal mixers and vulcanized using sulphur. Vulcanization is a thermochemical process that gives to the tires their performance characteristics in the consumption phase of the product lifecycle.

Table 2.1 Tires composition in the European Union [22]

Material	Car tire (%)	Truck tire (%)
Rubbers/Elastomers	48	45
Carbon black	22	22
Metal	15	25
Textile	5	--
Zinc oxide	1	2
Sulphur	1	1
Additives	8	5

2.2.3 Waste tire recycling

Different ways exist to recycle waste tires such as retreading, grinding, pyrolysis (to oil, monomers, carbon black) and reclaiming. The simplest approach of waste tire recycling is the grinding of vulcanizates and utilization of the tire reduced in powder (ground tire rubber, GTR). Grinding (size reduction) is the preferred recycling route for waste tires being associated with obvious economic and social benefits. To convert the whole tire into GTR the related technology comprises the following steps: shredding, separation (steel, textile), granulation, and classification. GTRs are produced by mechanical grinding at ambient temperature, at ambient temperature under wet condition, at high temperature and at cryogenic temperature. Prior to grinding to higher mesh sizes, i.e., smaller particle sizes, the tire is cut into relatively large and then shredded into smaller pieces. Ambient grinding is usually practiced in two-roll cracker-type mill. Though termed ‘‘ambient’’ the temperature may rise up to 130 °C during milling. The achievable particle size and particle size distribution of GTR depend on the milling sequences and mill type. Under wet (ambient) grinding the crumb rubber is cooled by water spraying. Afterward, water is separated from the GTR and the latter is dried [23].

Several methods have been proposed to prepare rubber powder. The conditions used in each method affect average particle size, particle size distribution, and particle shape greatly. The common methods of powdering the rubber vulcanizate are described under the following subsections [16].

2.2.3.1 Ambient grinding

Ambient grinding consists of passing the vulcanized rubber through the nip gap of a high powered shear mill or two roll mill at room temperature; the number of passes determines the particle size. The higher the number of passes, the greater is the size reductions; hence, the cost of ground rubber increases as the particle size decreases. In the case of scrap tires, the metal and fiber parts are first removed and the whole tire is cut into a chip from (~5 cm). The scrap tire particle size can be further reduced by the use of granulators, cracker mills and micromills.

2.2.3.2 Cryogenic grinding

The cryogenic grinding technique was commercialized in the late 1960s. In this process, initial particle size reduction is carried out at ambient temperature. Then, the rubber chips are cooled to subzero temperature by using liquid nitrogen, and the brittle material is then crushed to tiny particles by a hammer mill. In their frozen state, the particles are sieved. The major advantage of cryogenic grinding is the high production rate. Particle size is controlled by the immersion time in liquid nitrogen and by the mesh size of the screens used in the grinding chamber of the mill.

2.2.3.3 Wet grinding

In this process, tiny rubber chips in water are passed between hard, circular grinding plates that move concurrently and are lubricated by water. In a similar process called solution grinding, the rubber chips are swollen in a solvent and then led into the gap of grinding plates. Particle size is controlled by the time spent in the grinding process.

2.2.3.4 Extrusion

The extrusion process, produces polymer powder by employing a twin screw extruder that imposes compressive shear on the polymeric material, at selected temperatures. The channel depth of the screw decreases from feed zone to the outlet of extruder. By repeated passes through the extruder, particle of narrow size distribution and average diameter (as low as 40 to 60 μm) can be obtained.

2.2.3.5 Abrasion

This method is mostly confined to the preparation of tire buffing, which are obtained as a by-product of retreading. The method involves the removal of rubber particles from tire tread by an abrasion process. No formal studies have been made on the utilization of buffing, but it has been a normal practice in industries to reuse the tire buffing to make low-grade technical products by the revulcanization of the powder. The powder can be converted into useful products by sintering at high temperature under high pressure.

2.2.4 Characteristics of recovered rubber from waste tires

The principal material characteristics are summarized in Table 2.2 and a comparison of the different material outputs is also given. In Figure 2.15, the morphology and surface structure of scrap tire obtained from different process.

2.2.4.1 Shredded tires

The shreds are basically flat, irregularly shaped tire chunks with jagged edges that may or may not contain protruding sharp pieces of metal, which are parts of the steel plates or beads. The size of the tire shreds may range from as large as 460 mm to as small as 25 mm, with most particles within the 100 mm to 200 mm range. The average loose density of the tire shreds varies according to the size of the shreds, but can be expected to be between 390 kg/m^3 to 535 kg/m^3. The average compacted density ranges from 650 kg/m^3 to 840 kg/m^3. They are non-reactive under normal environmental conditions [22].

2.2.4.2 Tire chips

Tire chips are finer and more uniformly sized than tire shreds, ranging from 76 mm down to approximately 13 mm in size. Although the size of tire chips, like tire shreds, varies with the make and condition of the processing equipment, nearly all tire chip particles can be gravel sized. The loose density of tire chips can be expected to range from 320kg/m^3 to 490 kg/m^3. The compacted density of the tire chips ranges from 570 kg/m^3 to 730 kg/m^3. The chips have absorption values that range from 2.0 to 3.8 percent and are nonreactive under normal environmental conditions. The shear strength of tire chips varies according to the size and shape of the chips with friction

angles in the range of 19° to 26°, while cohesion values range from 4.3 kPa to 11.5 kPa. Tire chips have permeability coefficients ranging from 1.5 to 15 cm/sec [22].

2.2.4.3 Ground rubber

Ground rubber is made from whole tires, and 99.9 percent wire and fiber removed. Ground rubber is used in a variety of applications including loose fill playground surface nuggets, landscape covering and a variety of applications [24]. Ground rubber particles are intermediate in size between tire chips and crumb rubber. The particle sizing of ground rubber ranges from 9.5 mm to 0.85 mm [22].

2.2.4.4 Crumb rubber

Crumb rubber is made by size reducing the whole tires through additional granulators and classifiers. The size reduction process includes further reducing contaminants to meet specification of end use products. Ambient crumb rubber is processed at room temperature, while cryogenic crumb rubber is first frozen to very low temperature prior to grinding, producing clean, small particles with different physical characteristics than ambient crumb rubber. Crumb rubber is used in rubberized asphalt concrete, paving applications, and a variety of other tire derived products including synthetic turf infill and molded rubber products [24]. The majority of the particle sizes range within 1.2 mm to 0.42 mm. Some crumb rubber particles may be as fine as 0.075 mm. The specific gravity of the crumb rubber varies from 1.10 to 1.20 (depending on the type of production) and the product must be free from any fabric, wire and/or other contaminants [22].

Table 2.2 Summary of material characteristics [25]

Materials	Size (mm)	Key characteristics	Traditional materials
Cut tires	>300		
Shreds	50 – 300	Lightweight, low-compacted density ±0.5 t m^{-3}, high void	Crushed rock or gravel, large
Chips	10 – 50	Ratio with good water permeability between 10^{-1} and 10^{-3} m s^{-1}. Good thermal insulation and compressibility, low earth pressure and high friction road characteristics	Grain sand, lightweight clay or light expanded clay aggregate, fly ash from coal burning
Granulate (Ambient)	0.5 – 15	Cross-linked macro structure retains same characteristics as the tire; irregular shape; some thermal degradation, temperature stressed. May exhibit nominal degree of reduced cross-linking	Product: Virgin rubbers, EPDM, CE: clay, sand, gravel, fly ash from coal burning polyurethane
Granulate (Cryogenic)	0.5 – 5	Clean surfaces, regular particle size and shape, glossy, smooth surface, no surface decomposition or thermal stress	
Powder	<1	Dependent on technology: ambient/cryogenic characteristics as above	Virgin rubber, EPDM, other compounding materials

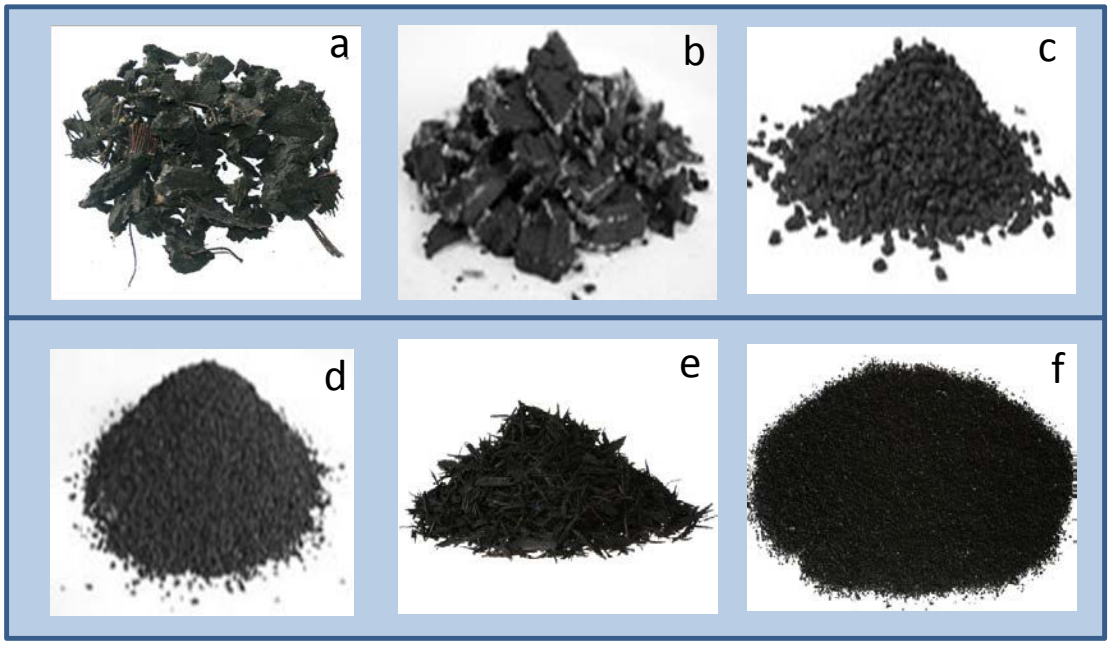

Figure 2.15 Scrap tire surface morphology comparison: (a) tire shred [26], (b) rubber chips, (c, d) granulates [27], (e) buffing and (f) crumb rubber [24].

2.2.5 Production and specifications of crumb rubber

Crumb rubber is a term usually applied to recycled rubber from automotive and truck scrap tires. There are two major technologies for producing crumb rubber – ambient mechanical grinding and cryogenic grinding. Of the two processes, cryogenic process is more expensive but it produces smoother and smaller crumbs.

2.2.5.1 Ambient mechanical grinding process

In ambient mechanical grinding process, the breaking up of a scrap tire happens at or above normal room temperature. Ambient grinding is a multi-step technology and uses whole or pre-treated car or truck tires in the form of shred or chips, or sidewalls or treads. The rubbers, metals and textiles are sequentially separated out. Tires are passed through a shredder, which breaks the tires into chips. The chips are fed into a granulator that breaks them into small pieces while removing steel and fiber in the process. Any remaining steel is removed magnetically and fiber through a combination of shaking screens and wind sifters. Finer rubber particles can be obtained through further grinding in the secondary granulators and the high-speed rotary mills. Ambient grinding is the production process used by the majority of crumb producers.

The machines most commonly used for fine grinding in ambient plants are: secondary granulators, high speed rotary mills, extruders or screw presses and cracker mills [16].

2.2.5.2 Cryogenic grinding process

Cryogenic grinding refers to the grinding of scrap tires at temperatures near -80 ^{o}C using liquid nitrogen or commercial refrigerants. Cryogenic processing generally uses pre-treated car or truck tires as feedstock, most often in the form of chips or ambiently produced granulate. Processing takes place at very low temperature using liquid nitrogen or commercial refrigerants to embrittle the rubber. It can be a four-phase system which includes initial size reduction, cooling, separation, and milling. The material enters a freezing chamber where liquid nitrogen is used to cool it from –80 to –120 °C, below the point where rubber ceases to behave as a flexible material and can be easily crushed and broken. Because of its brittle state, fibers and metal are easily separated out in a hammer mill. The granulate then passes through a series of magnetic screens and sifting stations to remove the last vestiges of impurities. This process requires less energy than others and produces rubber crumb of much finer quality [16].

Both ambient and cryogenic processing can be repeated to produce finer particles. Increasingly, the two with their attendant technologies, are combined into one continuous system in order to benefit from the advantages and characteristics of each and to reduce overall costs. The ambient system is generally used for the initial size reduction phases. The cryogenic system is used to further reduce the material in size and then to remove the metals and textiles. The outputs from either or both systems can be used directly or as feedstock for further processing.

2.2.5.3 Specifications

Crumb rubber is classified as number one, two and so on, depending on quality and size. Table 2.3 presents a summary of crumb rubber grades. However, crumb rubbers produced in industry should maintain certain quality requirements with respect to their grades and specifications. There is no national standard available in the United Kingdom, but a European standard is now underway. Most industries in the UK use their own specifications, although ASTM standards are widely used in many parts of the world. ASTM D5603-96 and ASTMD5644-96 are the two most widely used grading standards [22].

Table 2.3 Crumb rubber specification [22]

Grade	Size	Description
No.1 and 2 Tire Granule (minus 40 grades)	6.35 mm to less than 0.635 mm	*Guaranteed metal free.* Magnetically separated materials are not acceptable. Fluff from tire cord removed. Less than 0.635 mm refers to material that has been sized by passing through a screen with 40 holes per centimeter (referred as minus mesh 40 grades).
No.3 Tire Granule (minus 4 grades)	less than 6.35 mm	*Magnetically separated materials (these materials cannot be certified as metal free due to residual metal/oxide content.* Metal is magnetically separated. Fluff from tire cord removed. Less than 6.35 mm refers to material that has been sized by passing through a screen with 4 holes per centimeter.
No.4 Tire Granule (minus 80 grades)	6.35 mm to less than 0.3175 mm	*Magnetically Separated.* Fluff from tire cord removed. Less than 0.3175 mm refers to material that has been sized by passing through a screen with 80 holes per centimeter.

2.2.6 Uses of crumb rubber

As crumb rubber is free of metal and fiber it is used for different applications depending upon the size and requirement [28]:

- used to produce reclaimed rubber.
- used as tire derived fuel (TDF) in cement Kilns.
- used to replace virgin material.
- used for children's playground surfaces and tracks.
- used as soil amendment for sports turf.
- used in road construction.
- used for civil engineering purposes for construction.

Crumb rubber is sold as feedstock for chemical devulcanization or reclamation (pyrolysis) processes, added to asphalt for highway paving and pavement

sealers, or used for the production of a large number of recycled rubber-containing products. Some of the major applications of crumb rubber are athletic surfaces, automotive parts and tires, construction, landscape, walkways, extruded products, playground, rubber modified asphalt, sealants and rubber blends.

The work presented in this manuscript is the follow up of previous research carried out in the team. Firstly Sadaka *et al.* [29] studied the use of periodic acid for the controlled one-pot oxidative cleavage of carbonyl telechelic *cis*-1,4-oligoisoprenes (CTNR) and natural rubber (NR) as model compounds, then the application of this method was used to the degradation of ground tire waste rubber. Molecular weight analysis of the degraded material indicated that the reaction time and the periodic acid quantity can be used to control the degree of breakdown. Oligomers in the average molecular weight range of 700 - 5,000 g/mol were obtained and they showed to have ketone and aldehyde groups at the chain ends. Well-defined structures were obtained from waste tire crumbs following the same methodology, with an average molecular weight from 3,000 to 7,000 g/mol according to the periodic acid/ tire waste rubber ratio used. When the molar ratio of periodic acid to polymer was increased from 10%, 15%, 18% - 20% with a reaction time of 24 h, oligomeric products with molecular weights estimated by ^{1}H NMR spectroscopy of 3,280, 2,890, 1,880 and 1,580 g/mol respectively were obtained.

2.3 Polycaprolactone

2.3.1 General physicochemical properties

Poly(ε-caprolactone) (PCL) is a semicrystalline, biodegradable polymer having a melting point (T_m) of ~60 °C and a glass transition temperature (Tg) of ~ -60 °C. The repeating molecular structure of PCL homopolymer consists of five nonpolar methylene groups and a single relatively polar ester group. This structure gives PCL some unique properties and the presence of the hydrolytically unstable aliphatic-ester linkage causes the polymer to be biodegradable. This combination also gives PCL the unusual property of being compatible with numerous other polymers and PCL polymer blends having unique properties have been prepared [30].

2.3.2 Synthesis of polycaprolactone

Polycaprolactone was derived from the polymerization of monomer ε-caprolactone (Figure 2.16). The monomer can be produced through an oxidation process by microorganisms or using peracetic acid. The oxidation of cyclohexanol into adipic acid by microorganisms resulted in the formation of ε-caprolactone as an intermediary product [31]. The synthesis of ε-caprolactone also takes place when cyclohexanone is oxidized by peracetic acid [32]

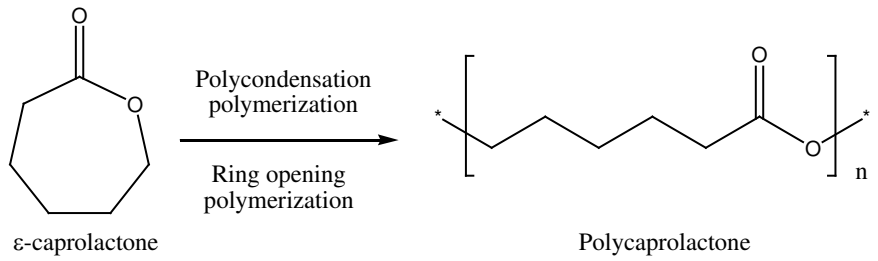

Figure 2.16 Polymerization of ε-caprolactone by polycondensation and ring opening polymerization techniques [33]

For the synthesis of PCL, the polymerization can take place through the condensation of 6-hydroxycaproic (6-hydroxyhexanoic) acid and the ring opening polymerization of ε-caprolactone. PCL polymerization by condensation of 6-hydroxycaproic (6-hydroxyhexanoic) acid is conducted under vacuum condition to remove the water produced during the reaction, thus inducing the formation of the polymer. There are also a few studies that describe the use of enzymes from microorganisms, like lipase, to synthesize PCL by polycondensation method [34]. However, polycondensation method usually results with a polymer with a lower molecular weight, whilst ring-opening polymerization can produce PCL with a higher molecular weight [32]. The synthesis of PCL via ring-opening polymerization route involved the use of catalysts and a wide range of catalytic systems, including metal-based, enzymatic and organic systems [32]. The catalysts included lithium diisopropylamide, magnesium aryloxide, triethylaluminium and stannous (II) ethylhexanoate [33].

2.4 Polyurethane foams

2.4.1 Polyurethane foam chemistry

There are two main reactions important in the production of polyurethane foams: the gas-production reaction (blow reaction) and the polymerization reaction (gelation reaction). To the manufacturer, balancing the respective rates of these two reactions provides the open celled morphology in the foam that is highly important for the physical properties. If the gelation, or cross-linking, reaction occurs too quickly, a tight close celled foam may result. If the blow, or gas-producing, reaction occurs too quickly, the cells may open before the polymer has enough strength to uphold the cellular structure, resulting in collapse of the foam. These two reactions must be kept in proper balance in order to obtain the desired product [35].

2.4.1.1 Gas-production reaction (blow reaction)

The reaction of water with isocyanate is a two-step process termed the blow reaction because, in addition to a polyurea product, a gas is evolved which plays a large role in blowing the liquid into a foam. The initial step of the blow reaction, which occurs through an intermediate is shown in Scheme 2.1, where a thermally unstable carbamic acid is generated. This carbamic acid then spontaneously decomposes yielding heat, carbon dioxide, and an amine functionality. The carbon dioxide diffuses into existing bubbles already nucleated in the liquid causing expansion of the foam. In addition to that, the heat generated will also play a large role in expanding the gas in the liquid to form the desired cellular morphology.

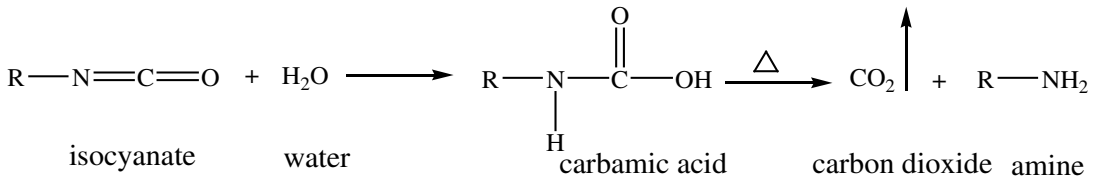

Scheme 2.1 First step of the blow reaction [35].

The amine functionality proceeds to the second step of the blow reaction. As shown in Scheme 2.2, it reacts with an additional isocyanate group to form a disubstituted urea linkage. The total heat given off in the reactions of Scheme

2.2 and Scheme 2.3 is approximately 47 kcal/mol. This second reaction can also be source of covalent cross-links if either the isocyanate has more than two functional groups or if polyfunctional (e.g. diethanolamine) have been added to the formulation.

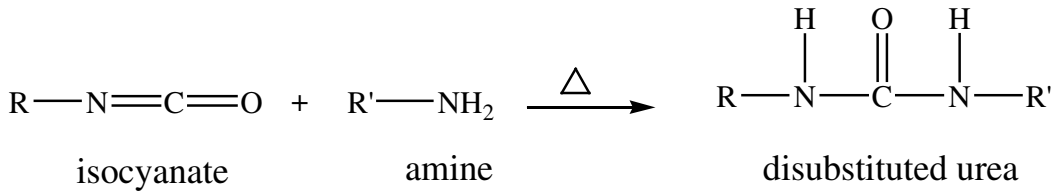

Scheme 2.2 Second step of the blow reaction [35].

There is an additional reaction which could also produce covalent cross-links. The formation of biuret linkages, as shown in Scheme 2.3, can occur if one of the hydrogens from the disubstituted urea product reacts with an isocyanate functionality. However, this reaction is reversible and generally does not occur below 100 °C, and no evidence exists which suggests that birurets are produced to a significant extent in typical polyurethane foams.

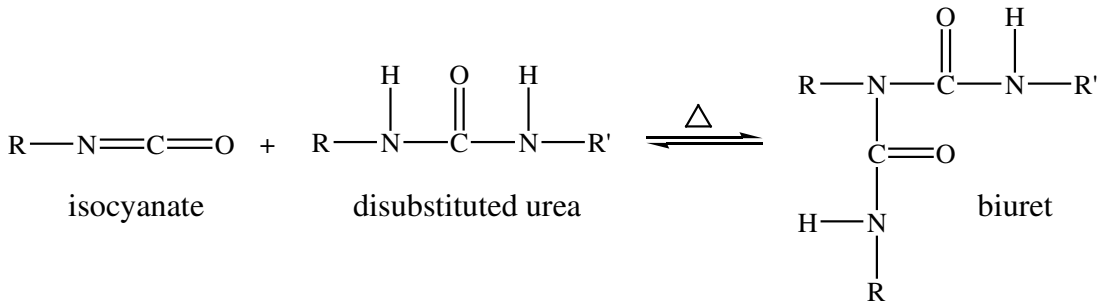

Scheme 2.3 Formation of a biuret linkage [35].

2.4.1.2 Polymerization reaction (Gelation reaction)

The polyurethane linkage is produced by the reaction of an alcohol functionality with an isocyanate group as shown in Scheme 2.4. This addition reaction is exothermic with a heat of reaction of approximately 24 kcal/mol of urethane. The nature of the R and R′ groups shown in Scheme 2.5 can vary depending on the selection of components in the formulation. Generally, one of these components is multifunctional so that these reactions lead to a covalent network.

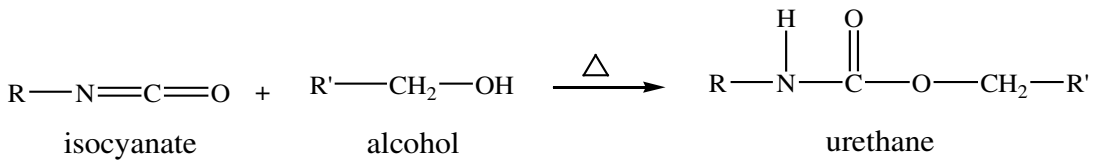

Scheme 2.4 The gelation or cross-linking reaction [35]

A side-reaction that can result from this urethane product is the allophanate forming reaction. This occurs when another isocyanate group reacts with the urethane linkage through the hydrogen on the nitrogen atom as is shown in Scheme 2.5. This formation reaction occurs mainly at high temperatures and is reversible. It is uncertain whether this reaction actually occurs in normal foam processes, as the catalysts utilized generally do not promote this reaction. Also, since it only occurs in significant levels above 110 °C, the allophanate reaction may reverse as the foam cools following production. If it does occur, it serves as an additional point of cross-linking; however, this side reaction has not been shown to actually occur in typical foam production.

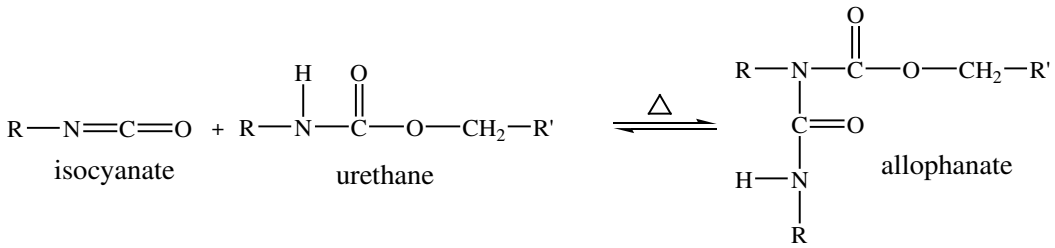

Scheme 2.5 Allophanate formation [35].

2.4.2 Type of polyurethane foams

One of the most desirable attributes of polyurethanes is their ability to be turned into foam [36]. Three types of foams can be formed, namely low density flexible foams, low density rigid foams and high density flexible foams.

2.4.2.1 Low density flexible foams

They are materials of densities 10-80 kg/m^3, composed of lightly crosslinked, open cells. Flexible foams are produced as slabstock or individually moulded and pads. Semi-rigid variants also have an open cell structure but different chemical formulations. An example of the cellular structure is shown in Figure 2.17 (a).

2.4.2.2 Low density rigid foams

They are highly crosslinked polymers with a closed cell structure-each bubble within material has unbroken walls so that gas movement is impossible. These materials have a strong structure in relation to their weight, combined with the outstanding thermal insulation properties. These foams must have at least 90 percent of closed cells and the density is above about 30 kg/m^3. An example of the cellular structure is shown in Figure 2.17 (b).

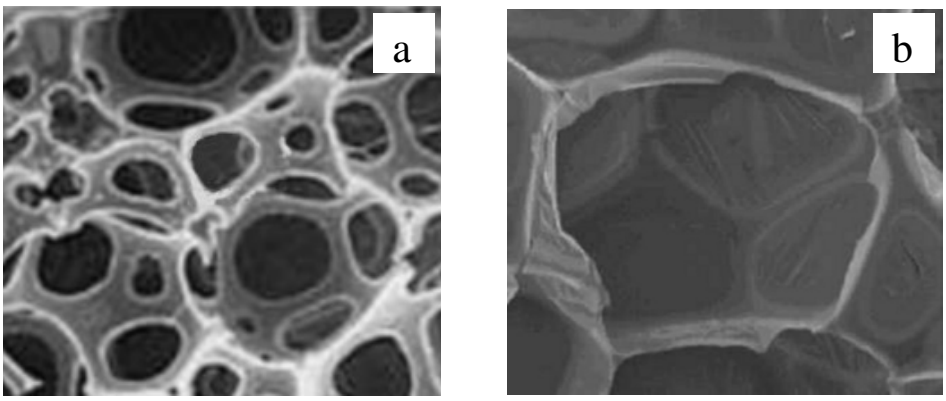

Figure 2.17 Morphology of flexible foam (a) and rigid foam (b) [37].

2.4.2.3 High density flexible foams

They are defined as those having densities above 100 kg/m^3. The range includes molded self-skinning foams and microcellular elastomers. Self-skinning or integral skin foam systems are used to make mould parts having a cellular core and a relatively high densities. There are two types:

a) Open cell core and an overall density in the range up to about 450 kg/m^3.

b) A largely closed cell or microcellular core and an overall density above about 500 kg/m^3.

Microcellular elastomers have a substantially uniform density in the range from about 400-800 kg/m^3 and those mostly closed cells. The biggest applications of self-skinning foams and microcellular elastomers are in mould parts for upholstery and vehicle trim and for shoe-soling.

Much of the polyurethanes produced are in the form of large blocks of foam, which are cut up for use in cushions, or for thermal insulation. The chemical

reaction can also take place in moulds, leading to, for example, a car bumper, a computer casing or a building panel. It may occur as the liquid reactants are sprayed onto a building surface or coated on a fabric [38].

2.4.3 Raw materials

The two major raw materials for making polyurethane foams are isocyanates and polyols.

2.4.3.1 Isocyanates

The isocyanate provides the source of NCO group to react with function groups from the polyol, water and other ingredients in the formulation. All the isocyanates used in the industry today contain at least two isocyanate groups per molecule. The most commercially viable methods of producing isocyanates involve the phosgenation of an amine (Scheme 2.6) [39].

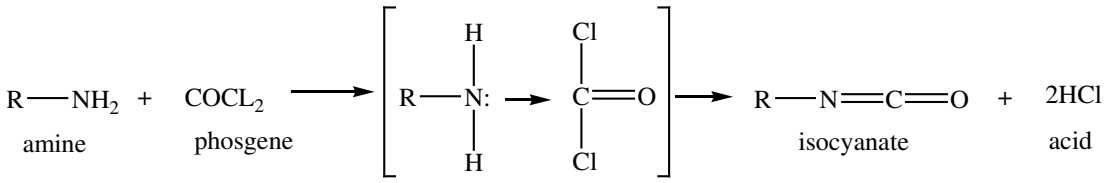

Scheme 2.6 The method of producing isocyanate [39].

This reaction is usually completed in a chlorinated aromatic solvent, which is employed to remove excess phosgene in later purification steps. Methylene diphenyl diisocyanate (MDI) and toluene diisocyanate (TDI) are two major kinds of isocyanates consumed in the global isocyanate market. Other types of isocyanates, like 1,6-hexane diisocyanate (HDI), isophorone diisocyanate (IPDI), 1,5-napthalene diisocyanate (NDI), 1,4-phenylene diisocyanate (PDI) are also used in different applications. Figures 2.18 to 2.20 show the chemical structures of these isocyanates.

In flexible foam, the isocyanate most commonly used is toluene diisocyanate (TDI). The two most important isomers of TDI are shown in Figure 2.18. The pure 2,4-TDI is more reactive than the pure 2,6-TDI [39].

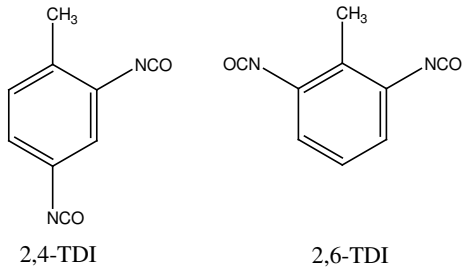

Figure 2.18 Chemical structure of toluene diisocyanate (TDI) [39].

Various forms of methylene diphenyl diisocyanate (MDI) are used in making high resiliency, semiflexible and microcellular foams. MDI is prepared from aniline, formaldehyde, and phosgene according to the general reaction scheme shown in Figure 2.19. The undistilled reaction mixture resulting from the phosgenation of the polyamine mixture contains varying amounts of di, tri and higher functionality polyisocyanates. The polymeric MDIs are differentiated by viscosity, functionality and reactivity. Blends of polymeric MDI with TDI are also used.

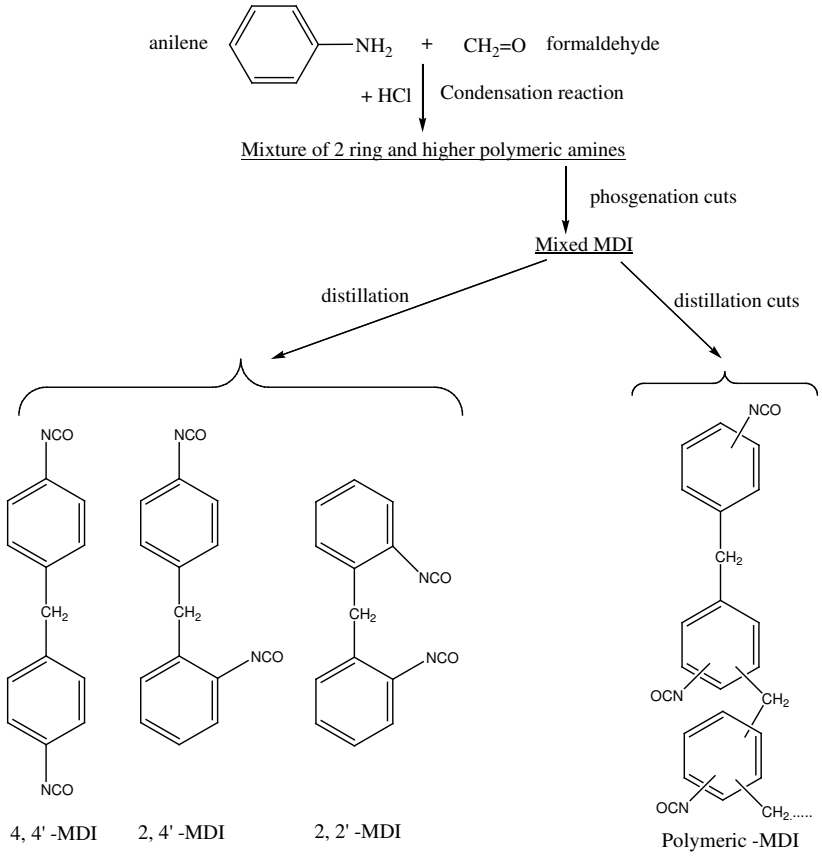

Figure 2.19 General scheme for MDI production [39].

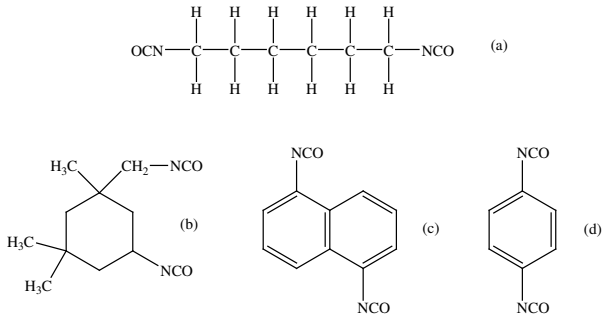

Figure 2.20 Chemical structure of (a) 1,6-hexane diisocyanate (HDI), (b) isophorone diisocyanate (IPDI), (c) 1,5-napthalene diisocyanate (NDI), and (d) 1,4-phenylene diisocyanate (PDI) [40].

2.4.3.2 Polyols

The polyol is a source of hydroxyl or other isocyanate reactive groups. Processing and properties of the resultant foam can be markedly influenced by the choice of starting polyol structure. The exact composition will be selected to tailor the foam for a given application and to allow its processing in commercial plants that differ widely in capabilities. Ninety percent of all flexible foams produced are made from polyether polyols. The other ten percent are polyester polyols [39] and examples of each type structure are shown in Figure 2.21.

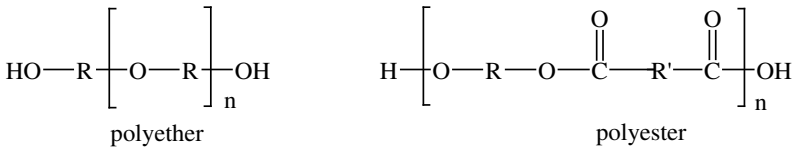

Figure 2.21 Example of polyether and polyester polyols

The polyether polyols may be grouped into the following categories:

- Polyoxypropylene diols,
- Polyoxypropylene triols,
- Polyoxypropylene tetrols and higher analogs,
- Ethylene oxide capped diols, triols, tetrols and higher analogs,
- Random and block polymers of the above in which the polyol is made with a mixture of ethylene and propylene oxide,
- Graft or copolymer polyols that contain stable dispersions of a solid particulate polymeric phase in the liquid polyol phase.

The polyether polyols are made by the reaction of epoxides (oxiranes) with an active hydrogen containing starter compounds as shown in Scheme 2.7 [41]. The polyester polyols are made by the polycondensation of multifunctional carboxylic acids and hydroxyl compounds as shown in Scheme 2.8 [42].

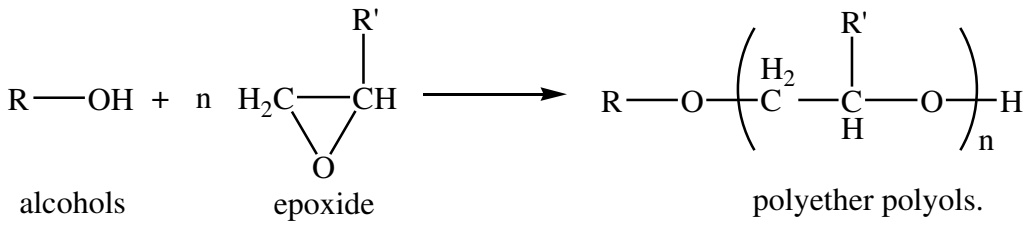

Scheme 2.7 Synthesis of polyether polyol [41].

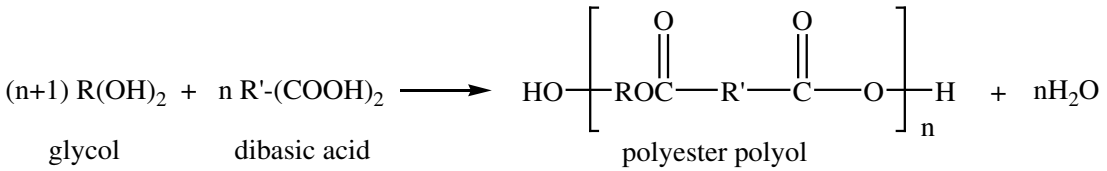

Scheme 2.8 Synthesis of polyester polyol [42].

Two important properties of polyols, functionality and equivalent weight, play a dominant role in the properties of the final product, polyurethane polymers. The functionality of polyols can be defined as the average number of functional groups reacting to isocyanate per molecule of polyol. The equivalent weight of polyols can be defined as follows:

$$\text{Equivalent weight} = \frac{\text{Molecular weight of polyols}}{\text{Functionality of polyols}} = \frac{56100}{\text{Hydroxyl number}}$$

The hydroxyl number (mg KOH/g) is milligrams of potassium hydroxide equivalent to the hydroxyl groups found in one gram of polyols [43]. The molecular structure of the polyol chains in equally important. The distinguishing characteristics of the polyols used to make polyurethanes are summarized in Table 2.5

Table 2.4 The relation between the properties of polyols and applications of polyurethane polymer [43].

Characteristics	Elastomers, Coatings, Flexible foams	Elastoplastics, Rigid coating, Rigid foams
Molecular weight range (Daltons)	1,000 – 6,500	150 – 1,000
Functionality	2.0 – 3.0	3.0 – 8.0
Hydroxyl number	28 – 160	250 – 1,000
Equivalent weight	500 – 3,000	70 – 800

In recent years, the price of petroleum polyols has escalated due to the continuous price increase in crude petroleum; moreover, consumption of petroleum products releases CO_2 and contributes to global warming, which is a serious environmental concern. These problems could be partially addressed by producing polyols from renewable resources.

2.4.3.3 Other additives

Catalysts

Catalysis plays a vital role in the preparation of polyurethane because it not only affects the rates of the chemical reactions responsible for chain propagation, extension, and cross-linking but also affects the ultimate properties of the resulting polymer. Catalysts are employed whose functions are not only to bring about faster rate of reaction but also to establish a proper balance between the chain-propagation reaction (primarily the hydroxyl-isocyanate reaction) and the foaming reaction. Another important function of catalysts is to bring about completion of the reactions resulting in an adequate ‘cure’ of the polymer.

The catalysts most commonly employed are tertiary amines and metal catalysts, especially tin catalysts. Tertiary amines are catalysts for the isocyanate-hydroxyl and the isocyanate-water reactions. The efficiency of tertiary amine catalysts depend on upon their chemical structure: it generally increases with the basicity of the amine and when the steric shielding of the amino nitrogen decreases. Some of the most commonly used tertiary amine catalysts are triethylenediamine, N-alkyl

morpholines, *N,N,N',N'*-Tetramethylethylenediamine, *N,N,N',N'*-Tetramethyl-1,3-butanediamine, *N,N'*-substituted piperazines, and dialkylanolamines [44].

Organometallic catalysts are used as gelation catalysts although they do affect the isocyanate-water blowing reaction. Organotins are the most widely used, but organomercury and organolead catalysts are also used. The mercury catalysts are very good for elastomers because they give a long working time with a rapid cure and very good selectivity towards the gelation. The lead catalysts are often used in rigid spray foams [44]. The relation between the type of catalyst and application is summarized in Table 2.6 and 2.7.

Table 2.5 Tertiary amine catalysts and their application [44].

Catalyst	**Characteristic and use**
N,N-Dimethylethanolamine (DMEA)	Inexpensive, used in flexible foams and in rigid foams. Acid scavenger for rigid-ester foams and fire retarded foams.
N,N-Dimethylcyclohexylamine (DMCHA)	Inexpensive, has a high odour, is used mainly in rigid foams.
Bis(N,N-Dimethylaminoethyl) ether (BDMAEE)	Excellent blowing catalyst used in flexible, high resilience and cold moulded foams.
N,N,N',N',N"-Pentamethyldiethylenetriamine (PMDETA)	Good blowing catalyst used in isocyanurate board stock and moulded rigid foams.
1,4-Diazabicyclo[2,2,2]octane (DABCO) (Also referred to as triethylenediamine (TEDA)	Very good amine gelation catalyst. Used in all types of foams.
2-(2-Dimethylaminoethoxy)ethanol (DMAEE)	Reactive catalyst used in low density packaging foams.
2-(2-Dimethylaminoethoxy) ethyl methyl-amino)ethanol	Excellent reactive low odour blowing catalyst used in high resilience and flexible foams. Low vinyl staining.
1-(Bis(3-dimethylamino)propyl) amino-2-propanol (Also referred to as N"-hydroxypropyl-N,N,N',N'	Low odour reactive catalyst used in rigid and high resilience foams. Replaces DMCHA in spray and is low vinyl

Table 2.5 (continued)

Catalyst	Characteristic and use
N,N',N'-Tris(3dimethylaminopropyl) hexahydrotriazine	Isocyanurate catalyst that provides back end cure. Decreases demould time of appliance foams.
Dimorpholinodiethylether (DMDEE)	Low odour catalyst used in one-component foams and sealants.
N,N-Dimethylbenzylamine	Characteristic smell used in polyester-based flexible foams, integral skin foams and for making prepolymers.
N,N,N',N",N"Pentamethyldipropyl enetriamine	Strong ammoniacal odour used for polyether-based slabstock foams and in semi-rigid foam moulding.
N,N'-Diethylpiperazine	Low odour balanced blow cure catalyst for flexible and semi-flexible systems.

Table 2.6 Organometallic catalysts and their application [44].

Catalyst	Characteristic and use
Stannous octoate	Polyether based slabstock and moulded flexible foams catalysis.
Dibutyltin dilaurate (DBTDL)	Microcellular, Reaction injection moulding (RIM) and cast elastomers catalysis.
Dibutyltin mercaptide	Hydrolysis resistant catalyst.
Phenylmercuric propionate	In glycol solution for potting compounds, as a powder for delayed action catalysis.
Lead octoate	Chain extension catalysis.
Potassium acetate/octoate (KA/KO)	General purpose catalyst, Isocyanurate foams
Quaternary ammonium formates (QAF)	General purpose catalyst, Isocyanurate foams
Ferric acetylacetonate	Catalyst for cast elastomer systems.

Surfactants

Polyurethane foams are made with the aid of nonionic silicone based surfactants. In broad terms, surfactants perform several functions:

- Lower surface tension,
- Emulsify incompatible formulation ingredients,
- Promote nucleation of bubbles during mixing,
- Stabilize the riding foam by reducing stress in thinning cell walls,
- Counteract the defoaming effect of any solids added to or formed during the foam reaction.

Among these functions, the stabilization of the cell walls is the most important. By doing this, the surfactant prevents the coalescence of rapidly growing cells until those cells have attained sufficient strength through polymerization to become self supporting. Without this effect, cell coalescence would lead to total foam collapse.

Selection of a surfactant for any given foam system is a task requiring literature review, supplier consultation, and small scale foam experimentation. Within each foam formulation, a minimum level of surfactant is needed to produce commercially acceptable foam. Figure 2.22 summarizes the basic effect of varying surfactant concentration in a TDI based flexible slabstock foam [39].

In the absence of a surfactant, a TDI based foaming system will normally experience catastrophic coalescence and exhibit the event known as boiling. With addition of a small amount of surfactant, stable yet imperfect foams can be produced. With increasing surfactant concentration, a foam system will show improved stability and cell size control. At optimum concentrations, stable open celled foams may be produced. At higher surfactant levels, the cell windows become over stabilized and the resulting foams are tighter with diminished physical properties. The surfactant requirements for slabstock foam made using a polymeric MDI isocyanate are typically much less demanding [39].

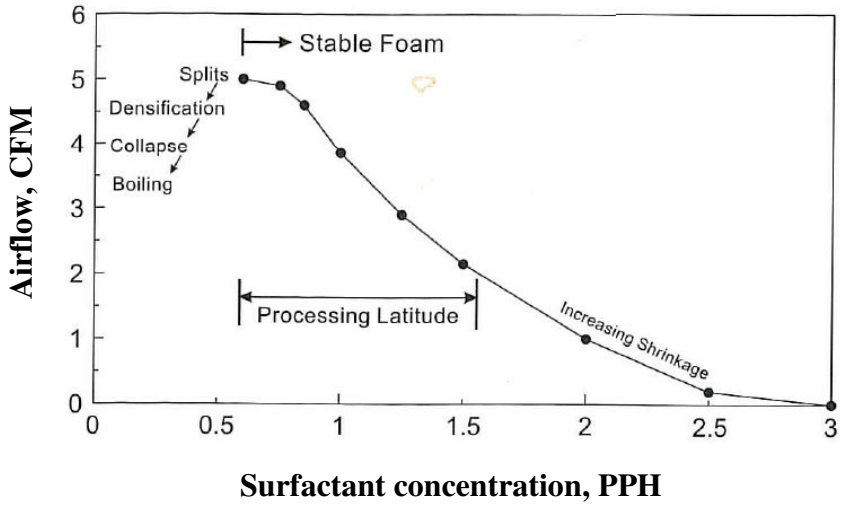

Figure 2.22 Typical effects of silicone surfactant in a TDI-based slabstock foam [39].

Chain extenders and cross linkers

Chain extenders (f=2) and cross linkers (f=3 or greater) are low molecular weight hydroxyl and amine terminated compounds that play an important role in the polymer morphology of polyurethane fibers, elastomers, adhesives, and certain integral skin and microcellular foams. The elastomeric properties of these materials are derived from the phase separation of the hard and soft copolymer segments of the polymer, such that the urethane hard segment domains serve as cross-links between the amorphous polyether (or polyester) soft segment domains. This phase separation occurs because the mainly non-polar, low melting soft segments are incompatible with the polar, high melting hard segments. The soft segments, which are formed from high molecular weight polyols, are mobile and are normally present in coiled formation, while the hard segments, which are formed from the isocyanate and chain extenders, are stiff and immobile. Because the hard segments are covalently coupled to the soft segments, they inhibit plastic flow of the polymer chains, thus creating elastomeric resiliency. Upon mechanical deformation, a portion of the soft segments are stressed by uncoiling, and the hard segments become aligned in the stress direction. This reorientation of the hard segments and consequent powerful hydrogen bonding contributes to high tensile strength, elongation, and tear resistance values. The choice of chain extender also determines flexural, heat, and chemical resistance properties. The most important chain extenders are ethylene glycol,

1,4-butanediol (1,4-BDO or BDO), 1,6-hexanediol, and cyclohexane dimethanol. All of these glycols form polyurethanes that phase separate well and form well defined hard segment domains, and are melt processable. They are all suitable for thermoplastic polyurethanes with the exception of ethylene glycol, since its derived bis-phenyl urethane undergoes unfavorable degradation at high hard segment levels. Diethanolamine and triethanolamine are used in flexible molded foams to build firmness and add catalytic activity. Diethyltoluenediamine is used extensively in RIM, and in polyurethane and polyurea elastomer formulations [45]. The chain extenders and cross linkers for polyurethane are shown in Table 2.8.

Table 2.7 Chain extenders and cross linkers [45].

	Molecular weight	Specific gravity	Melting point	Boiling point
Hydroxyl compounds - difunctional molecules				
ethylene glycol	62.1	1.110	-13.4	197.4
diethylene glycol	106.1	1.111	-8.7	245.5
triethylene glycol	150.2	1.120	-7.2	287.8
tetraethylene glycol	194.2	1.123	-9.4	325.6
propylene glycol	76.1	1.032	supercools	187.4
dipropylene glycol	134.2	1.022	supercools	232.2
1,3-propanediol	76.1	1.060	-28	210
1,3-butanediol	92.1	1.005	-	207.5
1,4-butanediol	92.1	1.017	20.1	235
neopentyl glycol	104.2	-	130	206
1,6-hexanediol	118.2	1.017	43	250
Hydroxyl compounds - trifunctional molecules				
glycerol	92.1	1.261	-	-
triethanolamine	149.2	1.124	-	-
Hydroxyl compounds - tetrafunctional molecules				
pentaerythritol	136.2	-	-	-
Amine compounds - difunctional molecules				
diethyltoluenediamine	178.3	1.022	-	-
dimethylthiotoluenediamine	214.0	1.208	-	-

Water

Water is a source of active hydrogens. Only demineralized water should be used for foam production. Isocyanate reacts with water to give carbon dioxide gas and polyurea molecules as shown in Scheme 2.1 and 2.2. The gas diffuses into nucleated bubbles and aids in foam expansion. The polyurea molecules enter into and contribute to the properties of the final polymer [39].

2.4.4 Polyurethane and polyurethane foams literature review

The state of the art of the literature concerning polyurethane foams is reported in the following sections.

2.4.4.1 Polyurethane foams from petroleum-based polyol

Kim and Kim [46] studied the effect of isocyanate index on the properties of rigid polyurethane foams by using HFC 365mfc as blowing agent. Rigid polyurethane foams (RPUFs) were fabricated from crude methylene diphenyl diisocyanate (CMDI) and polypropylene glycols (PPGs) by various isocyanate index. There was a tendency for the gel time to decrease and the tack-free time to increase with increasing index value. With increasing index value, the foam density and compression strength decreased and the glass transition temperature, dimension stability and thermal insulation increased, while the cell size and closed cell content were virtually unchanged.

Verdejo *et al.* [47] studied acoustic damping in flexible polyurethane foams filled with carbon nanotubes, with loading fractions of up to 0.2 wt% carbon nanotubes (CNTs): the foams were made by free-rising foaming using water as a blowing agent. Electron microscopy revealed an open cellular structure and a homogeneous dispersion of CNTs, although the incorporation of nanofiller affected the foaming process, foam density and cellular structure. The compressive strength of the foams did not show an improvement with increasing CNT content due to the variable foam structure. However, dense films generated by hot pressing the foams indicated a significant intrinsic reinforcement of the polymer, even at low loadings of CNTs. Most significantly, CNTs were found to increase the acoustic activity monotonically at concentrations up to 0.1 wt%.

2.4.4.2 Polyurethane foams from bio-based polyol

Because of environmental concerns and unstable petroleum price profiles, there is a trend toward substituting petroleum-based polyol with renewable resources. The use of natural resources in the synthesis of polyol for polyurethane foam preparation has been reported in the literature. For example, biopitch [48], rapeseed oil [49], wheat straw [50], palm oil [51], corn stover [52], sugarcane bagases [53] and soybean oil [54] have all been used for this purpose.

Araujo *et al.* [48] studied the effects of biopitch on the properties of flexible polyurethane foams. Biopitches are industrial residues obtained by the distillation of the tar recovered during eucalyptus charcoal production and can be used as a renewable polyol source. Flexible polyurethane foams were prepared with different proportions of biopitch and HTPB (hydroxyl-terminated polybutadiene) and using polymeric MDI (4,4' diphenyl methane diisocyanate), N,N dimethylcyclohexylamine as a catalyst and water as a blowing agent. Elemental analysis, thermal analysis (TGA/DSC), Fourier Transform Infrared Spectroscopy, scanning electronic microscopy and density results were used to discuss the contribution of biopitch to foams properties. The higher the biopitch content, the higher the thermal stability and the lower the density of the flexible foams (air atmosphere), whose behavior was similar to those of lignin-based polyurethanes.

Stirna *et al.* [49] prepared polyurethane foams from rapeseed oil polyols. By transesterifying rapeseed oil with triethanolamine or glycerol, polyols with a hydroxyl number of 290–310 mg KOH/g were synthesized. Water-blown rigid polyurethane foams (PUFs) with an isocyanate index of 150–250 were obtained from rapeseed oil polyols. Studies on the effect of the concentration of potassium oleate, the cyclotrimerization catalyst of isocyanate groups, on the degree of conversion of isocyanate groups were carried out using FTIR spectroscopy. The optimal physical and mechanical properties of the obtained PUFs were achieved at an isocyanate index of 150–200. Spray PUFs with good physical and mechanical properties were obtained from rapeseed oil polyol.

Wang and Chen [50] studied method of utilizing the biomass resource. Rapid liquefaction of wheat straw and preparation of biodegradable polyurethane foam (PUF) were studies. Wheat straw was rapidly liquefied in the mild condition.

The optimum liquefaction effect was obtained at steam-explosion pretreatment of wheat straw, liquefaction temperature of 140 ^{o}C, solvent/wheat straw ratio of 6:1, glycol : glycerol = 5, sulfuric acid of 5% and wheat straw of water content of 150%. During the liquefaction, lignin and cellulose were degraded. Hydroxyl value, acid value and viscosity of liquefied wheat straw were similar to those of petrochemical polyol. PUF based on liquefied wheat straw has high mechanical properties, which were comparable to those of conventional PUF. In addition, the kind of PUF had good water absorption and biological degradability. The above facts proved that liquefaction of wheat straw is an effective method to utilize the wheat straw and other agricultural straws. The method can utilize the rich resource of agricultural straw with little pollution and lessen the dependence of chemical industry on the oil. On the other hand, as a novel technology, liquefaction of the biomass has still many questions to overcome and more efforts are needed to perfect it.

Tanaka *et al*. [51] prepared polyurethane foams using a palm oil-based polyol (PO-p). At the first stage, palm oil was converted to monoglycerides as a new type of polyol by glycerolysis. The yield of the product reached 70% at reaction temperature of 90 ^{0}C by using an alkali catalyst and a solvent. At the second stage, PU foams were prepared from mixtures of the polyol and polyethylene glycol or diethylene glycol and an isocyanate compound. Characterization of the foams was carried out by thermal and mechanical analyses. The analyses showed that the chain motion of polyurethane became more flexible at the higher PO-p content in the whole polymer, which indicated that the monoglyceride molecules work as soft segments. The study here may lead to a development of a new type of polyurethane foams using palm oil as a raw material.

Wang *et al*. [52] studied the effects of Corn stover (CS) and ethylene carbonate (EC) ratio on structure and properties of polyurethane foams prepared from untreated liquefied corn stover with polymethylene polyphenylisocyanate (PAPI). CS was liquefied by using EC as liquefying solvent and sulfuric acid as a catalyst at 170 °C for 90 min. Polyurethane (PU) foams were prepared from liquefied corn stover (LCS) and PAPI by one-shot method at a [NCO]/[OH] ratio of 0.6 in the presence of a blowing agent, surfactant and co-catalyst. The effects of CS/EC ratio (w/w) on the structural, mechanical and thermal properties were studied by means of Fourier

Transform Infrared Spectroscopy, thermal analysis (TGA/DSC) and universal tensile machine. Fourier Transform Infrared Spectroscopy analysis indicated that urethane linkages were formed; free isocyanate groups existed in samples. All samples had a low thermal stability and decomposition occurred in four successive stages. With the increase in CS/EC ratio, the tensile strength and the Young's modulus first increased and then decreased, and the elongation at break decreased. Properties of LCS-PU foams can be changed by varying the CS/EC ratio.

Hakim *et al.* [53] prepared rigid polyurethane foam from sugar-cane bagasse polyol by the reaction of bio-polyol prepared from liquefied sugarcane bagasse (LBP) with commercial methylene diphenyl diisocyanate (MDI) and polyethylene glycol in the presence of N,N-dimethylcyclohexylamine as a catalyst, water as a chemical blowing agent, and silicon oil as a surfactant. The effect of partial replacement of polyethylene glycol polyol (PEG) by the prepared bio-polyol on physical and mechanical properties, thermal conductivity and thermal stability of polyurethane foam was studied. The obtained results revealed that, the prepared polyurethane foam showed longer cream and tack free times more than blank polyurethane foam (100% PEG). The foam density and the compressive strength improved with increasing of biomass-based polyol content. Increasing the percent of bio-polyol more than 30% replacement resulted in heterogeneous surface and irregular pore shape. Also thermal conductivity reduced from 0.035 to 0.029 $Wm^{-1}K^{-1}$ with increasing bio-polyol content. The structure of rigid polyurethane foam is shown in Figure 2.23.

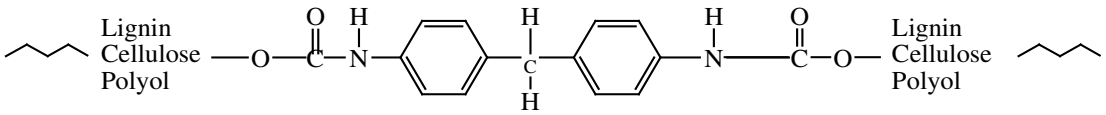

Figure 2.23 Structure of polyurethane foam prepared from bio-polyol [53].

Tan *et al.* [54] synthesized rigid polyurethane foams by substituting a polypropylene-based polyol with soybean oil-based polyol (SBOP). All the soy-based foams maintained a regular cell structure and had even smaller average cell size than the control foams. The density of soy-based foams was within 5% of the petroleum-derived polypropylene based polyol (Jeffol_ FX31-240), except that the density of foams from 100% SBOP was 17% higher. Soy-based foams also had comparable

initial thermal conductivity (k value) and closed cell content, higher T_g and compressive strength. However, while foams from 50% SBOP showed similar increase in k value to the 0% SBOP foams, under accelerated aging conditions, the 100% SBOP foams aged faster. Gas permeation tests performed on PU thin films showed higher N_2 permeation for PU thin films made from SBOP which is believed to be the cause of accelerated thermal aging.

Saetung *et al.* [55] prepared and studied the properties of flexible polyurethane foams based on hydroxytelechelic natural rubber. Flexible polyurethane foams were successfully prepared from a renewable source, hydroxytelechelic natural rubber (HTNR) having different molecular weights (1,000, 2,000 and 3,400 g/mol refer to HTNR1000, HTNR2000 and HTNR3400, respectively) and variation of epoxide contents (EHTNR, 0-35% epoxidation) by a one-shot technique. The chemical and cell structures as well as physico-mechanical, thermal, and acoustic properties were characterized and compared with commercial polyol analogs. The obtained HTNR based foams are open cell structures with cell dimensions between 0.38 and 0.47 mm. The HTNR1000 based foam exhibits better mechanical properties but lower elongation at break than those of analogous commercial polyol. However, the HTNR3400 based foam showed the best elastic properties. In a series of EHTNR based foams, the tensile and compressive strengths show a tendency to increase with increasing epoxide content and amount of 1,4-butanediol. The HTNR based foams demonstrate better low temperature flexibility than that of the foam based on commercial polyol. Moreover, the HTNR based polyurethane foams was found to be an excellent absorber of acoustics.

2.4.4.3 Polyurethane from NR and PCL based polyol

Polyurethanes prepared from natural rubber as a precursor have low rate of degradation due to the high resistance to biological attacks, hydrophobicity, and lack of functional groups recognizable by microbial enzymatic systems. In order to increase biodegradation of polyurethane, the addition of a biodegradable polyester segment as soft segment into the polyurethane chains can be tried. The biodegradation of the polyester occurs by hydrolysis resulting in the cleavage of polymer chains. Polycaprolactone (PCL) was widely used to synthesize biodegradable polyurethanes.

Heijkants *et al*. [56] synthesized polyurethanes based on poly(ε-caprolactone) (PCL) (750–2,800 g/mol) and 1,4-butane diisocyanate (BDI) with different soft segment lengths and constant uniform hard segment length in the absence of catalysts for the production of a degradable meniscus scaffold. First the polyester diols were endcapped with BDI yielding a macrodiisocyanate with a minimal amount of side reactions and a functionality of 2.0. Subsequently, the macrodiisocyanates were extended with 1,4-butanediol in order to obtain the corresponding polyurethane. The polyurethanes had molecular weights between 78 and 160 kg/mol. Above molar masses of 1,900 g/mol of the polyester-diol, crystalline PCL was found while the hard segment showed an increase in melting point from 78 to 122°C with increasing the hard segment content. The Young's modulus varied between 30 and 264 MPa.

Liu *et al*. [57] synthesized biodegradable aliphatic co-polyesters from ε-caprolactone, adipic acid, and 1,6-hexanediol by melt polycondensation method. The chemical structure and thermal properties of these copolymers were studied in detail. The water absorption behavior and hydrolytic degradation behavior of this co-polyester were also studied. With the increase in pentaerythritol, the water absorption behavior of the copolymers increased, but the water absorption didn't change distinctly with the content of caprolactone. The alkaline degradation behavior of these co-polyesters were also studied, the degradation rate increased with the increase in pentaerythritol and the caprolactone content. This aliphatic co-polyester prepolymer could be used to prepare the biodegradable poly(ester urethane), which might have potential application in the biomedical field.

Xie *et al*. [58] synthesized a novel biodegradable poly(ε-caprolactone)-poly(ethylene glycol)-based polyurethane (PCL-PEG-PU) with pendant amino groups by direct coupling of PEG ester of NH_2-protected-(aspartic acid) (PEG-Asp-PEG diols) and poly(ε-caprolactone) (PCL) diols with hexamethylene diisocyanate (HDI) under mild reaction conditions and by subsequent deprotection of benzyloxycarbonyl (Cbz) groups as shown in Figure 2.24. Gel permeation chromatography, ^{1}H Nuclear and ^{13}C Nuclear magnetic resonance studies confirmed the polymer structures. Differential scanning calorimetry and wide-angle X-ray diffraction results

indicated that the crystallinity of the copolymer enhanced with increasing PCL diols in the copolymer. The content of amino group in the polymer could be adjusted by changing the molar ratio of PEG-Asp-PEG diols to PCL diols. The results of this study provided a suitable method to prepare polyurethanes bearing hydrophilic PEG segments and reactive amino groups without complicate synthesis.

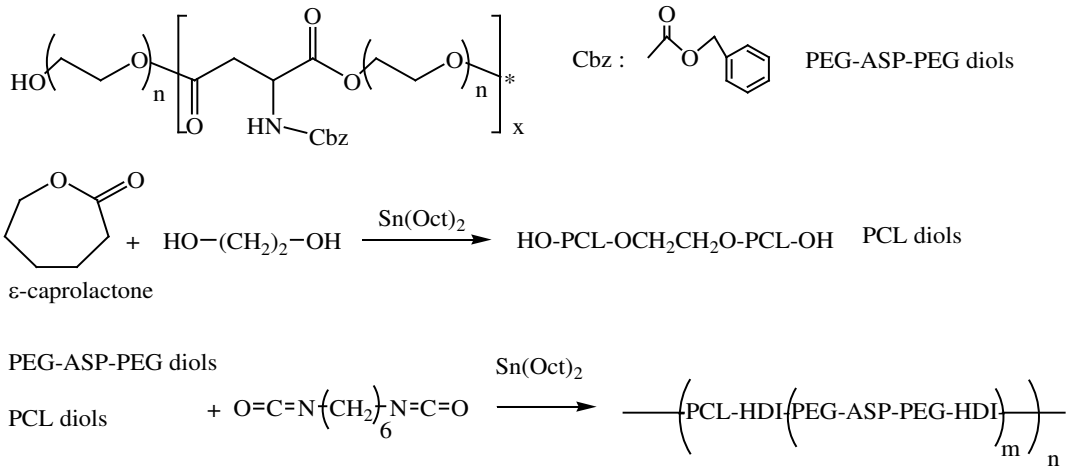

Figure 2.24 Synthesis of PCL diol and coupling reaction of PCL diols with PEG-Asp-PEG diols [58].

Jiang *et al.* [59] designed a series of nontoxic cross-linked waterborne polyurethanes and synthesized with isophorone diisocyanate (IPDI), poly(e-caprolactone) (PCL), poly(ethylene glycol) (PEG), 1,4-butandiol (BDO) and L-lysine without any other organic agent involved in the whole synthetic process. The bulk structures and properties were characterized by DSC and IR, mainly focusing on the effect of PEG amount. Their corresponding biodegradability was examined with Lipase AK. The result showed that the prepared waterborne polyurethanes had very good tensile properties, allowing them to be well used as biomaterials. And the change of tensile properties with increasing of amount of PEG in the polymers could be assigned to the change of microphase separation, as indicated by DSC and IR data. This work demonstrated a new synthetic approach that can be more promising to prepare both nontoxic and biodegradable polyurethanes for soft tissue engineering applications or drug delivery.

Jeon *et al*. [60] prepared poly(ε-caprolactone)-based polyurethane (PCL-PU) nanofibers containing silver nanoparticles by electrospinning of the 8 wt% PCL-PU solutions containing different amounts of $AgNO_3$ in a mixed solvent consisting of dimethylformamide (DMF) / tetrahydrofuran (THF) (7/3 w/w) for use in antimicrobial nanofilter applications. The average diameter of the pure PCL-PU nanofibers was 560 nm and decreased with increasing concentration of $AgNO_3$. The PCL-PU nanofiber mats electrospun with $AgNO_3$ exhibited higher tensile strength, tensile modulus, and lower elongation than the pure PCL-PU nanofiber mats. Small Ag nanoparticles were produced by the reduction of Ag^+ ions in the PCL-PU solutions. The average size and number of the Ag nanoparticles in the PCL-PU nanofibers were considerably increased after being annealed at 100°C for 24 h. They were all sphere-shaped and evenly distributed in the PCL-PU nanofibers, indicating that the PCL-PU chains stabilized the Ag nanoparticles well.

Panwiriyarat *et al.* [61] synthesized polyurethane polymer films by using hydroxyl terminated liquid natural rubber (HTNR) and poly(ε-caprolactone) (PCL) as soft segment and toluene-2,4 diisocyanate (TDI) as a hard segment. The PU samples were synthesized by solution polymerization. The suitable NCO:OH ratios were 0.84:1 to 1.20:1 and the $\overline{M}n$ of the derived PUs was 3,000-5,500 g/mol, determined by using gel permeation chromatography (GPC). The molecular weight tended to increase with increasing NCO:OH ratio. PU from PCL-HTNR block copolymer was synthesized by varying molar ratio between PCL and HTNR. The $\overline{M}n$ of HTNR was in the range of 1,700-8,000 g/mol. ^{1}H-NMR and FTIR were used to determine the formation of PU linkages. In another work, Panwiriyarat *et al.* [62] synthesized PU by using HTNR and PCL as a soft segment but the hard segment included isophoronediisocyanate and 1,4-butane diol (BDO), which was added as a chain extender. The addition of BDO in the PCL diol-based PU increased Young's modulus and tear strength but decreased the elongation at break resulting in a decrease in the tensile strength. By addition of a small amount of HTNR, the tensile properties and tear strength of PU increased significantly. The tensile behavior of PU was changed from a tough to a soft polymer with increasing HTNR content. In a follow up of the work (Panwiriyarat *et al.* [63]), the influence on mechanical

properties of three different diisocyanates and of the molecular weight of diols were investigated. An aliphatic diisocyanate (hexamethylenediisocyanate, HDI), an aromatic diisocyanate (toluene-2,4-diisocyanate, TDI) and a cycloalkane diisocyanate (isophoronediisocyanate, IPDI) were employed. PU containing TDI and IPDI showed a rubber-like behavior: low Young's modulus and high elongation at break. The crystalline domains in PU containing HDI acted as physical crosslinks, enhancing the Young's modulus and reducing the elongation at break, and they were responsible of the plastic yielding.

2.5 Biodegradation

2.5.1 General information

There is a world-wide research effort to develop biodegradable polymers as a waste management option for polymers in the environment. Biodegradation (i.e. biotic degradation) is a chemical degradation of materials (i.e. polymers) activated by the action of microorganisms. The most common definition of a biodegradable polymer is "a degradable polymer wherein the primary degradation mechanism is through the action of metabolism by microorganisms." Biodegradation is considered a type of degradation involving biological activity and is expected to be the major mechanism of loss for most chemicals released into the environment. This process refers to the degradation and assimilation of polymers by living microorganisms to produce degradation products.[64]

The American Society for Testing of Materials (ASTM) and the International Standards Organization (ISO) defined degradable plastics those which undergo a significant change in chemical structure under specific environmental conditions. These changes result in a loss of physical and mechanical properties, as measured by standard methods. Biodegradable plastics undergo degradation from the action of naturally occurring microorganisms such as bacteria, fungi, and algae. Plastics may also be designated as photodegradable, oxidatively degradable, hydrolytically degradable, or those which may be composted [65-68].

Biodegradation can be defined as the breakdown or mineralisation of an organic material due to microbial and/or fungal activity. The availability of oxygen

determines to which molecules the organic carbon is converted. If complete biodegradation takes place under aerobic conditions, the organic carbon of the material will be converted to carbon dioxide and water will be released (Scheme 2.9 (a)), while under anaerobic conditions, biogas, which is a mixture of carbon dioxide and methane, will be formed (Scheme 2.9 (b)). The organic carbon of the material is in both cases also partly converted to new biomass ($C_{biomass}$) and it is possible that some carbon is not converted or remains present under the form of metabolites ($C_{residual}$) (Figure 2.25) [69].

(a) $C_{sample} + O_2 \longrightarrow CO_2 + H_2O + C_{biomass} + C_{residual}$

(b) $C_{sample} \longrightarrow CO_2 + CH_4 + C_{biomass} + C_{residual}$

Scheme 2.9 The biodegradation of carbon under: (a) aerobic conditions; (b) anaerobic conditions.

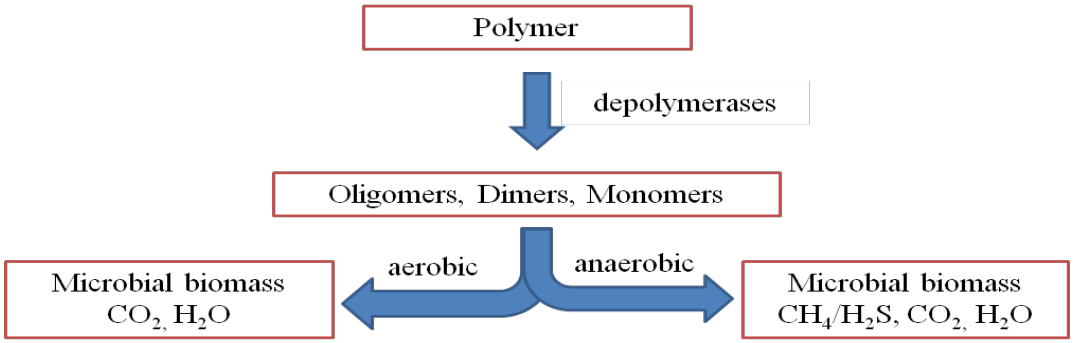

Figure 2.25 Scheme of polymer degradation under aerobic and anaerobic conditions [69].

When the end products are CO_2, H_2O, or CH_4, the degradation is called mineralization (Figure 2.26). It is important to note that bio-deterioration and degradation of polymer substrate can rarely reach 100% and the reason is that a small portion of the polymer will be incorporated into microbial biomass, humus and other natural products. The primary products will be microbial biomass, CO_2, CH_4 and H_2O under methanogenic (anaerobic) conditions e.g. landfills/compost [70].

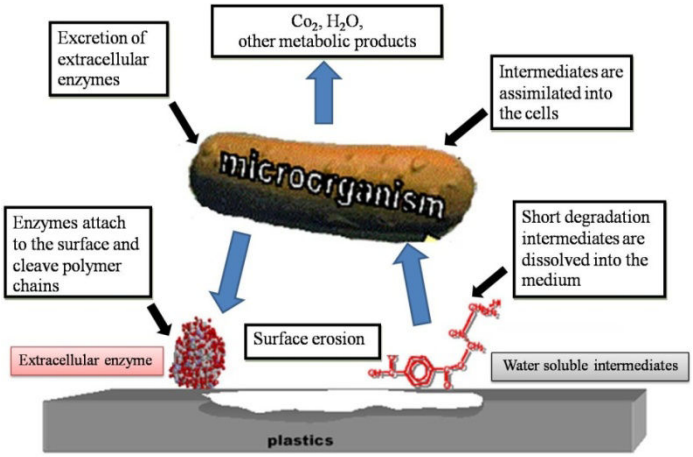

Figure 2.26 Classification of the biodegradable polymers [71].

Bacteria important in the biodegradation process include, *inter alia*, *Bacillus* (capable of producing thick-walled endospores that are resistant to heat, radiation and chemical disinfection), *Pseudomonas*, *Klebsiella*, *Actinomycetes*, *Nocardia*, *Streptomyces*, *Thermoactinomycetes*, *Micromonospora*, *Mycobacterium*, *Rhodococcus*, *Flavobacterium*, *Comamonas*, *Escherichia*, *Azotobacter* and *Alcaligenes* (some of them can accumulate polymer up to 90% of their dry mass) [2, 7-9]. Temperature is one of the most important factors affecting microorganism growth. Also important are sources of carbon and nitrogen, and pH. Fungi active in the biodegradation process are *Sporotrichum, Talaromyces, Phanerochaete, Ganoderma, Thermoascus, Thielavia, Paecilomyces, Thermomyces, Geotrichum, Cladosporium, Phlebia, Trametes, Candida, Penicillium, Chaetomium,* and *Aerobasidium* [8, 10-12].

2.5.2 Biodegradation test

Guidelines for biodegradation test were developed by the Organization for Economic Cooperation and Development (OECD) in 1981. CEN (European committee for standardisation), ISO (International Organization for Standardization) and ASTM (American Society for Testing and Materials) also developed biodegradability testing methods for organic chemicals and also for more complex materials. The major part of these standards is based on the principles of the OECD guidelines [72].

The extent of the biodegradation of degradable plastics is undergoing considerable re-examination. Marine areas, soil, sewage, and composts represent complex biological environments. A large number of microorganisms from different species and genera are present in these environments. These microorganisms display a broad range of polymer-degrading abilities ranging from the complete degradation of a polymer in one environment to the slight degradation of the same polymer in another environment. Consequently, for a biodegradable polymer to be used for a certain application, the polymer should necessarily degrade in the environment of end usage and not necessarily degrade in other environments. For example, biodegradable agricultural mulch films should degrade when they are in contact with soil microorganisms but not necessarily degrade in a marine environment. Therefore, a good method for the evaluation of biodegradability should consider the end usage of the polymer and the environment of end usage. American Standard Testing Methods (ASTM) and the Organization for Economic Cooperation and Development (OECD) have proposed several test methods [72,73].

Testing methods of biodegradable polymers can be subdivided into five categories (i.e. Modified Sturm test, Closed bottle test, Petri dish screen, Environmental chamber method and Soil burial test).

2.5.2.1 Modified Sturm test

The modified Sturm test seems to be the preferred technique for polymeric materials. It has been specified by the Italian authorities for assessing biodegradable polymers and is currently being evaluated by the Biodegradable Plastics Group of the International Biodeterioration Research Group. The test operates under aerobic conditions, the test substance provides the sole source of carbon, it is exposed to a low level of inoculum. The test is run for 28 days without any acclimatization period.

The process of the Sturm method is as follows. To a chemically defined mineral nutrient solution free of organic carbon, the test substance is added at two concentrations (10 and 20 $mg.L^{-1}$). An inoculum of sewage microorganisms is added (1–20 x 10^6 mL^{-1}) to the solution. The test system with suitable controls are incubated at ambient temperatures with stirring for 28 days. The CO_2 evolved is

trapped in alkali and measured as carbonate by either titration or with the use of a carbon analyzer.

After analysis of the data with respect to suitable blank controls the total amount of CO_2 produced by the polymer over the test period is determined and calculated as that percentage of the total CO_2 which the polymer could have theoretically produced based upon its total carbon content. Because a proportion of carbon will be incorporated into biomass, the total CO_2 and hence calculated biodegradation levels can never reach 100%. With this in mind, more realistic levels have been recommended. For a chemical substance to be regarded as readily biodegradable, it should decompose and lose 60% of its initial weigh within 28 days.

2.5.2.2 Closed bottle test

The closed bottle test method is as follows. A predetermined amount of the test substance is added to a chemically defined mineral salt solution. The solution is inoculated with sewage microorganisms and then dispersed into closed bottles. The bottles are incubated in the dark at 20±1 °C and periodically assessed for their dissolved oxygen contents. The oxygen demand is calculated and compared with theoretical or chemical oxygen demand of the test substance. Polymers have to be prepared as finely divided powders and their continuous dispersion in the nutrient solution assured [73].

2.5.2.3 Petri dish screen

This test is used in USA (ASTM), German (DIN), French (AFNOR), Swiss (SN) and international (ISO) standards. The principle of this method involves facing the test material (2.5 x 2.5 cm^2) on the surface of mineral salts agar in a Petri dish containing no additional carbon source. The test material and agar surface are sprayed or painted with a standardized mixed inoculum of known fungi or bacteria. The Petri dishes are sealed and incubated at a constant temperature between 21 and 28 days. The test material is then examined for the amount of growth on its surface. The more growth on the surface, the more likely it is that the material is intrinsically able to support growth and thus the greater the likelihood that it will fail in service. Weight loss, mechanical or electrical tests can all be carried out on the test materials after exposure provided that the correct types of specimen (e.g. dumbbells) have been used in the test.

2.5.2.4 Environmental chamber method

The environmental chamber employs high humidity (90%) situations to encourage microbial (in particular fungal) growth. Strips or prefabricated components of the test materials are hung in the chamber, sprayed with a standard mixed inoculum of known fungi in the absence of additional nutrients and then incubated for 28 to 56 days at a constant temperature. A visual assessment is subsequently made and a rating given based on the amount of growth on the material. This test is particularly stringent and was designed to simulate the effects of high humidity conditions on electronic components and electrical equipment. The growth of fungi across a printed circuit board can result in a gross system failure in a computer system or in military equipment. Such a test is valuable in assessing how biodegradable polymers will perform under such conditions whilst in service.

2.5.2.5 Soil burial test

Tests based upon this methodology evaluate in-service soil contact exposure. The material is buried in soil beds prepared in the laboratory using standard sieved soil; often a commercial soil-based compost. The soil beds are normally conditioned for up to four weeks prior to use and may be supplemented with organic fertilizer to encourage an active microbial flora. The microbial activity is tested using a cotton textile strip which should lose 90% of its tensile strength within 10 days of exposure to the soil. Currently no other reference materials are recommended, although for plastic materials a standard alternative able to demonstrate the degradation capabilities of the microbial flora with respect to plastic should be sought. The soil beds containing the samples are incubated at a constant temperature for between 28 days and 12 months. The moisture content is normally set at 20–30%, although it is better calculated as a percentage (40–50%) of the soil's maximum water holding capacity. This then accounts for different soil structures and ensures that the soil does not become unduly wetted or is too dry for optimal microbial activity. Samples are removed for assessment of changes or a light microscopy and SEM examination to assess surface damage and to look for the presence and nature of microbial growth. Physical factors such as fragmentation and embrittlement can also be assessed in these tests. Finally, the samples can be used to 'bait' microorganisms involved in the degradation process. These microbes once isolated and characterized

can be incorporated into the petri dish screen as alternatives or additions to the current list [73].

2.5.3 Biodegradation of natural rubber

Natural rubber (NR) is a biopolymer that is synthesized by more than 2000 plant species, most of them belong to Euphorbiaceae or Compositaceae, and by some fungi [74]. Natural rubber refers to a coagulated or precipitated product obtained from the milky secretion (latex) of the rubber plants (*Hevea Brasiliensis*), which forms non-linked polymer chains having molecular masses of about 10^6 Da with elastic properties. Latex serves as a clogging material during healing of wounds caused by mechanical injury of plants. Natural rubber consists of C_5H_8 units (isoprene), each containing one double bond in the cis configuration [75]. The microbial susceptibility of natural rubber (NR) either in the raw or in the vulcanized state was sufficiently examined and reviewed. Soil is a rich source of microorganisms, both bacteria and fungi, which can degrade natural as well as synthetic rubbers and utilize them as carbon and energy sources [76]. Several microorganisms were isolated from such experiments, and pure cultures were tested for their rubber degrading potential. Results showed that actinomycetes were almost the only organisms able to considerably decompose NR and to use the rubber hydrocarbon as a carbon source [77,78]. Several serious difficulties hamper investigation of microbial degradation of rubber. Rubber biodegradation is a slow process, and the growth of bacteria utilizing rubber as a sole carbon source is also slow. Therefore, incubation periods extending over weeks or even months are required to obtain enough cell mass or degradation products of the polymers for further analysis. This is particularly true for members of the clear-zone forming group. Periods of 10-12 weeks have to be considered for *Streptomyces coelicolor* 1A [74], *Thermomonospora curvata* E5 [79], or *Streptomyces* sp. strain K30; the only exception is *Xanthomonas* sp. strain 35Y [80]. Although members of the non-clear-zone-forming group exhibit slightly faster growth, cultivation periods of at least 4-6 weeks are also required for *Gordonia westfalica* [81] and *Bacillus* sp. S-10 [82] to determine whether a putative mutant is able to grow on the polymer.

2.5.3.1 Natural rubber degrading bacteria

Many bacterial strains that are able to utilize rubber as the sole source of carbon and energy, have been described during the last hundred years [75,83]. These bacteria can be divided into two groups, which follow different strategies to degrade rubber. Members of the first group form translucent halos if they are cultivated on solid media containing dispersed latex particles, indicating the excretion of rubber cleaving enzymes. The most potent representatives in this group belong to actinomycetes from *Actinoplanes, Streptomyces,* and *Micromonospora* [76]. Members of the second group do not form halos and do not grow on latex plates; they require direct contact with the polymer. They grow adhesively at the surface of rubber particles in liquid culture, and they represent the most potent rubber degrading bacterial strains. This group comprises mycolic acid containing *Actinobacteria* belonging to the genera *Gordonia, Mycobacterium*, and *Nocardia*. Some new rubber-degrading strains belonging to the *Corynebacterium*, *Nocardia, Mycobacterium* group, such as *Gordonia polyisoprenivorans* strains VH2 and Y2K, G. *westfalica* strain Kb1, and *Mycobacterium fortuitum* strain NF4, were isolated [84]. All rubber-degrading species described so far are mesophilic species, with only one exception, identified as a *Streptomyces* sp. closely related to *Streptomyces albogriseolus* and *Streptomyces viridodiastaticus*, which was able to grow at temperatures up to 50 °C and belong to the so-called clear zone forming group of rubber degrading bacteria. The author has reported on the existence of holes in the rubber material, beneath the adhering *Actinomycetes* colonies, both in liquid mineral culture and on agar plates coated by purified NR films, and concluded that under these conditions increase in biomass could only have taken place at the expense of the rubber hydrocarbon. A new rubber degrading strain *Bacillus* sp. AF 666, was isolated through enrichment and NR latex overlay (latex film plates) in the author's laboratory [85]. One disadvantage of latex overlay agar plates is that all rubber degrading bacteria cannot be cultivated in this way, because most of them do not form halos on agar plates. Besides this, a very small amount of polyisoprene is locally available to allow formation of visible colonies by these organisms.

2.5.3.2 Natural rubber degrading fungi

Kwiatkowska et al. [86] performed soil burial tests of NR vulcanized sheets of definite composition and detected substantial weight losses reaching up to 40% of the initial weight after 91 days. These authors isolated a fungal strain *Fusarium solani* from the surface of rubber and claimed its degradation by this strain. In a study by Williams in 1982, the author isolated a fungal strain, *Penicillium variabile* from deteriorated NR sample after soil burial. Spore suspensions inoculated on to NR smoked sheet in a humidity cabinet led to a successive increase of biomass on the NR surface, as shown by cell protein determination every 14 days, and was accompanied by a weight loss of rubber strips up to 13% after 56 days. However, further increase in biomass and in weight loss beyond this time period could not be determined. Using solution viscosity measurement as analytical tool, the author estimated a 15% reduction in the molecular weight of polyisoprene after 70 days [87]. Several rubber deteriorating fungi were isolated from mineral agar plates containing powdered NR as sole substrate and also from the surface of deteriorated tire material. The fungal strains *F. solani*, *Cladosporium cladosporioides* and *Paecilomyces lilacinus* were grown on the surface of rubber after 20 days of incubation. Using GPC, a relative reduction of the molecular weight up to 20% was detected and even a decrease in intrinsic viscosity up to 35% [84]

2.5.3.3 Biodegradation process for reclaiming of rubber

Biological attack of natural rubber latex is quite facile. But addition of sulphur and numerous other ingredients to rubber reduces biological attack. A recent approach was to utilize a chemolithotrope bacteria in aqueous suspension for attacking powder elastomers on the surface only, so that after mixing with virgin rubber diffusion of soluble polymer chains is facilitated and bonding during vulcanization becomes again possible.

The biodegradation of the *cis*-1, 4-polyisoprene chain was achieved by a bacterium belonging to the genus *Nocardia,* leading to considerable weight loss of different soft types of NR vulcanizates. The microbial desulphurization or devulcanization of particle surfaces was investigated in order to increase the possibility of producing high quality rubber products containing a larger percentage of recycled rubber. Old tires with 1.6% sulphur were treated with different species of

Thiobacillus ferrooxidans, *T. thiooxidans*, *T. thioparus* in shaked flasks and in a laboratory reactors. The sulphur oxidation depends to a large extent on the particle size. The best results were obtained with *T. thioparus* with a particle size of 100-200 mm. 4.7% of the total sulphur of the rubber powder was oxidized to sulphate within 40 days [88].

2.5.4 Biodegradation of polycaprolactone

The biodegradation of PCL occurs relatively slowly and the rate of degradation ranges from several months to several years, depending on the molecular weight and crystallinity of the polymer and the conditions of degradation. The degradation of PCL produces various acidic, low molecular weight products such as succinic acid, butyric acid, valeric acid and hexanoic acid [89]. Investigation into the mechanism of *in vivo* PCL degradation suggested that the process was attributed to random hydrolytic chain scission of the ester linkages, potentially due to the OH radical formation [90]. The hydrolytic degradation of PCL was autocatalysed by carboxylic acids generated during hydrolysis and took place in two stages, beginning with a drop in the molecular weight while retaining the mass and shape, then followed with the fragmentation of the polymer and mass loss when the molecular weight reaches 5000 [33]. Hydrolytic degradation was highly dependent on polymer crystallinity and hydrophilicity, with low crystallinity and high hydrophilicity accelerating the polymer degradation rate due to increased water penetration [33].

Biodegradation of PCL can also occur by an enzymatic mechanism. Enzymatic degradation took place by surface erosion, with a preferential attack of the amorphous regions prior to crystalline regions. Lipase was the best characterized enzyme for PCL biodegradation. Lipase produced by microorganisms such as *Rhizopus delemer*, *Rhizopus arrhizus* and *Pseudomonas* have been shown to be effective at degrading PCL [91], while porcine pancreatic lipase and *Candida cylindracea* lipase had no effect [33]. Enzymatic degradation took effect faster than hydrolytic degradation. PCL microparticles exhibit pores and channels on the surface after 9 weeks of *in vitro* degradation with lipase, while, without the presence of lipase, no significant change was observed [92]. Similarly, PCL networks were shown to degrade faster through enzymatic degradation than hydrolysis, with an 18% mass loss measured within 14 weeks with lipase, while it took 60 weeks to reach a similar mass loss in the absence of lipase [93].

2.5.5 Biodegradation of polyurethane

Urethane bond produced by the diisocyanate poly addition process is the characteristic chain link of Polyurethane. Growth of microorganisms could not be supported by PU and so the biodegradation was also found incomplete. PU degradation proceeded in a selective manner, with the amorphous regions being degraded prior to the crystalline regions. Also, PU's with long repeating units and hydrolytic groups would be less likely to pack into high crystalline regions as normal polyurethane, and these polymers were more accessible to biodegradation [88].

The PU *depolymerases* of the microorganisms have not been examined in detail, although due to the presence of ester linkage most degradation is carried out by *esterases*. *Comamonas acidovorans* TB-35 utilized a polyester PU containing polydiethyleneglycol adipate as the sole source of carbon but not the polyether PU. Polyester PU degradation by *porcine pancreatic elastase* was ten times faster than its activity against polyether PU [88]. *C. acidovorans* canned completely degraded 50 mg of PU dissolved in mineral salt medium at 303 K. The products of degradation were adipic acid and diethylene glycol. Absence of any metabolites confirmed that urethane linkage was not cleaved [88].

The degradation of PU is inhibited by the presence of a detergent that does not inhibit the hydrolysis of a water-soluble ester compound, suggesting that degradation proceeded via a two-step mechanism namely,

1. Hydrophobic adsorption to the polymer surface, followed by
2. Hydrolysis of the ester bond of PU.

The deduced protein sequence contained a signal sequence, the lipase box and catalytic triad, and three hydrophobic domains, which played a role in the hydrophobic adsorption of the enzyme to the polymer surface. It was found that two proteolytic enzymes, *papain* and *urease* degraded medical polyester PU [94]. Bacteria like *Corynebacterium* sp. and *Pseudomonas aeruginosa* could degrade PU in the presence of basal media [95]. Several fungi are observed to grow on PU surfaces and especially *Curvularia senegalensis* was observed to have a higher PU degrading activity. Although cross linking was considered to inhibit degradation, *papain* was found to diffuse through the film and broke the structural integrity by hydrolyzing the urethane and urea linkage producing free amine and hydroxyl group.

2.5.6 The related publications

Demirtas *et al.* [96] studied the biodegradability of a polyurethane foam under anaerobic conditions. The experimental protocols for the assessment of PU biodeterioration included bioavailability assays using batch shake-flask and soil reactors, continuous flow soil and sludge bioreactors, analytical and physical measurements of PU deterioration. The microbial deterioration of PU was investigated by measuring the physical properties (weight loss, tensile strength) of PU plugs before and after bioassays, chemical structure measurements using Fourier transform infrared spectroscopy (FTIR) and measurement of growth of microorganisms (microbial counts). The experimental results have shown that the studied PU foam is likely not biodegradable under anaerobic conditions. Neither weight loss nor a change in the tensile strength of the PU material after biological exposure was observed. The Fourier transform infrared spectroscopy chemical signature of the PU foams was also nearly identical before and after biological exposure. The composition of the PU material (aromatic polyester and polyether PU) used in this study could have played a significant role in its resistance to microbial attack during the short-term accelerated experiments.

Gorna and Gogolewski [97] prepared linear biodegradable polyurethanes with varying ratios of the hydrophilic-to-hydrophobic segment. The hydrophilic segment was based on poly(ethylene oxide-propylene oxide-ethylene oxide) diols (Pluronic®). The hydrophobic segment was based on poly(ε-caprolactone) diol. Viscosity-average molecular weights and the polydispersity index of the polyurethanes were in the range of 38,000–85,000 daltons and 1.2–3.2, respectively. Polymers absorbed 3.9% of water depending on the chemical composition. The tensile strength, the Young's modulus and the elongation at break of polymers were in the range of 11–46 MPa, 4.5–91 MPa and 370–960%, respectively. The glass transition and the soft segment melting temperatures were -60 to -21.5°C and 30–55°C, respectively. Degradation in vitro caused 2% mass loss, 15–80% reduction of molecular weight and slight reduction of polydispersity at 48 weeks. The extent of degradation was dependent on the polymer composition and the hydrophilic segment content. At a comparable degradation time the materials containing Pluronic® were degraded most. Degradation of polyurethanes caused insignificant changes of the pH of the medium.

2.6 Characterizations

2.6.1 Mechanical properties

2.6.1.1 Tensile testing

Tensile tests are performed for several reasons. The results of tensile tests are used in selecting materials for engineering applications. Tensile properties frequently are included in material specifications to ensure quality, often measured during development of new materials and processes, so that different materials and processes can be compared, and often used to predict the behavior of a material under forms of loading other than uniaxial tension [98]. A tensile specimen is shown in Figure 2.27.

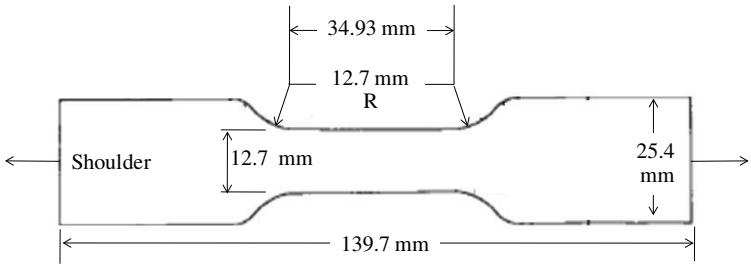

Figure 2.27 Typical tensile specimen, showing a reduced gage section and enlarged shoulders (ASTM D 3574 Test E).

A tensile test involves mounting the specimen in a machine and subjecting it to tension. The tensile stress (σ) and the strain (ε) are defined in equation (2.1) and (2.2), respectively.

$$\sigma = \frac{F}{A_0} \qquad (2.1)$$

$$\varepsilon = \frac{\Delta L}{L_0} \qquad (2.2)$$

Where F is the tensile force and A_0 is the initial cross-sectional area of the gage section. L_0 is the initial gage length and ΔL is the change in gage length ($L-L_0$). When a solid material is subjected to small stresses, the bonds between the molecules are stretched. When the stress is removed, the bonds relax and the material returns to its original shape. This reversible deformation is called elastic deformation. At higher stresses, planes slide over one another. This deformation, which is not recovered when the stress is removed, is termed plastic deformation. For most

materials, the initial portion of the curve is linear. The slope of this linear region is called the elastic modulus or Young's modulus (E) as shown in equation (2.3).

$$E = \frac{\sigma}{\varepsilon} \qquad (2.3)$$

The stress-strain curves of tensile test are shown in Figure 2.28. The tensile strength (ultimate strength) is defined as the highest value of engineering stress. Up to the maximum load, the deformation should be uniform along the gage section. With ductile materials, the tensile strength corresponds to the point at which the deformation starts to localize, forming a neck (Figure 2.28a). Less ductile materials fracture before they neck (Figure 2.28b). In this case, the fracture strength is the tensile strength. Indeed, very brittle materials do not yield before fracture (Figure 2.28c). Such materials have tensile strengths but not yield strengths.

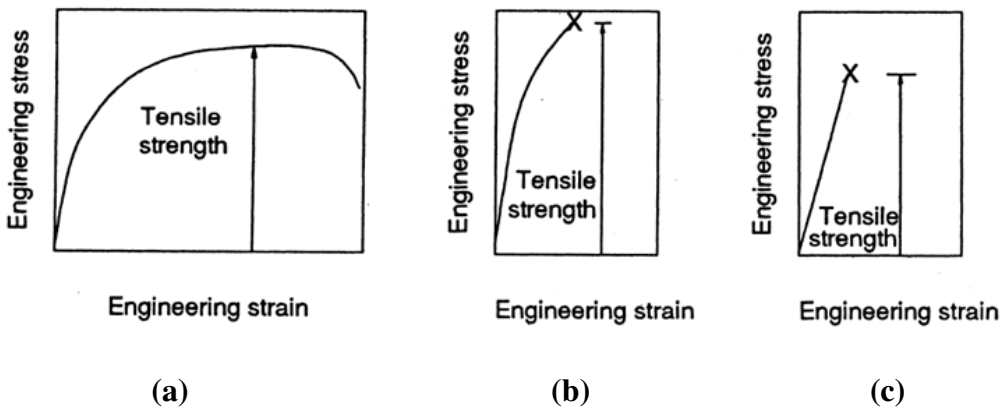

Figure 2.28 Stress-strain curves of (a) ductile, (b) semi-ductile and (c) brittle materials [98].

2.6.1.2 Compression testing

The mechanical behavior of solid foams under compressive loading is probably the primary property that distinguishes them from non-cellular solids. Typical stress-strain curves for solid foams made from three different kinds of solid materials can be distinguished: elastomeric foams, elastic-plastic foams and elastic-brittle foams. They all have similar characteristics i.e. linear elasticity at low stresses, followed by an extended plateau terminating in a regime of densification, whereby the stress rises steeply. These characteristics are different from those of common solid materials such as metals, which normally do not have an extended stress-strain plateau under compression [99].

In all the three types of solid foam, initial linear elasticity arises primarily from the bending of cell struts, and in closed cell foams, stretching of the membranes in the cell walls and changes in fluid pressure inside the cells. On the other hand, the mechanisms corresponding to the stress-strain plateau are different for the three types of foam – elastic buckling for elastomeric foams, formation of plastic hinges in elastic-plastic foams and brittle crushing in elastic-brittle foams.

The long plateau in the compressive stress-strain curve endows foams with a very high compressibility and enables them to exert a relatively constant stress up to a very high strain. These two characteristics make foam an ideal material for cushioning purposes because the low and constant stress contribute to comfort and for crash protection (e.g. in helmets), because the foam is able to absorb kinetic energy while limiting the stress transmitted to relatively low levels.

Compression set tests are intended to measure the ability of rubber compounds to retain elastic properties after longed action of compressive stresses. The actual stressing service may involve the maintenance of a definite deflection, the constant application of a known force, or the rapidly repeated deformation and recovery resulting from intermittent compressive forces. Though the latter dynamic stressing, like the others, produces compression set, its effects as a whole are simulated more closely by compression flexing or hysteresis tests. Therefore, compression set tests are considered to be mainly applicable to service conditions involving static stresses. Tests are frequently conducted at elevated temperatures.

2.6.2 Thermal gravimetric analysis (TGA)

TGA is an analytical technique used to determine a material's thermal and/or oxidative stabilities and its fraction of volatile components by monitoring the weight change that occurs as a specimen is heated. Figure 2.29 shows an example of thermobalance. The measurement is normally carried out in air or in an inert atmosphere, such as Helium (He) or Argon (Ar), and the weight is recorded as a function of increasing temperature. The measurement is performed in a lean oxygen atmosphere (1-5% O_2 in N_2 or He) to slow down oxidation. The TGA and derivative thermogravimetric analysis (DTG) curves generally are plotted between mass and temperature, as illustrated in Figure 2.30. The TGA curve shows the plateau of constant weight (region A), the mass loss portion (region B), and another plateau of constant mass (region C) [100].

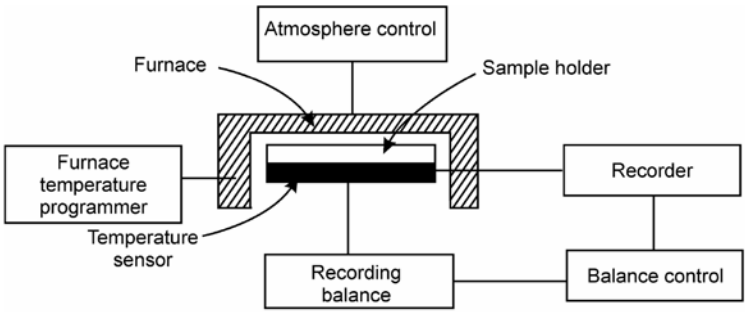

Figure 2.29 TGA diagram of a thermobalance [101].

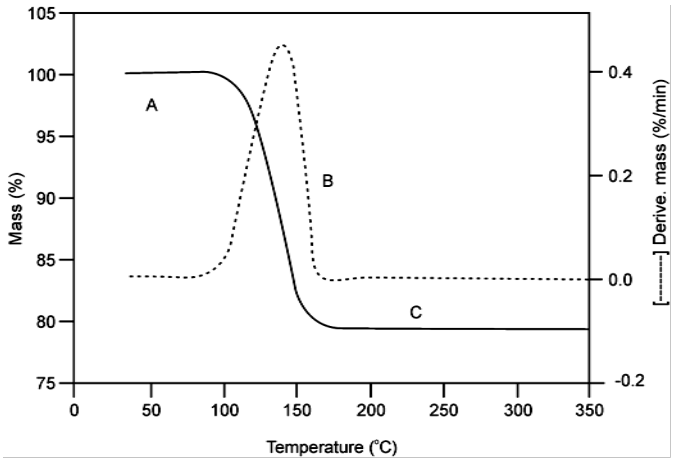

Figure 2.30 Typical TGA and DTG curves [102].

2.6.3 Nuclear magnetic resonance spectroscopy (NMR)

NMR is a technique that exploits the magnetic properties of certain atomic nuclei. The basic arrangement of an NMR spectrometer is shown in Figure 2.31. When placed in the magnetic field of NMR, active nuclei (e.g. ^{1}H, ^{13}C) absorb electromagnetic radiations at a frequency characteristic of the isotope. The resonant frequency, the energy of the absorption, and the intensity of the signal are proportional to the strength of the magnetic field. Any motion of a charged particle has an associated magnetic field, meaning a magnetic dipole is created, just like an electrical current in a loop creates a magnetic dipole, which in a magnetic field corresponds to a magnetic moment μ (Figure 2.32) [103]. The operation gives a locator number called the Chemical Shift, having units of parts per million (ppm), and designated by δ symbol. ^{1}H-NMR provides information related to the molecular structure. This is particularly important for copolymers where such information may, for example, help to determine reactivity ratios and, for vinyl polymers, can give an immediate indication of the presence of unreacted monomer.

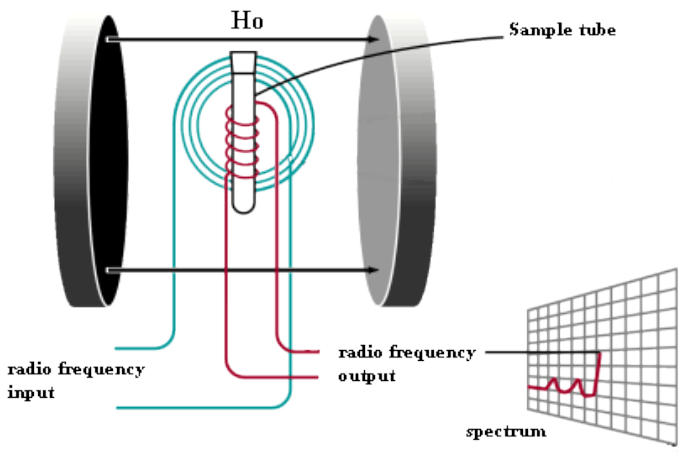

Figure 2.31 The basic arrangement of NMR spectrometer [103].

Figure 2.32 A spinning nucleus can be regarded as a microscopic magnet [103].

2.6.4 Fourier transform infrared spectroscopy (FTIR)

Infrared spectroscopy (IR) is the most important of vibrational spectroscopies. It is used for the determination and identification of molecular structure. IR and Raman spectroscopy are complementary techniques. Generally, IR spectroscopy is used for a measurement of the asymmetric vibrations of polar groups while Raman spectroscopy is suitable for the symmetric vibrations of non-polar groups [104]. The schematic diagram of the optical layout of IR spectrometer is shown in Figure 2.33. In the IR active mode an oscillating electric dipole moment in polymeric molecules must take place. Figure 2.34 expresses the modes of vibration of the bonds and IR activities. The plus and minus signs indicate the partial charges on atoms and the arrows means the direction of motion [105].

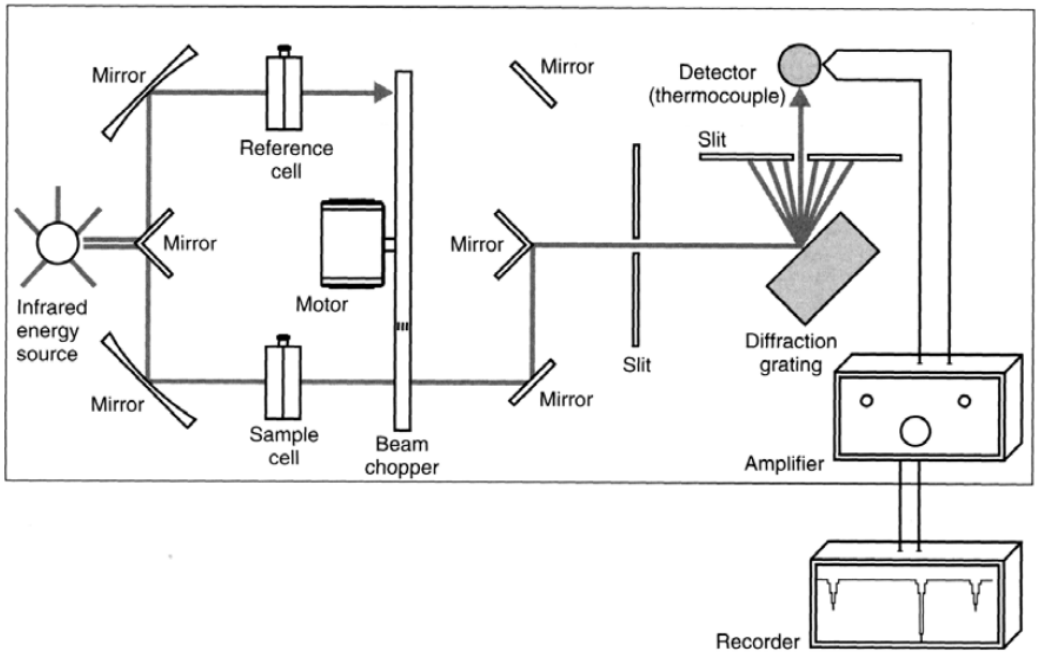

Figure 2.33 Schematic diagram of the optical layout of IR spectrometer [104].

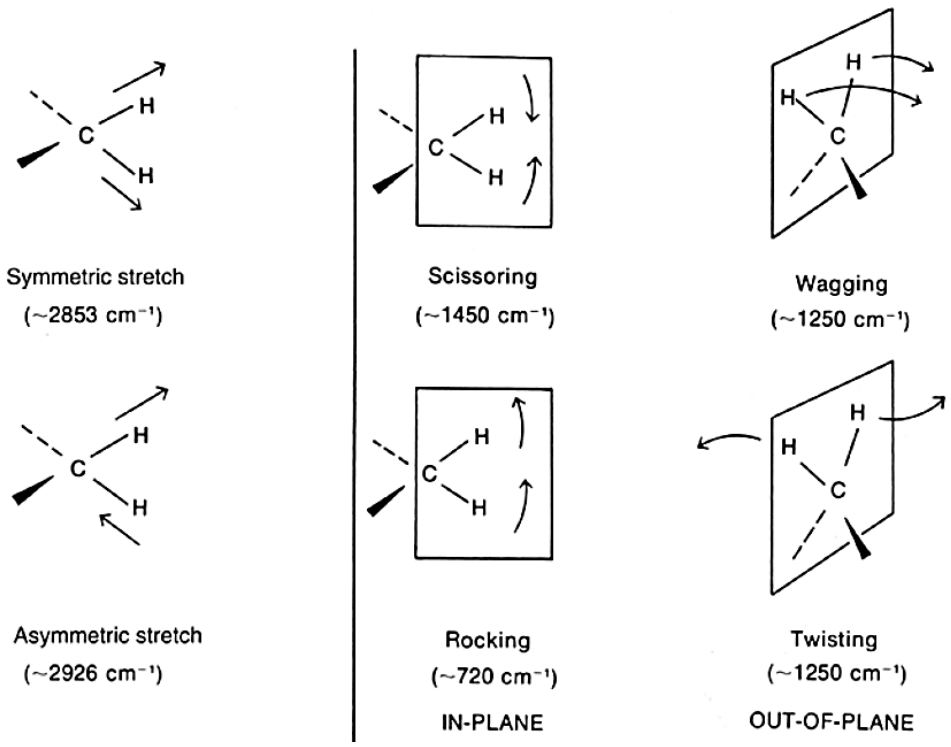

Figure 2.34 Stretching and bending vibrational modes for a CH_2 group [106].

2.6.5 Scanning electron microscope

The scanning electron microscope uses a focused beam of high-energy electrons to generate a variety of signals at the surface of solid specimens. The signals that derive from electron sample interactions reveal information about the sample including surface morphology, chemical composition, crystalline structure and orientation of materials making up the sample. In most applications, data are collected over a selected area of the surface of the sample, and a 2-dimensional image is generated that displays spatial variations in these properties. When the primary electron enters a specimen it travels some distance into the specimen before hitting a particle. After hitting an electron or a nucleus, etc., the primary electron will continue on in a new trajectory. This is known as scattering. It is the scattering events that are most interesting, because it is the components of the scattering events (not all events involve electrons) that can be detected. The result of the primary beam hitting the specimen is the formation of a teardrop shaped reaction vessel as shown in Figure

2.35 [107]. The brightness of the signal depends on the number of secondary electrons reaching the detector. If the beam enters the sample perpendicular to the surface, then the activated region is uniform about the axis of the beam and a certain number of electrons "escape" from within the sample. As the angle of incidence increases, the "escape" distance of one side of the beam will decrease, and more secondary electrons will be emitted. Thus steep surfaces and edges tend to be brighter than flat surfaces, which results in images with a well-defined, three-dimensional appearance. Using the signal of secondary electrons image resolution less than 0.5 nm is possible.

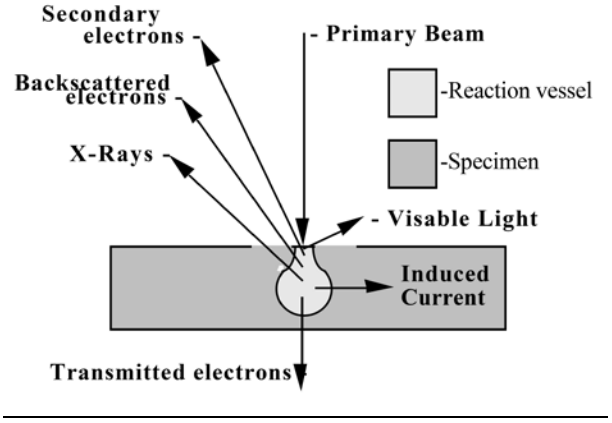

Figure 2.35 Diagram of electron beam and specimens [107].

2.6.6 Gel permeation chromatography (GPC)

Gel permeation chromatography (GPC), a type of size exclusion chromatography (SEC), is a technique that employs porous non-ionic gel beads to separate polymers in solution. Beads containing pores of various sizes and distributions are packed into a column in GPC. Such beads are commonly made of glass or cross-linked polystyrene. A solvent is pumped through the column and then a polymer solution in the same solvent is injected into the column. Fractionation of the polymer sample results as different-sized molecules are eluted at different times. Fractionation of molecules in GPC is governed by hydrodynamic volume rather than by molecular weight. The largest polymers in the solution cannot penetrate the pores within the cross-linked gel beads, so they will elute first as they are excluded and their retention volume is smaller. The smallest polymer molecules in the solution are

retained in the interstices (or the voids) within the beads, and so require more time to elute and their retention volume is bigger (Figure 2.36) [105].

The resulting chromatogram is therefore a weight distribution of the polymer as a function of retention volume or retention time. In order to obtain a molecular weight distribution, the column must be calibrated by using fractions of known molecular weight so to relate molecular weight to the eluted volume. Commercially available PS samples with narrow molecular weight distributions are often used as calibration standards. A calibration curve is produced by plotting the logarithm of molecular weight versus the elution volume as illustrated in Figure 2.37.

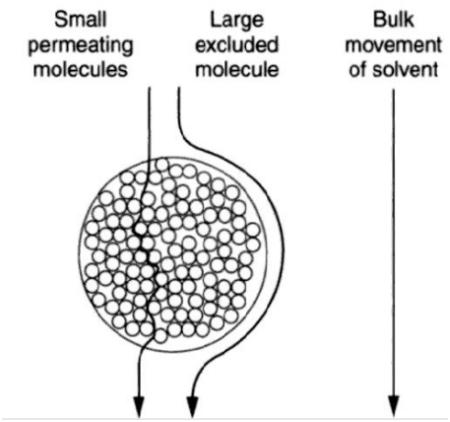

Figure 2.36 Illustration of the separation of polymer molecules of different sizes [105].

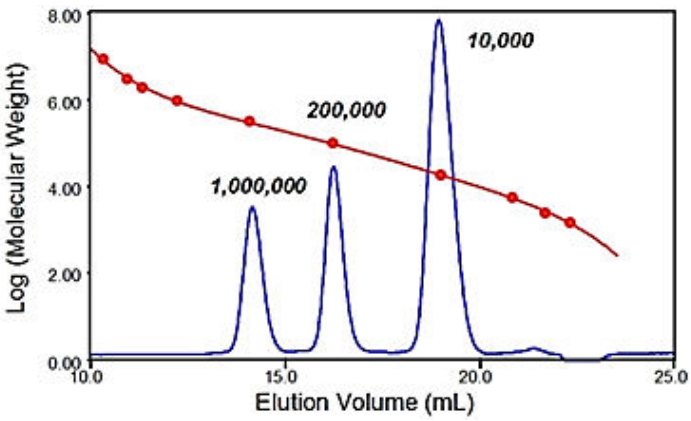

Figure 2.37 The general form of a calibration curve and chromatogram of different sizes of polymer [108].

2.7 References

1. Uraneck, C.A., Hsieh, H.L. and Buck, O.G. 1960. Telechelic Polymers. Journal of polymer science. 16: 535-539.
2. Nor, H.M. and Ebdon, J.R. 1998. Telechelic liquid natural rubber: A review. Progress in Polymer Science. 23: 143-177.
3. Tangpakdee, J., Mizokoshi, M., Endo, A. and Tanaka, Y. 1998. Novel method for preparation of low molecular weight natural rubber latex. Rubber Chemistry and Technology. 71(4): 795-802.
4. Cunneen, J.I. 1973. Research and the improvement of trie performance. NR Technology. 4: 65.
5. Ravindran, T., Nayar, M.R.G. and Francis, J.D. 1986. A novel method for the preparation of hydroxyl terminated liquid natural rubber. Die Makromolekulare Chemie, Rapid Communications. 7(3): 159-163.
6. Gupta, S.K., Kurup, M.R., Devadoss, E., Muthiah, R. and Thomas, S. 1985. Development and evaluation of a novel binder based on natural rubber and high-energy polyurethane/composite propellants. Journal of Applied Polymer Science. 30(3): 1095-1112.
7. Burfield, D.R. and Gan, S.N. 1977. Determination of epoxy groups in natural rubber by degradation methods. Polymer. 18(6): 607-611.
8. Reyx, D. and Campistron, I. 1997. Controlled degradation in tailor-made macromolecules elaboration. Controlled chain-cleavages of polydienes by oxidation and by metathesis. Die Angewandte Makromolekulare Chemie. 247(1): 197-211.
9. Mauler, R.S., Guaragna, F.M., Gobbi, D.L. and Samios, D. 1997. Sonochemical degradation of 1,4-cis-polyisoprene using periodic acid-solvent and temperature effect European Polymer Journal. 33(3): 399-402.
10. Phinyocheep, P., Phetphaisit, C.W., Derouet, D., Campistron, I. and Brosse, J.C. 2005. Chemical degradation of epoxidized natural rubber using periodic acid: Preparation of epoxidized liquid natural rubber. Journal of Applied Polymer Science. 95(1): 6-15.

11. Gillier-Ritoit, S., Reyx, D., Campistron, I., Laguerre, A. and Pal Singh, R. 2003. Telechelic cis-1,4-oligoisoprenes through the selective oxidolysis of epoxidized monomer units and polyisoprenic monomer units in cis-1,4-polyisoprenes. Journal of Applied Polymer Science. 87(1): 42-46.
12. Thanki, P.N., Reyx, D., Campistron, I., Laguerre, A. and Singh, R.P. 2004. Metathetic alkenolysis of unsaturated units in polymers and copolymers—application to the synthesis of epoxy-functionalized oligomers and organic compounds. European Polymer Journal. 40(11): 2611-2616.
13. Marmo, J.C. and Wagener, K.B. 1993. Acyclic diene metathesis (ADMET) depolymerization. Synthesis of mass-exact telechelic polybutadiene oligomers. Macromolecules. 26(8): 2137-2138.
14. Solanky, S.S., Campistron, I., Laguerre, A. and Pilard, J.-F. 2005. Metathetic selective degradation of polyisoprene: Low-molecular-weight telechelic oligomer obtained from both synthetic and natural rubber. Macromolecular Chemistry and Physics. 206(10): 1057-1063.
15. Pilard, J.F., Campistron, I., Sadaka, F. and Laguerre, A. 2011. Method for preparing telechelic oligomers from tire waste. WO 2011101551 A1, August 25.
16. De, S.K., Isayev, A.I. and Khait, K. 2005. Rubber recycling. CRC Press Taylor & Fancis. United state of america 131-134.
17. Cardy, B. 2011. Independent news & technical information for the auto industry. http://www.autoindustryinsider.com/?p=1371 (accessed 15/02/2016)
18. Frederick, J.S. Tyre Manufacturing. 2011 [updated; cited]. Available from: http://www.iloencyclopaedia.org/component/k2/131-80-rubber-industry/tyre-manufacturing (accessed 12/26/2015).
19. Peralta, E.J.F. 2009. Study of the interaction between bitumen and rubber. Master Thesis in Civil Engineering, School of engineering, University of Minho, Portugal.
20. Kaster & Falvey, P.A. Tire Manufacturing Processes. http://tirefailures.com/PDF_vf/whitepaper.pdf (accessed 15/02/2016).
21. Carne, P.C. 2009. Study of compatibilization methods for High Density Polyethylene and Ground Tyre Rubber: Exploring new routes to recycle scrap

tyres. Ph.D. Thesis, Department of Chemical Engineering , University of Catalonia, Barcelona, Spain

22. Rahman, M. 2004. Characterisation of dry process crumb rubber modified asphalt mixtures. Ph.D. Thesis. School of civil engineering, University of nottingham, United Kingdom.
23. Karger-Kocsis, J., Mészáros, L. and Bárány, T. 2013. Ground tyre rubber (GTR) in thermoplastics, thermosets, and rubbers. J Mater Sci. 48(1): 1-38.
24. CalRecycle. 2016. Tire-Derived Product (TDP) Descriptions and Case Studies. http://www.calrecycle.ca.gov/tires/products/Feedstock/default.htm (accesses 15/02/2016).
25. Shulman, V.L. 2011. Chapter 21 - Tyre recycling. In: Waste. Letcher, T. and Vallero, D., Ed. Academic Press: Boston. p. 297-320.
26. Shercom Industries. 2015. Tire derived aggregate (Tire Shred). http://www.shercomindustries.com/tireshred (accesses 15/02/2016).
27. RETIRE ABEE. 2009. Products - Rubber granulates in various granulations. http://www.dkretire.gr/en/products/?m=1 (accessed 15/02/2016).
28. Rafique, R.M.U. 2012. Life Cycle Assessment of Waste Car Tyres at Scandinavian Enviro Systems. Master of Science Thesis, Department of Chemical and Biological Engineering, Chalmers University of Technology, Göteborg, Sweden.
29. Sadaka, F., Campistron, I., Laguerre, A. and Pilard, J.-F. 2012. Controlled chemical degradation of natural rubber using periodic acid: Application for recycling waste tyre rubber. Polymer Degradation and Stability. 97(5): 816-828.
30. Perrin, D.E. and English, J.p. 1997. Polycaprolactone. Overseas publisher association, Amsterdam
31. Thomas, S.M., DiCosimo, R. and Nagarajan, V. 2002. Biocatalysis: applications and potentials for the chemical industry. Trends in Biotechnology. 20(6): 238-242.
32. Labet, M. and Thielemans, W. 2009. Synthesis of polycaprolactone: a review. Chemical Society Reviews. 38(12): 3484-3504.

33. Daud, M.F. 2013. An organized 3D in vitro model for peripheral nerve studies. Ph.D. Thesis, Department of Material Science and Engineering, University of Sheffield, United Kingdom.
34. Mahapatro, A., Kumar, A. and Gross, R.A. 2004. Mild, solvent-free ω-hydroxy acid polycondensations catalyzed by candida a ntarctica Lipase B. Biomacromolecules. 5(1): 62-68.
35. Kaushiva, B.D. 1999. Structure-property relationships of flexible polyurethane foams. Ph.D. Thesis, Virginia Polytechnic Institute and State University, Blacksburg, Virginia, United States.
36. Gayathri, R. 2013. Studies on polyurethane and its hybrid foams with micro and nano fillers for low frequency sound absorption. Master of technology thesis, Department of Polymer Engineering, BS Abdur Rahman University, Vandalur, Chennai, India.
37. Saetung, A. 2009. Preparation of Polyurethane Foams from Hydroxytelechelic Oligoisoprenes Obtained by Controlled Degradation of Natural Rubber: Study of Their Physico-mechanical, Thermal, and Acoustic Properties. PhD Thesis, Prince of Songkla University, Pattani, Thailand and University of Maine, France.
38. The essential chemical industry online. 2013. Polyurethanes. http://www.essentialchemicalindustry.org/polymers/polyurethane.html (accesses 16/02/2016).
39. Klempner, D. and Sendijarevic, V. 2004. Handbook of polymeric foams and foam technology. 2nd Hanser publishers: Munich
40. TU, Y.-C. 2008. Polyurethane foams from novel soy-based polyols. PhD Thesis, Faculty of the Graduate School, University of Missouri, Jesse Hall, Columbia.
41. Boustead, I. 2005. Eco-profiles of the European Plastics Industry: Polyols. Brussels.
42. Sin, L.C. 2008. Rigid and flexible polyurethane foams production from palm oil-based polyol. PhD Thesis. University of malaya, Kuala lumpur: Malaysia.
43. Szycher, M. 1999. Szycher 's handbook of polyurethanes. CRC Press: Florida.
44. Yee, K.K. 2005. Aqueous polyurethane dispersion with non-yellowing and good bonding strength for water borne polyurethane footwear adhesives

applications. Master of science thesis, Department of chemistry, National university of singapore, Singapore

45. Daga, P. 2009. Polyurethane. http://www.scribd.com/doc/17492117/Polyurethane#scribd (acessed 17/02/2016).
46. Kim, S.H., Kim, B.K. and Lim, H. 2008. Effect of isocyanate index on the properties of rigid polyurethane foams blown by HFC 365mfc. Macromolecular research. 16(5): 467-472.
47. Verdejo, R., Stämpfli, R., Alvarez-Lainez, M., Mourad, S., Rodriguez-Perez, M.A., Brühwiler, P.A. and Shaffer, M. 2009. Enhanced acoustic damping in flexible polyurethane foams filled with carbon nanotubes. Composites Science and Technology. 69(10): 1564-1569.
48. Araújo, R.C.S., Pasa, V.M.D. and Melo, B.N. 2005. Effects of biopitch on the properties of flexible polyurethane foams. European Polymer Journal. 41(6): 1420-1428.
49. Stirna, U., Sevastyanova, I., Misane, M., Cabulis, U. and Beverteb, I. 2006. Structure and properties of polyurethane foams obtained from rapeseed oil polyols. Proceedings of the estonian academy of sciences chemistry. 55: 101-110.
50. Wang, H. and Chen, H.-Z. 2007. A novel method of utilizing the biomass resource: Rapid liquefaction of wheat straw and preparation of biodegradable polyurethane foam (PUF). Journal of the Chinese Institute of Chemical Engineers. 38(2): 95-102.
51. Tanaka, R., Hirose, S. and Hatakeyama, H. 2008. Preparation and characterization of polyurethane foams using a palm oil-based polyol. Bioresource Technology. 99(9): 3810-3816.
52. Wang, T.P., Li, D., Wang, L.J., Yin, J., Chen, X.D. and Mao, Z.H. 2008. Effects of CS/EC ratio on structure and properties of polyurethane foams prepared from untreated liquefied corn stover with PAPI. Chemical Engineering Research and Design. 86(4): 416-421.
53. Hakim, A.A., Nassar, M., Emam, A. and Sultan, M. 2011. Preparation and characterization of rigid polyurethane foam prepared from sugar-cane bagasse polyol. Materials Chemistry and Physics. 129(1–2): 301-307.

54. Tan, S., Abraham, T., Ference, D. and Macosko, C.W. 2011. Rigid polyurethane foams from a soybean oil-based Polyol. Polymer. 52(13): 2840-2846.
55. Saetung, A., Rungvichaniwat, A., Campistron, I., Klinpituksa, P., Laguerre, A., Phinyocheep, P., Doutres, O. and Pilard, J.-F. 2010. Preparation and physico-mechanical, thermal and acoustic properties of flexible polyurethane foams based on hydroxytelechelic natural rubber. Journal of Applied Polymer Science. 117(2): 828-837.
56. Heijkants, R.G.J.C., Calck, R.V., Tienen, T.G., Groot, J.H., Buma, P., Pennings, A.J., Veth, R.P.H. and Schouten, A.J. 2005. Uncatalyzed synthesis, thermal and mechanical properties of polyurethanes based on poly(ε-caprolactone) and 1,4-butane diisocyanate with uniform hard segment. Biomaterials. 26(20): 4219-4228.
57. Liu, C., Qian, Z., Gu, Y., Fan, L., Li, J., Chao, G., Jia, W. and Tu, M. 2006. Synthesis, characterization, and thermal properties of biodegradable aliphatic copolyester based on caprolactone, adipic acid, and 1,6-hexanediol. Materials Letters. 60(1): 31-38.
58. Xie, Z., Lu, C., Chen, X., Chen, L., Hu, X., Shi, Q. and Jing, X. 2007. A facile approach to biodegradable poly(ε-caprolactone)-poly(ethylene glycol)-based polyurethanes containing pendant amino groups. European Polymer Journal. 43(5): 2080-2087.
59. Jiang, X., Li, J., Ding, M., Tan, H., Ling, Q., Zhong, Y. and Fu, Q. 2007. Synthesis and degradation of nontoxic biodegradable waterborne polyurethanes elastomer with poly(ε-caprolactone) and poly(ethylene glycol) as soft segment. European Polymer Journal. 43(5): 1838-1846.
60. Jeon, H.J., Kim, J.S., Kim, T.G., Kim, J.H., Yu, W.-R. and Youk, J.H. 2008. Preparation of poly(ε-caprolactone)-based polyurethane nanofibers containing silver nanoparticles. Applied Surface Science. 254(18): 5886-5890.
61. Panwiriyarat, W., Tanrattanakul, V., Pilard, J.-F. and Khaokong, C. 2011. Synthesis and characterization of block copolymer from natural rubber, toluene-2,4-diisocyanate and poly(ε-caprolactone) diol - based polyurethane. Materials Science Forum. 695: 316-319.

62. Panwiriyarat, W., Tanrattanakul, V., Pilard, J.-F., Pasetto, P. and Khaokong, C. 2013. Physical and thermal properties of polyurethane from isophorone diisocyanate, natural rubber and poly(ε-caprolactone) with high NCO:OH content. Advanced Science Letters. 19(3): 1016-1020.
63. Panwiriyarat, W., Tanrattanakul, V., Pilard, J.-F., Pasetto, P. and Khaokong, C. 2013. Effect of the diisocyanate structure and the molecular weight of diols on bio-based polyurethanes. Journal of Applied Polymer Science. 130: 453-462.
64. Leja, K. and Lewandowicz, G. 2010. Polymer biodegradation and biodegradable polymers – a review. Polish Journal of Environmental Studies. 19: 255-266.
65. Bastioli, C. 2005. Handbook of biodegradable polymers: smithers rapra publishing, United Kingdom.
66. Chandra, R. and Rustgi, R. 1997. Biodegradation of maleated linear low-density polyethylene and starch blends. Polymer Degradation and Stability. 56(2): 185-202.
67. Kolybaba, M., Tabil, L.G., Panigrahi, S., Crerar, W.J., Powell, T. and Wang, B. 2003. Biodegradable polymers past, present, and future. The 2003 CSAE/ASAE Annual Intersectional MeetingSponsored by the Red River Section of ASAEQuality Inn & Suites301 3rd Avenue NorthFargo, North Dakota, USA. 1-15.
68. Müller, R.J. 2005. Biodegradability of polymers: Regulations and methods for testing. In: Biopolymers Online. Ed. p.
69. Mortier, N. and De Wilde, B. 2014. Review of Standard Testing methods and specifications for measuring biodegradation of bio-based materials in fresh water. International conference of agricultural engineering AgENG 2014 Zurich 6-10 July.
70. Shah, A.A., Hasan, F., Hameed, A. and Ahmed, S. 2008. Biological degradation of plastics: A comprehensive review. Biotechnology Advances. 26(3): 246-265.
71. Avérous, L. 2008. Chapter 21 - Polylactic Acid: Synthesis, Properties and Applications. In: Monomers, Polymers and Composites from Renewable Resources. Gandini, M.N.B., First Ed. Elsevier: Amsterdam. p. 433-450.
72. Organisation for Economic Co-operation and Development. 1993. OECD guidelines for testing of chemicals. CO2 evolution test. . OECD 301 B, Paris, France.

73. Chandra, R. and Rustgi, R. 1998. Biodegradable polymers. Progress in Polymer Science. 23: 1273–1335.
74. Bode, H.B., Kerkhoff, K. and Jendrossek, D. 2001. Bacterial degradation of natural and synthetic rubber. Biomacromolecules 2: 295-303.
75. Rose, K. and Steinbüchel, A. 2005. Biodegradation of natural rubber and related compounds: Recent insights into a hardly understood catabolic capability of microorganisms. Applied and Environmental Microbiology. 71(6): 2803-2812.
76. Imai, S., Ichikawa, K., Muramatsu, Y., Kasai, D., Masai, E. and Fukuda, M. 2011. Isolation and characterization of Streptomyces, Actinoplanes, and Methylibium strains that are involved in degradation of natural rubber and synthetic poly(cis-1,4-isoprene). Enzyme and Microbial Technology. 49(6–7): 526-531.
77. Heisey, R.M. and Papadatos, S. 1995. Isolation of microorganisms able to metabolize purified natural rubber. Applied and Environmental Microbiology. 61(8): 3092-3097.
78. Tsuchii, A., Suzuki, T. and Takeda, K. 1985. Microbial degradation of natural rubber vulcanizates. Applied and Environmental Microbiology. 50(4): 965-970.
79. Ibrahim, E.M.A., Arenskötter, M., Luftmann, H. and Steinbüchel, A. 2006. Identification of poly(cis-1,4-isoprene) degradation intermediates during growth of moderately thermophilic actinomycetes on rubber and cloning of a functional lcp homologue from nocardia farcinica Strain E1. Applied and Environmental Microbiology. 72(5): 3375-3382.
80. Tsuchii, A. and Takeda, K. 1990. Rubber-degrading enzyme from a bacterial culture. Applied and Environmental Microbiology. 56(1): 269-274.
81. Bröker, D., Arenskötter, M., Legatzki, A., Nies, D.H. and Steinbüchel, A. 2004. Characterization of the 101-Kilobase-Pair Megaplasmid pKB1, Isolated from the rubber-degrading bacterium gordonia westfalica Kb1. Journal of Bacteriology. 186(1): 212-225.
82. Shah, Z., Shah, A.A., Hameed, A. and Hasan, F. 2009. Effect of pretreatments on enhanced degradation of polyisoprene rubber by newly isolated Bacillus sp. strain S10. Journal of the Chemical Society of Pakistan. 31(4): 638-646.

83. Rose, K., Tenberge, K.B. and Steinbüchel, A. 2005. Identification and characterization of genes from Streptomyces sp. Strain K30 responsible for clear zone formation on natural rubber latex and poly(cis-1,4-isoprene) rubber degradation. Biomacromolecules. 6(1): 180-188.

84. Shah, A.A., Hasan, F., Shah, Z., Kanwal, N. and Zeb, S. 2013. Biodegradation of natural and synthetic rubbers: A review. International Biodeterioration & Biodegradation. 83: 145-157.

85. Shah, A.A., Hasan, F., Shah, Z., Mutiullah and Hameed, A. 2012. Degradation of polyisoprene rubber by newly isolated bacillus sp. AF-666 from soil. Appl Biochem Microbiol. 48(1): 37-42.

86. Kwiatkowska, D., Zyska, B.J. and Zankowicz, L.P. 1980. Microbiological deterioration of natural rubber sheet by soil microorganisms. Biodeterioration 4: 135-141.

87. Williams, G.R. 1982. The breakdown of rubber polymers by microorganisms. International Biodeterioration Bulletin 18: 31-36.

88. Premraj, R. and Doble, M. 2005. Biodegradation of polymers. Indian journal of biotechnology. 4: 186-193.

89. Sanchez, J.G., Tsuchii, A. and Tokiwa, Y. Degradation of polycaprolactone at 50 °C by a thermotolerant Aspergillus sp. Biotechnology Letters. 22(10): 849-853.

90. Ali, S.A.M., Zhong, S.P., Doherty, P.J. and Williams, D.F. 1993. Mechanisms of polymer degradation in implantable devices: I. Poly(caprolactone). Biomaterials. 14(9): 648-656.

91. Mochizuki, M., Hirano, M., Kanmuri, Y., Kudo, K. and Tokiwa, Y. 1995. Hydrolysis of polycaprolactone fibers by lipase: Effects of draw ratio on enzymatic degradation. Journal of Applied Polymer Science. 55(2): 289-296.

92. Chen, D., Bei, J. and Wang, S. 2000. Polycaprolactone microparticles and their biodegradation. Polymer Degradation and Stability. 67(3): 455-459.

93. Castilla-Cortázar, I., Más-Estellés, J., Meseguer-Dueñas, J.M., Escobar Ivirico, J.L., Marí, B. and Vidaurre, A. 2012. Hydrolytic and enzymatic degradation of a poly(ε-caprolactone) network. Polymer Degradation and Stability. 97: 1241-1248.

94. Phua, S.K., Castillo, E., Anderson, J.M. and Hiltner, A. 1987. Biodegradation of a polyurethane in vitro. Journal of Biomedical Materials Research. 21(2): 231-246.

95. Howard, G.T. 2002. Biodegradation of polyurethane: a review. International Biodeterioration & Biodegradation. 49: 245 - 252.

96. Urgun-Demirtas, M., Singh, D. and Pagilla, K. 2007. Laboratory investigation of biodegradability of a polyurethane foam under anaerobic conditions. Polymer Degradation and Stability. 92(8): 1599-1610.

97. Gorna, K. and Gogolewski, S. 2002. In vitro degradation of novel medical biodegradable aliphatic polyurethanes based on ϵ-caprolactone and Pluronics® with various hydrophilicities. Polymer Degradation and Stability. 75(1): 113-122.

98. Davis, J.R. 2004. Tensile Testing, Second Edition. Materials Park, Ohio, USA.

99. Ridha, M. 2007. Mechanical and failure properties of rigid polyurethane foam under tension. PhD Thesis, Department on mechanical engineering, National university of Singapore, Singapore.

100. Sepe, M.P. 1997. Thermal analysis of polymers. . iSmithersRapra Publishing, Shrewsbury, SY4 4NR, United Kingdom.

101. Suresh, S. 2015. Analytical chemistry (Thermogravimetric analysis). http://wwwslidesharenet/sureshselvaraj108/thermogravimetric-analysis (accessed 25/01/2016).

102. PerkinElmer. 2012. Thermogravimetric analysis (TGA). A Beginner's Guide. In. Ed. PerkinElmer, Inc: Waltham. p. 1-19.

103. Gerothanassis, P.I., Troganis, A., Exarchou, V. and Barbarossou, K. 2002. Nuclear magnetic resonance (NMR) spectroscopy: Basic principles and phenomena and their applications to chemistry, biology and medicine. Chemistry Education Research and Practice in Europe. 3: 229-252.

104. Larkin, P. 2011. Infrared and Raman spectroscopy; principles and spectral interpretation. In. Ed. Elsevier, San Diego, USA. p.

105. Stuart, B.H. 2002. Polymer analysis. John Wiley & Sons, Hoboken, NJ, USA.

106. Åmand, L.E. and Tullin, C.J. 1999. The theory behind FTIR analysis application examples from measurement at the 12 MW Circulating Fluidized Bed Boiler at Chalmers Department of Energy Conversion Chalmers University of Technology, Göteborg, Sweden.

107. Dunlap, M. and Adaskaveg, J.E. 1997. Introduction to the scanning electron microscope: Theory, practice, and procedures. Facility for advanced instrumentation. Rutgers School of Dental Medicine, NJ, USA.

108. Malvern Instruments. 2013. GPC/SEC Conventional calibration. http://particularsciencesie/psl/technology/sec-gpc/conventional-cal/ (accessed 25/01/2016).

CHAPTER 3

MATERIALS AND METHODOLOGY

3.1 Materials

All materials used in this research work are listed in Table 3.1

Table 3.1 List of materials

Chemicals	Abbreviation Formula	Specification	Producer
Block natural rubber (STR5 CV60)	C_5H_8	Mooney viscosity ML (1+4) 100 °C = 60	Jana Concentrated Latex, Co., Ltd., Thailand
Periodic acid	H_5IO_6	- colorless crystals, reactant for synthesized CTNR - 99% purity, D = 1.4 g/cm^3 - $\overline{M}w$ = 227.941 g/mol	Sigma - Aldrich Co., LLC, USA
Sodium borohydride	$NaBH_4$	- white powder, reactant for synthesized HTNR - 98% purity, D = 1.07 g/cm^3 - $\overline{M}w$ = 37.83 g/mol	Acros Organics Co.,USA
Sodium bicarbonate	$NaHCO_3$	- white powder, purified agent - 99.7% purity, D = 2.16 g/cm^3 - $\overline{M}w$ = 84.01 g/mol	Sigma-Aldrich Co., LLC, USA
Magnesium sulfate (anhydrous)	$MgSO_4$	- white powder, purified agent - 97% purity, D =2.66 g/cm^3 - $\overline{M}w$ = 120.37 g/mol	Fisher Scientific UK Ltd., England
Sodium thiosulfate pentahydrate	$Na_2S_2O_3.5H_2O$	- white crystals, purified agent - 99.5% purity, D = 1.74 g/cm^3 - $\overline{M}w$ = 248.21 g/mol	RCI labscan Ltd., Thailand
Sodium chloride	NaCl	- white powder, purified agent - 99% purity, D = 2.17 g/cm^3 - $\overline{M}w$ = 58.44 g/mol	RCI labscan Ltd., Thailand
Tetrahydrofuran (THF)	C_4H_8O	- 99% purity, D = 0.89 g/cm^3 - $\overline{M}w$ = 72.11 g/mol, solvent - boiling point = 65-66 °C	RCI labscan Ltd., Thailand

Table 3.1 (continued)

Chemicals	Abbreviation Formula	Specification	Producer
Dichloromethane	CH_2Cl_2	- 99.8% purity, solvent - $\overline{M}w$ = 84.93 g/mol - boiling point = 40 °C - D = 1.33 g/cm^3	RCI labscan Ltd., Thailand
Polymethylene Polyphenylpoly isocyanate (Lupranate®M20S)	$[C_6H_3(NCO)CH_2]$ n	- dark brown liquid - % NCO = 31.5 - viscosity 200 cPs at 25 °C - D = 1.23 g/cm^3, $\bar{f}_n$ = 2.7	BASF Polyurethanes GmbH, Germany
Polycaprolactone diol	$(C_6H_{10}O_2)n$	- solid (waxy), polyol - $\overline{M}w$ = 2,000 g/mol - D = 1.07 g/cm^3	Sigma-Aldrich Co., LLC, USA
Silicone surfactant	TEGOSTAB B 8110	- viscous liquid, stabilizer - polyether-modified polysiloxane	Evonik Industries, Germany
Triethylene diamine (Dabco 33-LV)	$C_6H_{12}N_2$	- viscous liquid (colorless) - $\overline{M}w$ = 112.17 g/mol - mixture of 33% triethylene diamine and 67% dipropylene glycol - amine catalyst	Sigma-Aldrich Co., LLC, USA
Dibutyltin dilaurate (Dabco T-12)	$C_{32}H_{64}O_4Sn$	- viscous liquid (yellow) - $\overline{M}w$ = 631.56 g/mol - tin catalyst	Sigma-Aldrich Co., LLC, USA
1,4-Butanediol	$C_4H_{10}O_2$	- viscous liquid, 99% purity - D = 1.0171 g/cm^3 - $\overline{M}w$ = 90.12 g/mol - chain extender	Sigma-Aldrich Co., LLC, USA
Sodium hydroxide	NaOH	- white solid, 99% purity - $\overline{M}w$ = 40 g/mol - trap CO_2 in biodegradation test	Merck Ltd., Germany
Barium hydroxide octahydrate	$Ba(OH)_2.8H_2O$	- white solid, 98% purity - $\overline{M}w$ = 315.48 g/mol - trap CO_2 in biodegradation test	QReC:Quality reagent chemical, New Zealand
Iron(III) chloride hexahydrate	$FeCl_3.6H_2O$	- yellow powder, 99% purity - $\overline{M}w$ = 270.32 g/mol - mixture of culture medium for biodegradation test	QReC:Quality reagent chemical, New Zealand

Table 3.1 (continued)

Chemicals	Abbreviation Formula	Specification	Producer
Potassium dihydrogen orthophosphate (anhydrous)	KH_2PO_4	- white crystals solid - $\overline{M}w$ = 136.09 g/mol - PH (5% solution) = 4.3-4.5 - mixture of culture medium for biodegradation test	RCI labscan Ltd., Thailand
Potassium phosphate dibasic (anhydrous)	K_2HPO_4	- white powder - $\overline{M}w$ = 174.8 g/mol - PH (5% solution) = 8.5-9.6 - mixture of culture medium for biodegradation test	RCI labscan Ltd., Thailand
Disodium hydrogen phosphate dihydrate	$Na_2HPO_4.2H_2O$	- white crystals solid - $\overline{M}w$ = 177.99 g/mol - PH (5% water) = 9-9.2 - mixture of culture medium for biodegradation test	RCI labscan Ltd., Thailand
Ammonium chloride	NH_4Cl	- white crystals powder - $\overline{M}w$ = 53.49 g/mol - PH (5% solution) = 4.5-5.5 - mixture of culture medium for biodegradation test	RCI labscan Ltd., Thailand
Magnesium sulfate heptahydrate	$MgSO_4.7H_2O$	- colorless crystals - $\overline{M}w$ = 264.48 g/mol - PH (5% water) = 5-8 - mixture of culture medium for biodegradation test	RCI labscan Ltd., Thailand
Calcium chloride dihydrate	$CaCl_2.2H_2O$	- white powder - $\overline{M}w$ = 147.01 g/mol - PH (5% solution) = 4.5-8.5 - mixture of culture medium for biodegradation test	RCI labscan Ltd., Thailand

3.2 Instruments

All instruments used in this research are listed in Table 3.2

Table 3.2 List of instruments

Instruments	Model	Producer
Nuclear Magnetic Resonance Spectrometer (^{1}H-NMR)	(1) Bruker®Avance 400 spectrometer (2) UNITY INOVA®500	Bruker, Corp., USA Varian Inc., Germany
Fourier Transform Infrared Spectrometer (FTIR)	(1) Nicolet Avatar®370 DTGS FTIR spectrometer (2) Tensor®27	Thermo Electronic Corp., USA Bruker Corp., Germany
Gel Permeation Chromatography (GPC)	ThermoFiningan SEC instrument	Thermo Electronic Corp., USA
Thermal Gravimetric Analytical Instrument (TGA)	TGA® Q500	TA instrument, USA
Thermal analyzer (TG-DSC)	STA 449 F3-Jupiter	NETZSCH, Germany
Scanning Electron Microscope (SEM)	Quanta®400 FEI	JEOL Co., Japan
Evaporator	BUCHI®Rotavapor	BUCHI Laborttechnik AG, Switzerland
Tensile testing machine:	Universal Instron®3365	Instron, USA
Hot air oven	UM 400	MEMMERT Co., Ltd., Germany
Vacuum oven	VD53	Binder Co., Ltd., Germany
Homogenizer	Ystral: Laboratory Series X10	Ystral gmbh, Germany

3.3 Methodology

In this section, experimental procedures used for the synthesis of the oligomers from natural rubber are described; the results of the products characterization, such as nuclear magnetic resonance spectra, infrared spectra, and molecular weights from size exclusion chromatography will be presented in chapter 4.

3.3.1 Synthesis of telechelic oligomer (TNR) from natural rubber

3.3.1.1 Carbonyl telechelic natural rubber (CTNR)

Natural rubber (NR, 60 g) was cut in crumbs and dissolved in tetrahydrofuran (THF, 1.5 L) in a jacketed reaction flask equipped with a mechanical stirrer, for 24 h at room temperature. Periodic acid (H_5IO_6, 27.44 g) was suspended in THF (300 mL) and slowly dropped into the NR solution, and the reaction was maintained at 30 °C for 24 h. At the end of the reaction, the solution was filtered by using filter paper. THF was evaporated and then the polymer was dissolved again in dichloromethane (CH_2Cl_2). The solution was washed twice with a mixture of saturated sodium bicarbonate solution ($NaHCO_3$) and 20 w/v% of sodium thiosulphate solution ($Na_2S_2O_3$), and washed again with a saturated sodium chloride solution (NaCl) [1-7]. Then, the organic phase was dried over $MgSO_4$ overnight. After filtration, the solvent was evaporated and the product was dried in a vacuum oven. The sample was analyzed by ^{1}H-NMR, FTIR and GPC. The reaction is described in Scheme 3.1.

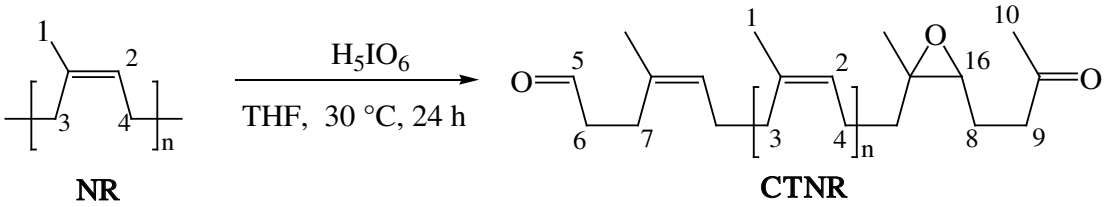

Scheme 3.1 Carbonyl telechelic oligomers (CTNR) preparation.

Molecular weight of CTNR can be obtained from the ^{1}H-NMR spectrum using the calculation in equation (1) [5].

$$M_{n,NMR\text{-}CTNR} = \left\{\frac{4I_2 \times 68}{I_{9,6}}\right\} + 100 \quad \ldots\ldots\ldots\ldots\ldots\ldots\ldots\ldots\ldots\ldots (1)$$

Where (I_2) represents the integration of the ethylenic "2" proton of the repeating unit, at δ 5.12 ppm; ($I_{9,6}$) is the integration of the 4 protons in the two methylenic groups in position 9 and 6 at the chain ends (δ 2.45 and 2.49 ppm respectively); 68 g/mol is the molecular weight of the isoprene repeating unit; 100 is the molecular weight of the $-CH_2CHO$ and $-CH_2COCH_3$ chain ends.

3.3.1.2 Hydroxyl telechelic natural rubber (HTNR)

Sodium borohydride ($NaBH_4$, 3.78 g, 5 equivalents) was dissolved in THF (333 mL) in a jacketed reaction flask equipped with a mechanical stirrer. CTNR (40 g, 1 equivalent) was dissolved in THF (285 mL) and slowly dropped into $NaBH_4$ solution in the reactor. The reaction was run at 60 °C for 24 h. After, a mixture of THF (25 mL) with ice (75 g) was added in the reactor to hydrolyze the functional group to hydroxyl group. After, the organic solution was washed with saturated NaCl solution and dried over $MgSO_4$ [1-12]. The solution was filtered, the solvent was evaporated and the polymer was dried in the vacuum oven. The sample was analyzed by ^{1}H-NMR, FTIR and GPC. The reaction is described in Scheme 3.2.

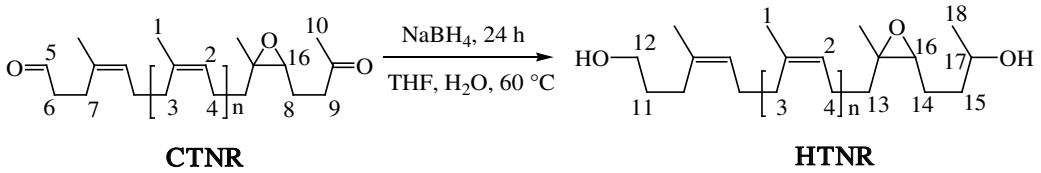

Scheme 3.2 Hydroxyl telechelic oligomers (HTNR) preparation.

Molecular weight average of HTNR from ^{1}H-NMR can be calculated by the relationship in equation (2) [7].

$$M_{n,NMR\text{-}HTNR} = \left\{\frac{2I_2 \times 68}{I_{12}}\right\} + 104 \quad \ldots\ldots\ldots\ldots\ldots\ldots\ldots\ldots\ldots\ldots\ldots\ldots(2)$$

Where (I_2) represents the integration of proton signal of the ethylenic proton at 5.12 ppm, and (I_{12}) represents the integration of the two CH_2 protons on the carbon of the primary alcohol chain end, at 3.65 ppm. The oligomers were stored at room temperature, protected from light. (see Figure 4.4 in Chapter 4)

3.3.2 Synthesis of telechelic oligomers from waste tires

3.3.2.1 Carbonyl telechelic waste tires (CTWT)

Small molecules and waste tire additives contained in the waste tire crumbs (average size = 0.63 – 1 mm) were extracted in a soxhlet apparatus using THF, for 24 h. Then the waste tires crumbs (200 g) were suspended in THF (2 L) in a jacketed reaction flask equipped with a mechanical stirrer, for 24 h, at room

temperature. H_5IO_6 (106 g) suspended in THF (1.178 L) was added dropwise to the suspension in the reactor. The reaction solution was stirred at 30 °C for 24 h. At the end of reaction, a solid fraction containing a small amount of partially dissolved waste tires crumbs was separated from the CTWT solution. The solution was washed twice with a mixture of a solution of saturated $NaHCO_3$ and a 20 w/v% solution of $Na_2S_2O_3$. These washing steps allowed the partial elimination of carbon black, which went into the aqueous phase. The organic phase was filtered through a sintered glass funnel containing a layer of Celite powder (5 cm height) and then washed with saturated NaCl. This phase was dried over $MgSO_4$ overnight, filtered and evaporated under reduced pressure [5,7]. The sample was analyzed by ^{1}H-NMR, FTIR and GPC. Scheme 3.3 shows the synthesis of CTWT.

3.3.2.2 Hydroxyl telechelic waste tires oligomers (HTWT)

Sodium borohydride ($NaBH_4$, 10 g) was dissolved in THF (900 mL) in a reaction flask equipped with a magnetic stirrer. A solution of CTWT (30 g) in THF (390 mL) was added dropwise to a solution of $NaBH_4$. The reaction solution was kept at 60 °C for 24 h and then hydrolyzed by adding the mixture of THF (70 mL) with ice (200 g) dropwise, at room temperature. After that, the solution was washed with a saturated NaCl solution and dried over $MgSO_4$ [7]. After filtration, the solvent was evaporated and the polymer was dried in a vacuum oven. The sample was analyzed by ^{1}H-NMR, FTIR and GPC and the relative results are reported in chapter 4. The reaction is described in Scheme 3.4.

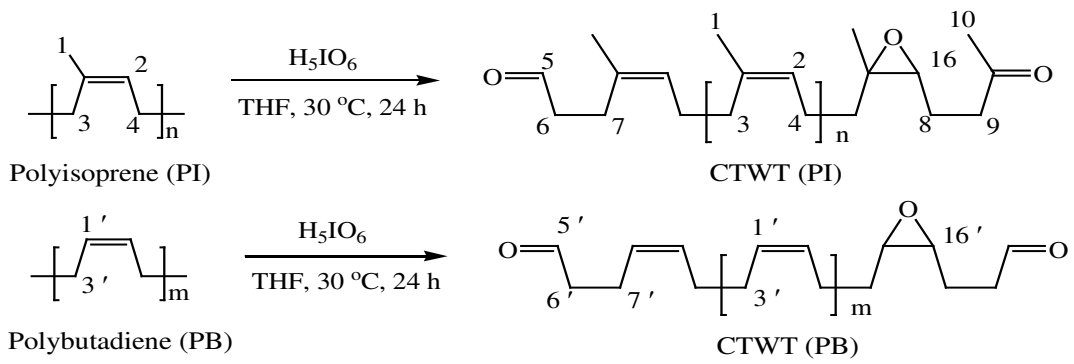

Scheme 3.3 Synthesis of carbonyl oligomers from waste tires (CTWT).

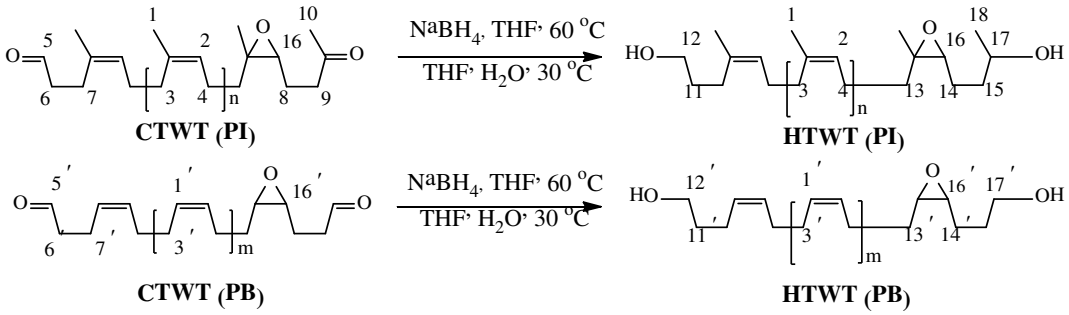

Scheme 3.4 Reduction reaction of carbonyl telechelic oligomer from waste tires to obtain hydroxyl oligomers.

3.3.3 Preparation of bio-based polyurethane foams from HTNR, HTWT and polycaprolactone diol (PCL)

The bio-based polyurethane foams (bio-PUFs) were prepared by the one-shot technique. The ingredients were mixed together at once and allowed to cure. Polyol (HTNR, HTWT and PCL), water, surfactant (B8110), chain extender (BDO), catalyst (DABCO-33LV and DABCO-T12) and dichloromethane were mixed with a homogenizer under vigorous stirring, followed by addition of P-MDI to the mixture and continuously stirred by homogenizer at a speed of 11,000 rpm until the liquid started whitening (creaming time) [6,7]. The mixture was poured into a plastic mould, the size of which was 12.5 × 17.5 × 4.5 cm for a total weight of polyols equal to 35 g, and 3× 4 × 7 cm for a total weight of polyol equal to 4 g. The sample was kept in an oven at 60 °C for 24 h. The foam formulation was chosen by using the NCO index of 100. The molecular weights of HTNR and PCL were 2,000 g/mol (HTNR2000 and PCL2000) whereas the molecular weight of HTWT was 1,500 g/mol. The molar ratios of HTNR/PCL and HTWT/PCL were 1/0, 1/0.5, 1/1 and 0.5/1. Foam formulations are listed in Table 3.3 and 3.4. Creaming time, rising time and tack free time were determined during foam preparation.

Table 3.3 Formulations of foams (Bio-PUFs) using HTNR and PCL as precursors

Samples	PUF1	PUF2	PUF3	PUF4
Ratio of HTNR and PCL by mole	1/0	1/0.5	1/1	0.5/1
Ingredients	Weight (g)			
HTNR2000	35	23.5	17.7	11.8
PCL2000	0	11.5	17.3	23.1
Dichloromethane	8.75	8.75	8.75	8.75
1,4-Butanediol	0.17	0.17	0.17	0.17
Dabco 33-LV	0.26	0.26	0.26	0.26
Dabco T-12	0.18	0.18	0.18	0.18
B8110	0.61	0.61	0.61	0.61
water	1.40	1.40	1.40	1.40
P-MDI	26.1	26.1	26.2	26.2

Table 3.4 Formulation of Bio-PUFs by using HTWT and PCL as precursors

Samples	PUF5	PUF6	PUF7	PUF8
Ratio of HTWT and PCL by mole	1/0	1/0.5	1/1	0.5/1
Ingredients	Weight (g)			
HTWT-1500	4	2.21	1.53	0.95
PCL-2000	0	1.79	2.47	3.06
Dichloromethane	1	1	1	1
1,4-Butanediol	0.02	0.02	0.02	0.02
Dabco 33-LV	0.03	0.03	0.03	0.03
Dabco T-12	0.02	0.02	0.02	0.02
B8110	0.07	0.07	0.07	0.07
Water	0.16	0.16	0.16	0.16
P-MDI	3.33	3.18	3.13	3.08

3.3.4 Kinetic rate of bio-PUFs formation

The kinetic rate of bio-based PUFs formation mainly depended on some properties of foam such as creaming time, rising time and tack free time [13]. The creaming time is the beginning of the foam rise. At this point, the color of the mixed reactants changed from dark brown to a lighter color. The rising time is the time when the foam reach the maximum height [14]. The tack free time is the time at which the outer surface of the foam loses its stickiness and the cross-linked PUFs can be removed from the mold [15]. These times were measured with a digital stopwatch timer device during the bio-PUFs preparation.

3.3.5 Physical and mechanical properties

3.3.5.1 Density

The density of the polyurethane foams was measured according to ASTM D 3574 Test A. Five specimens were cut to have a dimension of 10 mm x 10 mm x 10 mm. Then, these specimens were precisely weighed. The result of the weight (M) divided by volume (V) of the specimens was a density in a unit of kg/m^3.

3.3.5.2 Cell size

Cell dimension of polyurethane foams was determined by using a JEOL® JSM-6510LV scanning electron microscope at a voltage of 10 kV and magnification of 37X. Cell size was measured by the program JEOL scanning electron microscope calculating the average diameter of 20 cells per image.

3.3.5.3 Tensile properties

The tensile strength and elongation at break of polyurethane foams were measured with a crosshead speed of 500 mm/min according to ASTM D 3574 Test E by using a universal tensile testing machine. Five dumbbell shaped specimens were cut using a type A die. The tensile strength was calculated by dividing the maximum breaking force (F) by the original cross-sectional area of the specimen (A) and reported in a unit of kilopascal (kPa) as shown in equation (9). The ultimate elongation was also calculated by subtracting the original distance between the bench marks (d_0) from the total distance between the bench marks at the break point (d_b) and expressed the difference as a percentage of the original distance as shown in equation (10).

$$\text{Tensile strength (kPa)} = \frac{F}{A} \quad \ldots\ldots\ldots\ldots\ldots\ldots\ldots\ldots\ldots\ldots(9)$$

$$\text{Elongation at break (\%)} = \frac{(d_b - d_0)}{d_0} \times 100 \ldots\ldots\ldots\ldots\ldots\ldots\ldots(10)$$

3.3.5.4 Compressive strength

The compressive strength of the polyurethane foams was investigated according to ASTM D 3574 Test C by using a universal tensile testing machine. The dimension of specimens was 50 mm x 50 mm x 25 mm. The specimens were compressed to 50% of their original thickness at a speed of 50 mm/min and the final force was determined after 60 s (F). The compressive strength was obtained from the average value of three specimens tested per sample and was reported in units of kilopascal (kPa) as shown in equation (11).

$$\text{Compressive strength (kPa)} = \frac{F}{A} \quad \ldots\ldots\ldots\ldots\ldots\ldots\ldots\ldots(11)$$

3.3.5.5 Compression set

The compression set is the percentage change of the original thickness after the specimens have been constantly deflected under a specific condition of temperature and time according to ASTM D 3574 Test D. The dimension of the specimens was 50 mm x 50 mm x 25 mm. These specimens were deflected at 50% of their measured original thickness. All specimens were kept at 70 °C for 22 h, then removed from the apparatus, left at room temperature for 30 min and finally their thickness was measured. The compression set value was calculated as shown in equation (12).

$$\text{Compression set (\%)} = \frac{(T_0 - T_f)}{T_0} \times 100 \ldots\ldots\ldots\ldots\ldots\ldots\ldots\ldots(12)$$

T_0 = original thickness of test specimens (mm)

T_f = final thickness of test specimens

3.3.6 Characterizations

3.3.6.1 Nuclear magnetic resonance spectroscopy (^{1}H-NMR)

Deuterated chloroform ($CDCl_3$-*d*) was used as a solvent and tetramethylsilane was used as the internal standard. 30 mg of sample were dissolved in $CDCl_3$-*d* and charged in a NMR tube. ^{1}H spectra were recorded on a Bruker 400 Fourier transform spectrometer at 400.13 MHz.

3.3.6.2 Fourier transform infrared spectroscopy (FTIR)

The FTIR was used to determine the presence of functional groups in the telechelic oligomers and bio-PUFs. The samples were scanned at a frequency range of 600 – 4,000 cm^{-1} with an attenuated total reflection (ATR) mode.

3.3.6.3 Gel permeation chromatography (GPC)

Number average molecular weight ($\overline{M}_n$), weight average molecular weight ($\overline{M}w$) and dispersity (Đ) were measured at 35 °C on a ThermoFinnigan SEC instrument (equipped with a SpectraSYSTEM AS1000 autosampler, a SpectraSYSTEM UV2000 and a SpectraSYSTEM RI150 detectors), using a polymer laboratories (PL) gel 5 mm MIXED-D columns, calibrated with a series of standard polystyrenes (580– 483×10^3 g/mol). THF (1 mL/min) was used as an eluent.

3.3.6.4 Thermal gravimetric analysis

Thermogravimetric analysis (TGA) was performed on a TA Instrument and Thermal analyzer with an initial heating rate 10 °C/min, under nitrogen, in the range 25-1,000 °C. The sample weight was 5 mg.

3.3.6.5 Scanning electron microscopy (SEM)

The SEM was carried out to study the cell structure and cell size of bio-PUFs by using scanning electron microscopy at a voltage of 15 kV and magnification of 37X. The bio-PUFs were cut with a blade into rectangular slices: 15 x 15 x 3 mm. Each sample slice was sputter coated with a thin gold layer before observation.

3.3.7 Biodegradation Tests

3.3.7.1 Preparation of liquid culture medium

Liquid culture medium for foam biodegradation experiments was prepared according to OECD 301 B [16]: Solution A: K_2HPO_4 (21.75 g), KH_2PO_4 (8.5 g), $Na_2HPO_4.2H_2O$ (33.4 g) and NH_4Cl (0.5 g); solution B: $CaCl_2.2H_2O$ (36.4 g); solution C: $MgSO_4.7H_2O$ (22.5 g); solution D: $FeCl_3.6H_2O$ (0.25 g). For each solution the salts were dissolved in 1 L of water then, to obtain the final culture medium, 10 mL of solution A, 1 mL of solution B, 1 mL of solution C and 1 mL of solution D were added to 987 mL of water to make a total of 1 L solution.

3.3.7.2 Biodegradation by the STURM test

The principle of the widely used CO_2 evolution test (OECD 301 B), also known as the Sturm test, was the determination of the ultimate biodegradability of organic compounds by aerobic microorganisms. In this test, HTNR/PCL foams in Table 3.3, HTWT/PCL foams in Table 3.4, sodium benzoate (positive control), LDPE (light density polyethylene, negative control) and a blank (culture medium only) were used as samples. Microorganisms were taken from sewage in the latex rubber factories (Top glove technology (Thailand). Co., Ltd.). The amount of microorganisms in the test culture medium was 30 mg solid/L. CO_2 was determined as an evidence of the biodegradation. A schematic diagram of the biodegradability testing system in this study is shown in Figure 3.1. Experiments were carried out in tightly closed erlenmeyer flasks. The test set up consisted in a first part for air pretreatment (NaOH, 2.5 M and $Ba(OH)_2$, 0.02 M) to eliminate the CO_2 at the entrance. The test flask contained 250 mL of culture medium and sample (70 mg of total organic carbon/L of liquid culture medium), and was aerated with 1 to 2 bubbles of CO_2-free air per second. Each test flask was connected to a series of three flasks containing 100 mL of a 0.02 M $Ba(OH)_2$ solution [17]. The system was monitored every 2 days for 60 days by titration of the solution contained in the last flask of the circuit. The theoretical amount of CO_2 ($ThCO_2$), in grams per flask, was calculated by the following equation (13) [18]:

$$ThCO_2 = M_{TOT} \times C_{TOT} \times \frac{44}{12} \quad \text{.....(13)}$$

where $ThCO_2$ is the theoretical amount of carbon dioxide which can be produced by the sample, in grams per test flasks; M_{TOT} is the total dry solids in grams, in the sample added into the test flasks at the beginning of the test; C_{TOT} is the proportion of total organic carbon in the total dry solids in the sample, in grams per gram; 44 and 12 are the molecular mass of carbon dioxide and atomic mass of carbon, respectively.

The carbon dioxide generated during the biodegradation test was captured by 100 mL of a 0.02 M $Ba(OH)_2$ solution and consequently precipitated as $BaCO_3$. The amount of CO_2 evolution was determined by titrating the remaining $Ba(OH)_2$ from each trap with 0.2 M HCl to the phenolphthalein end-point. The total amount of CO_2 evolution was calculated by reference to the blank control flask. The percentage of biodegradation of the sample was calculated according to the equation (14) [18].

$$\% \text{ Biodegradation} = \left[\frac{(CO_2)t - (CO_2)b}{ThCO_2} \right] \times 100 \quad \text{.....(14)}$$

Where $(CO_2)t$ represent the cumulative amount of carbon dioxide evolved in each test flask containing the sample material, and $(CO_2)b$ represent the cumulative amount of carbon dioxide evolved in the blank flask, in grams per flask.

Number of colonies of bacteria in the sewage water before and after biodegradation test (0 and 60 days, respectively) was determined. The number of colonies (Colony formation units, CFU/mL) was counted through visual examination of growth on Plate Count Agar (PCA) [19]. 30 mg of the sewage water was mixed with 1 L of liquid culture medium, and 1 mL of this solution was used. It was diluted with saline in order to obtain the concentration of 1:1,000. Then, 0.1 mL of this diluted solution was dropped onto a Petri dish containing PCA. The Petri dish was thermostated for 3 days at 30 °C and the colony growth was visually observed.

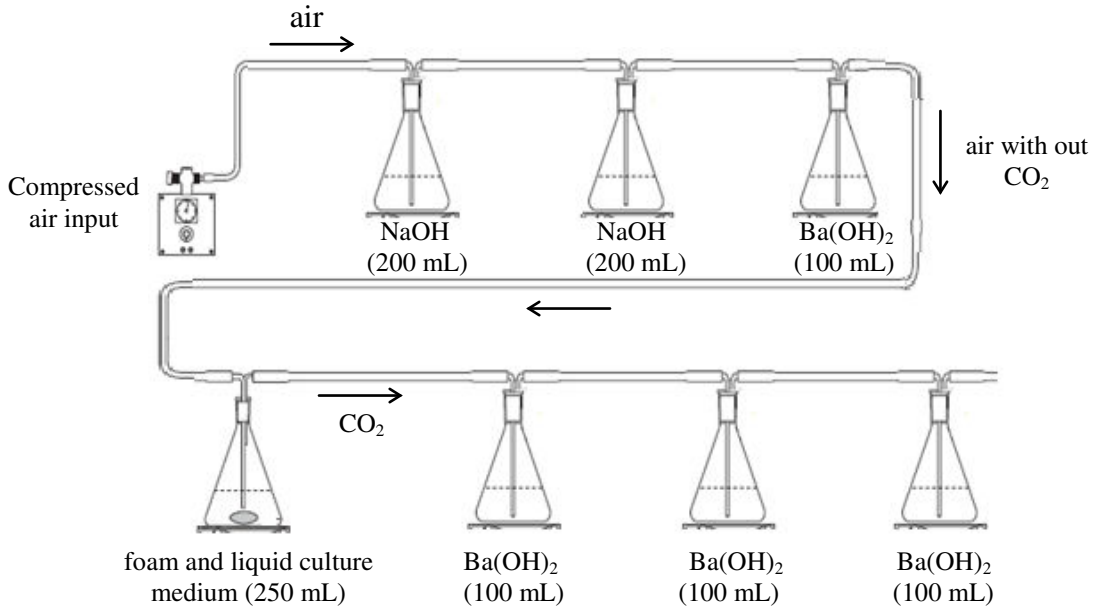

Figure 3.1 A schematic diagram of biodegradability testing system.

3.4 References

1. Panwiriyarat, W., Tanrattanakul, V., Pilard, J.-F. and Khaokong, C. 2011. Synthesis and characterization of block copolymer from natural rubber, toluene-2,4-diisocyanate and poly(ε-caprolactone) diol - based polyurethane. Materials Science Forum. 695: 316-319.
2. Panwiriyarat, W., Tanrattanakul, V., Pilard, J.-F., Pasetto, P. and Khaokong, C. 2013. Effect of the diisocyanate structure and the molecular weight of diols on bio-based polyurethanes. Journal of Applied Polymer Science. 130: 453-462.
3. Panwiriyarat, W., Tanrattanakul, V., Pilard, J.-F., Pasetto, P. and Khaokong, C. 2013. Preparation and properties of bio-based polyurethane containing polycaprolactone and natural rubber. J Polym Environ. 21(3): 807-815.
4. Panwiriyarat, W., Tanrattanakul, V., Pilard, J.-F., Pasetto, P. and Khaokong, C. 2013. Physical and thermal properties of polyurethane from isophorone diisocyanate, natural rubber and poly(ε-caprolactone) with high NCO:OH content. Advanced Science Letters. 19(3): 1016-1020.

5. Sadaka, F., Campistron, I., Laguerre, A. and Pilard, J.-F. 2012. Controlled chemical degradation of natural rubber using periodic acid: Application for recycling waste tyre rubber. Polymer Degradation and Stability. 97(5): 816-828.
6. Saetung, A., Rungvichaniwat, A., Campistron, I., Klinpituksa, P., Laguerre, A., Phinyocheep, P., Doutres, O. and Pilard, J.-F. 2010. Preparation and physico-mechanical, thermal and acoustic properties of flexible polyurethane foams based on hydroxytelechelic natural rubber. Journal of Applied Polymer Science. 117(2): 828-837.
7. Tran, T.K.N., Pilard, J.-F. and Pasetto, P. 2015. Recycling waste tires: Generation of functional oligomers and description of their use in the synthesis of polyurethane foams. Journal of Applied Polymer Science. 132(1): 1-11.
8. Kebir, N., Campistron, I., Laguerre, A., Pilard, J.F., Bunel, C. and Jouenne, T. 2007. Use of telechelic cis-1,4-polyisoprene cationomers in the synthesis of antibacterial ionic polyurethanes and copolyurethanes bearing ammonium groups. Biomaterials. 28(29): 4200-4208.
9. Kébir, N., Campistron, I., Laguerre, A., Pilard, J.-F., Bunel, C., Couvercelle, J.-P. and Gondard, C. 2005. Use of hydroxytelechelic cis-1,4-polyisoprene (HTPI) in the synthesis of polyurethanes (PUs). Part 1. Influence of molecular weight and chemical modification of HTPI on the mechanical and thermal properties of PUs. Polymer. 46(18): 6869-6877.
10. Kébir, N., Morandi, G., Campistron, I., Laguerre, A. and Pilard, J.-F. 2005. Synthesis of well defined amino telechelic cis-1,4-oligoisoprenes from carbonyl telechelic oligomers; first studies of their potentialities as polyurethane or polyurea materials precursors. Polymer. 46(18): 6844-6854.
11. Saetung, A., Kaenhin, L., Klinpituksa, P., Rungvichaniwat, A., Tulyapitak, T., Munleh, S., Campistron, I. and Pilard, J.-F. 2012. Synthesis, characteristic, and properties of waterborne polyurethane based on natural rubber. Journal of Applied Polymer Science. 124(4): 2742-2752.

12. Saetung, A., Rungvichaniwat, A., Campistron, I., Klinpituksa, P., Laguerre, A., Phinyocheep, P. and Pilard, J.-F. 2010. Controlled degradation of natural rubber and modification of the obtained telechelic oligoisoprenes: Preliminary study of their potentiality as polyurethane foam precursors. Journal of Applied Polymer Science. 117: 1279-1289.
13. Seo, W.J., Park, J.H., Sung, Y.T., Hwang, D.H., Kim, W.N. and Lee, H.S. 2004. Properties of water-blown rigid polyurethane foams with reactivity of raw materials. Journal of Applied Polymer Science. 93(5): 2334-2342.
14. Piszczyk, Ł., Strankowski, M., Danowska, M., Haponiuk, J.T. and Gazda, M. 2012. Preparation and characterization of rigid polyurethane–polyglycerol nanocomposite foams. European Polymer Journal. 48(10): 1726-1733.
15. Singh, H., Sharma, T.P. and Jain, A.K. 2007. Reactivity of the raw materials and their effects on the structure and properties of rigid polyurethane foams. Journal of Applied Polymer Science. 106(2): 1014-1023.
16. Gautam, R., Bassi, A.S., Yanful, E.K. and Cullen, E. 2007. Biodegradation of automotive waste polyester polyurethane foam using Pseudomonas chlororaphis ATCC55729. International Biodeterioration & Biodegradation. 60(4): 245-249.
17. Watcharakul, S., Umsakul, K., Hodgson, B., Chumeka, W. and Tanrattanakul, V. 2012. Biodegradation of a blended starch/natural rubber foam biopolymer and rubber gloves by Streptomyces coelicolor CH13. Electronic Journal of Biotechnology. 15(1): 1-13.
18. Leejarkpai, T., Suwanmanee, U., Rudeekit, Y. and Mungcharoen, T. 2011. Biodegradable kinetics of plastics under controlled composting conditions. Waste Management. 31(6): 1153-1161.
19. Jurconi, B., Feher, L., Doca, N., Vlase, T., Lazăr, C., Ţibru, I. and Ştefănescu, M. 2007. Evaluation of oily soil biodegradability by means of thermoanalytical methods. J Therm Anal Calorim. 88(2): 373-375.

CHAPTER 4

RESULTS AND DISCUSSION

4.1 Preparation and properties of bio-based polyurethane foam (PUF) from polycaprolactone diol (PCL) and natural rubber (NR)

4.1.1 Synthesis of carbonyl telechelic natural rubber (CTNR)

The ^{1}H-NMR spectrum of NR is presented in Figure 4.1, in which the chemical shift at 5.1 ppm belongs to methine proton (-C=C**H**-) of NR. The methylene (-C**H**$_2$-) and methyl proton (-C**H**$_3$) were assigned at 2.0 ppm and 1.6 ppm, respectively. To obtain carbonyl telechelic oligomers (CTNR) some of the carbon-carbon double bonds in the polyisoprene backbone were chemically oxidized by the reaction of periodic acid. This reaction allows targeting a desired molecular weight by adjusting the amount of added periodic acid. Figure 4.2 represents the ^{1}H-NMR spectrum of CTNR and all the chemical shifts of CTNR are listed in Table 4.1 [1-7].

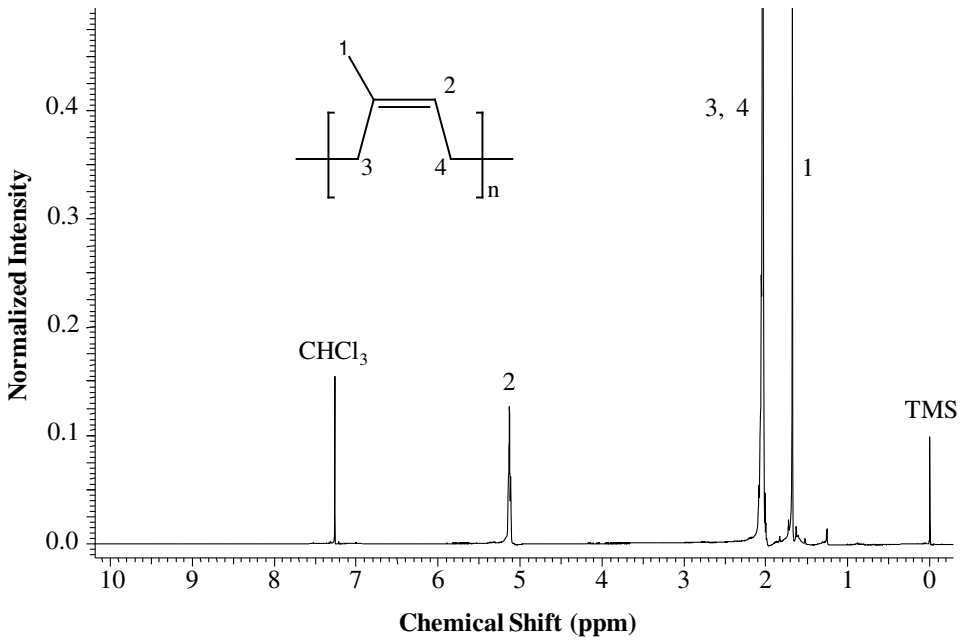

Figure 4.1 ^{1}H-NMR spectrum of natural rubber (NR).

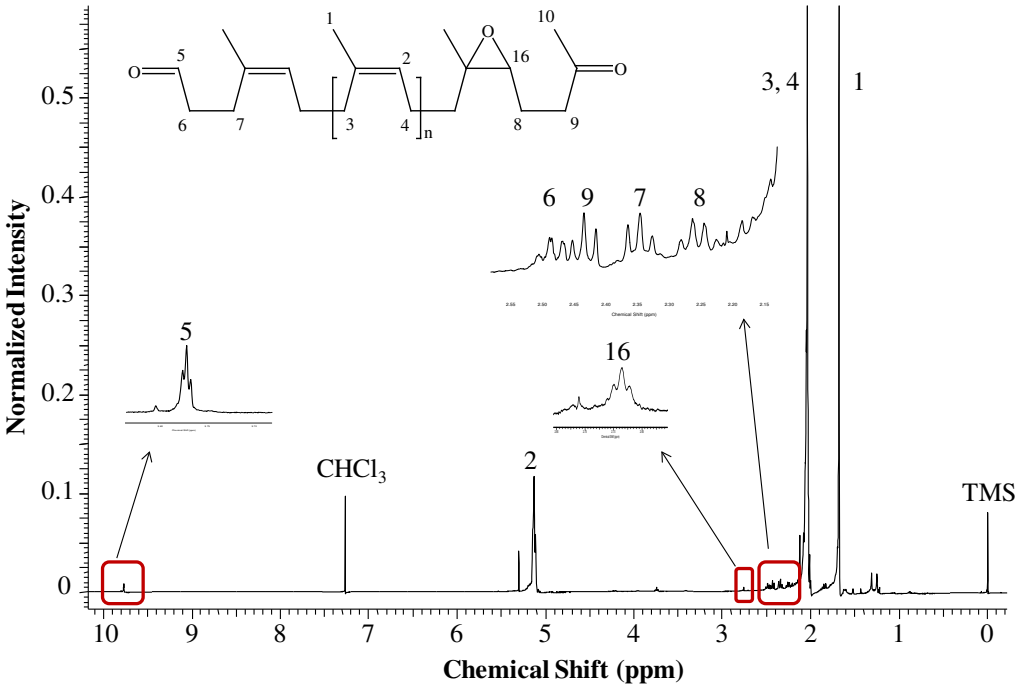

Figure 4.2 ^{1}H-NMR spectrum of CTNR.

Table 4.1 Chemical shift assignment of CTNR [1-7]

Functional group	Chemical shift (ppm)	Functional group	Chemical shift (ppm)
–C(O)**H**	9.77 (H_5)	$CH_3C(O)CH_2$**CH_2**–	2.25 (H_8)
–C=C**H**–	5.12 (H_2)	$CH_3C(O)$**CH_2**–	2.13 (H_{10})
–**CH_2**C(O)H	2.49 (H_6)	–**CH_2**–	2.00 (H_3)
$CH_3C(O)$**CH_2**–	2.43 (H_9)	–**CH_3**	1.67 (H_1)
–**CH_2**CH_2C(O)H	2.34 (H_7)	–C(O)–C**H**–	2.7 (H_{16})

The signals at 2.1, 2.15-2.6 and 9.77 ppm in the CTNR were assigned to the signals of three types of proton adjacent to carbonyl group (C***H_3***-C(O), C***H_2***-C(O) and ***H***-C(O), respectively) [6]. The functional groups and the molecular structure of CTNR were also investigated by using FTIR technique as shown in Figure 4.3. Table 4.2 shows the assignment of the functional groups. The absorption band of the carbonyl group at 1725 cm^{-1} appeared in the CTNR spectrum.

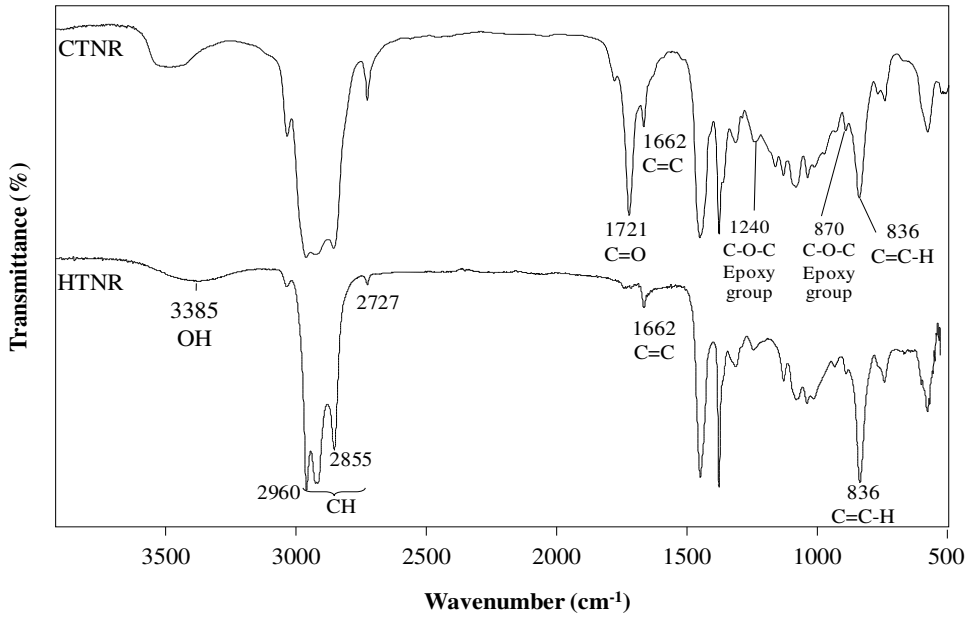

Figure 4.3 FTIR spectra of CTNR and HTNR.

Table 4.2 Wavenumber and functional groups of CTNR and HTNR [1-4,6,8-14]

Wavenumber (cm^{-1})	Functional group	Wavenumber (cm^{-1})	Functional group
3473 (CTNR)	ν (O-H) side reaction	1662	ν (C=C)
3385 (HTNR)	ν (O-H)	1451, 1375	δ (CH_2, CH_3)
2730-2900	ν (CH_2, CH_3)	836	δ (C=C–H)
1721 (CTNR)	ν (C=O)	1240	Symmetric ν(C-O-C) in epoxide groups,
1737 (HTNR)	ν (C=O)	870	Asymmetric ν(C-O-C) in epoxide groups,

ν = Stretching, δ = bending

The reaction of the periodic acid is a two-step mechanism: the first molecule forms an epoxide on some of the polyisoprene carbon-carbon double bonds, then the second molecule finishes the oxidation by breaking completely the covalent bond and forming the carbonyl chain ends. However, some of the epoxide groups remain not opened at the end of the reaction and their presence is evidenced by the peak at 2.7 ppm and 870 or 1240 cm^{-1} in NMR and FTIR spectrum of CTNR, respectively.

The average molecular weights ($\overline{M}n$ and $\overline{M}w$) and polydispersity instead of polydispersity index (Đ) of CTNR are listed in Table 4.3. This characterization was determined by GPC calibrated with polystyrene standards. The various molecular weights of CTNR were obtained by varying the amount of periodic acid (H_5IO_6). The targeted molecular weight of CTNR in this work was 2,000 g/mol. Thus only in the synthesis of CTNR3, the amount of periodic acid was calculated by multiplying by the required number of mole by the factor 4, to obtain a molecular weight of CTNR close to the target one. Molecular weight values obtained from polystyrene equivalent were converted to actual values by using Benoit's factor, B = 0.67 [3,15]. The relation of both values can be defined by $\overline{M}n$-GPC = B x $\overline{M}ps$ where $\overline{M}n$-GPC corresponds to real molecular weights of CTNR and $\overline{M}ps$ is molecular weight obtained from standard polystyrene. These obtained values are comparable with those obtained by ^{1}H-NMR method. In addition, the average functionality of CTNR was calculated in previous works [6,7,9]. It was found that the molecular weight of CTNR depended on ratio of periodic acid and NR: i.e. the molecular weight decreased with increasing ratio between periodic acid and NR. The optimum reaction time for periodic acid to cut NR chain was 24 h based on the preliminary studies [7].

Table 4.3 Characteristics of carbonyl telechelic natural rubber (CTNR)

Code	mass(H_5IO_6)/ mass(NR)	Yield (%)	$\overline{M}n$-NMR (g/mol)	$\overline{M}n$-GPC (g/mol)	$\overline{M}w$-GPC (g/ mol)	Đ
CTNR1	0.23	71	2,900	3,000	6,600	2.19
CTNR2	0.27	85	2,700	1,700	3,700	2.12
CTNR3	0.46	69	1,700	1,600	3,900	2.38

4.1.2 Synthesis of hydroxyl telechelic natural rubber (HTNR)

The ketone and aldehyde end-groups of CTNR were reduced to hydroxyl end-groups using sodium borohydride. The ^{1}H-NMR spectrum of HTNR is displayed in Figure 4.4 and the chemical shifts of HTNR are listed in Table 4.4. The HTNR spectrum did not show the signal of the aldehyde group at 9.77 ppm but the signal of the CH_2 and CH proton in α position of hydroxyl end group appeared at 3.65

and 3.80 ppm, respectively. Some of the epoxide groups in CTNR remain not opened at the end of the reaction and their presence is evidenced by the peak at 2.7 ppm relative to the H_{16} proton (Figure 4.4, HTNR spectrum). It contained ~ 5.6 mol% epoxidation. The determination of the percentage of epoxide is important because it was shown that the rigidity of the foams increases with this parameter [8].

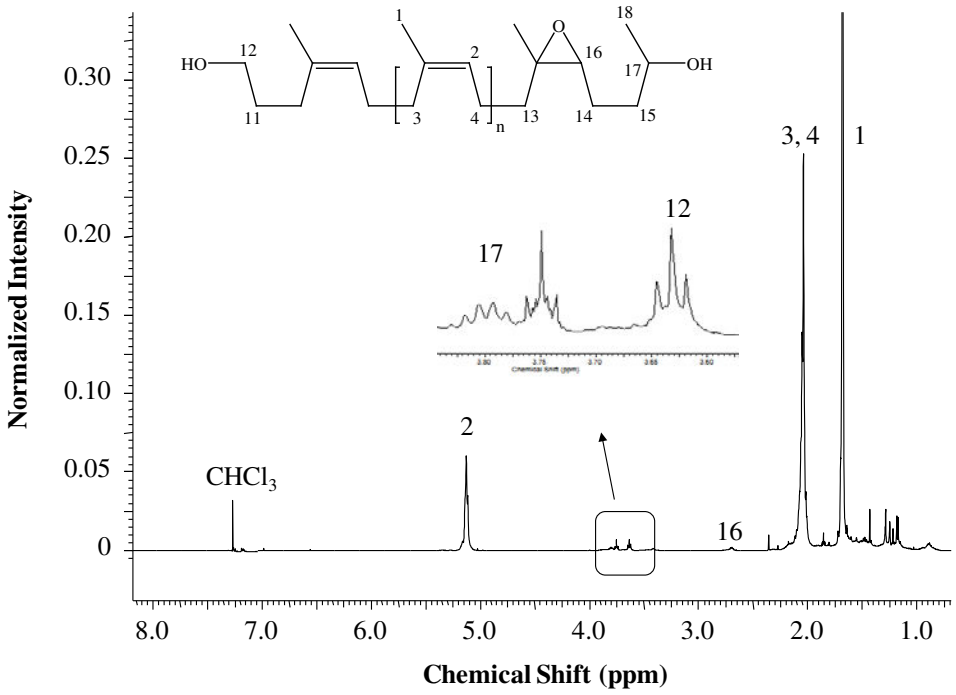

Figure 4.4 ^{1}H-NMR spectrum of HTNR.

The FTIR spectrum of HTNR is shown in Figure 4.3 and the assignment of the functional groups is listed in Table 4.2. The new peak at 3385 cm^{-1} for O-H stretching from the hydroxyl group was observed while the absorption band of carbonyl group at 1725 cm^{-1} disappeared. This result confirmed that the carbonyl group in the CTNR was completely changed to the hydroxyl group in the HTNR.

The average molecular weights ($\overline{M}n$ and $\overline{M}w$) and polydispersity instead of polydispersity index (Đ) of HTNR are shown in Table 4.5. The characterization and calculation were similar to those of CTNR. It was found that, the molecular weight of HTNR depended on ratio of periodic acid and NR [7].

Table 4.4 Chemical shift assignment of HTNR [1,3-5,7,9,11,13]

Functional group	Chemical shift (ppm)
–C=C**H**–	5.12 (H_4)
–C**H**OH	3.80 (H_9)
–C**H**$_2$OH	3.65 (H_1)
–C**H**$_2$–	2.00 (H_2)
–C**H**$_3$	1.67 (H_3)
–CH(OH)–C**H**$_3$	1.20 (H_{10})
–C(O)–C**H**–	2.7 (H_{16})

For this work, the targeted molecular weight of HTNR was 2,000 g/mol, and the obtained molecular weight of HTNR3 was 1,800 g/mol. Therefore, HTNR3 was used as a precursor to synthesize PUF from PCL and HTNR.

Table 4.5 Characteristics of hydroxyl telechelic natural rubber (HTNR)

Code	Starting material	mass($NaBH_4$) (g)	Yield (%)	$\overline{M}$n-NMR (g/mol)	$\overline{M}$n-GPC (g/mol)	$\overline{M}$w-GPC (g/ mol)	Đ
HTNR1	CTNR1	7.32	69	4,400	3,400	11,100	3.2
HTNR2	CTNR2	7.16	87	2,600	1,300	3,100	2.4
HTNR3	CTNR3	7.4	66	1,800	1,600	3,900	2.4

4.1.3 Synthesis and characterization of PUFs from HTNR and PCL

The functional groups of PUFs were identified by FTIR. Figure 4.5 illustrates the FTIR spectra of PUFs and Table 4.6 summarizes the assignment of their functional groups. The expected chemical structure of PUF from HTNR and PCL is shown in Figure 4.6

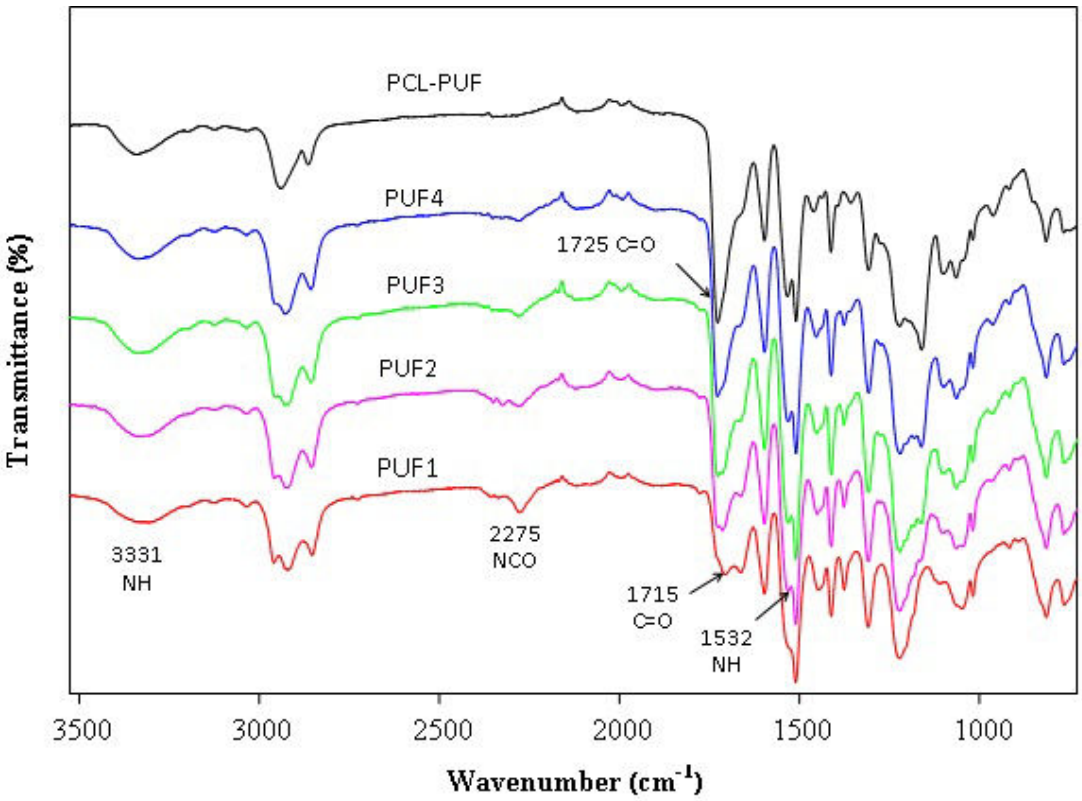

Figure 4.5 FTIR spectra of PUFs from HTNR and PCL.

Generally the characteristics of the urethane linkages were represented by the -NH stretching vibration (3200–3500 cm^{-1}) and the -NH bending vibration (1525-1550 cm^{-1}). These two main characteristics were observed in the PUF1 (NR-PUF) at 3331 and 1532 cm^{-1}, respectively. Another strong peak was noticed at 1715 cm^{-1} and assigned to the carbonyl stretching of the C=O, which was hydrogen bonded with the NH group of the hard segment. The PCL-PUF also showed the same main characteristic frequencies, except there was no peak at 2277 cm^{-1} which belongs to the free –NCO. This result indicated that the reaction between –NCO and –OH in PCL-PUF was completed. PUF2-PUF4 were synthesized from a mixture of HTNR and PCL diol and their FTIR spectra looked similar to that of PUF1 (NR-PUF). It is noticeable that the absorption band at 1715 cm^{-1} in PUF2-PUF4 increased with the increasing PCL content, indicating more hydrogen bonding [16].

Table 4.6 Wavenumber and functional groups of PUFs from HTNR, PCL and P-MDI [8,11-14,17-23]

Wavenumber (cm^{-1})	Functional group
3331	N–H stretching in urethane group, hydrogen bond NH with oxygen (carbonyl)
2730-2900	$–CH_2–$ and $–CH_3$ stretching in aliphatic compounds
2270-2280	–N=C=O stretching in isocyanates (free isocyanate)
1725	–C=O stretching, non-hydrogen boned carbonyl urethane group
1700-1720	–C=O stretching, hydrogen bonded carbonyl urethane group
1662	–C=C– stretching in aliphatic alkenes
1500-1600	–C=C– stretching in aromatic compound
1532	N–CO stretching and N–H bending in urethane group
1451	$–CH_2–$ bending in aliphatic compounds
1410	–C–N stretching (amide III band) in primary amide
1375	$–CH_3$ bending in aliphatic compounds
1308	N–H bending and C–N stretching in urethane group
1220	amide III and C–O stretching in urethane group
1046	–C–N stretching of $C–NH_2$ in primary aliphatic amines
815	C=C–N bending in isocyanate

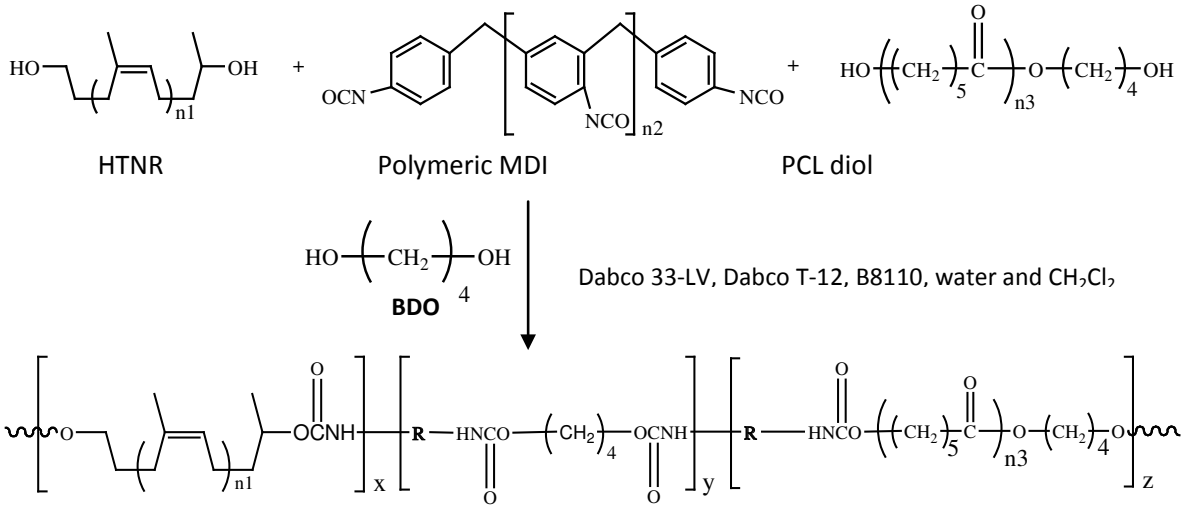

Figure 4.6 Chemical structure and reaction route of the PUF from HTNR and PCL.

4.1.4 Physical properties of PUFs from HTNR and PCL

In this part, the effect of molar ratio between HTNR and PCL (1/0, 1/0.5, 1/1 and 0.5/1) on the physical properties (foam formation rate, density and cell size) of PUFs were studied following the formulation in Table 3.3. These results are shown in Table 4.7 and Figure 4.7-4.9

Table 4.7 Physical properties of PUFs from HTNR and PCL

Code	HTNR/ PCL	Creaming Time (s)	Rising Time (s)	Tack Free Time (s)	Density (kg/m^3)	Cell Size (mm)
PUF1	1/0	25	132	216	30.80±1.95	0.42±0.07
PUF2	1/0.5	50	171	330	24.08±1.56	0.44±0.03
PUF3	1/1	45	173	277	25.20±1.39	0.55±0.10
PUF4	0.5/1	40	108	210	27.67±2.32	0.59±0.11

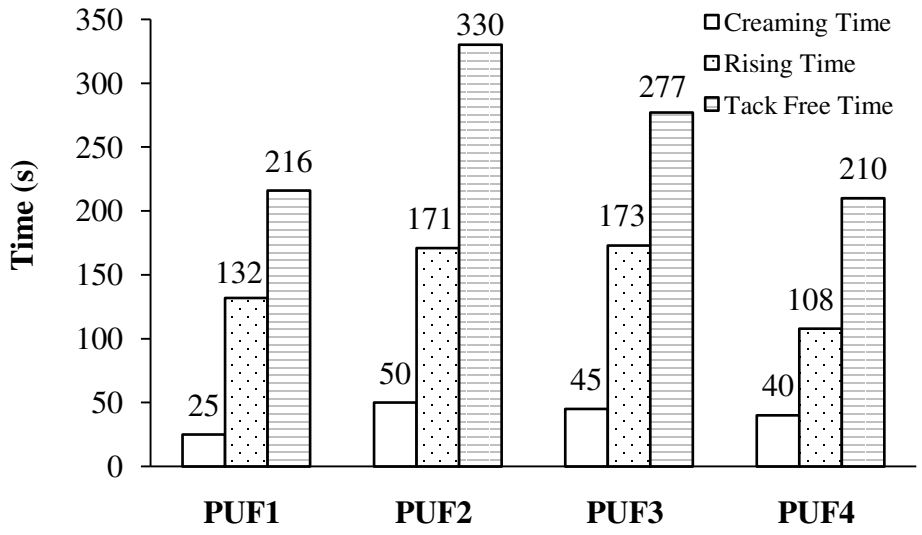

Figure 4.7 Kinetic characteristic of PUFs from HTNR and PCL.

Foam formation rate was determined by the creaming, rising and tack free time (Table 4.7 and Figure 4.7). The use of mixed diols (HTNR and PCL) induced different foam formation rate from the use of HTNR alone. Creaming time is the time measured from the beginning of mixing until the mixture had changed color and began to rise. It could indicate a time for obtaining a homogeneous mixture.

Therefore, it was expected that PUF2-PUF4 showed a longer creaming time than PUF1 because of the additional PCL. The molar ratio of HTNR/PCL also strongly affected the rising and tack free time. When HTNR content was equal or higher than PCL content (PUF2 and PUF3), the creaming, rising and tack free time were higher than those of the NR-PUF (PUF1). In contrast, when HTNR content was lower than PCL (PUF4), the rising and tack free time dropped and was lower than that of NR-PUF. Based on the preliminary study [24], PCL-PUF showed higher foam formation rate than NR-PUF. These results indicated that the hydroxyl groups from PCL are more reactive than the hydroxyl groups from HTNR leading to shorter tack free time in PUF2-PUF4. Viscosity of the mixture may play a major role in the rising time. Higher viscosity was able to retard the rising time.

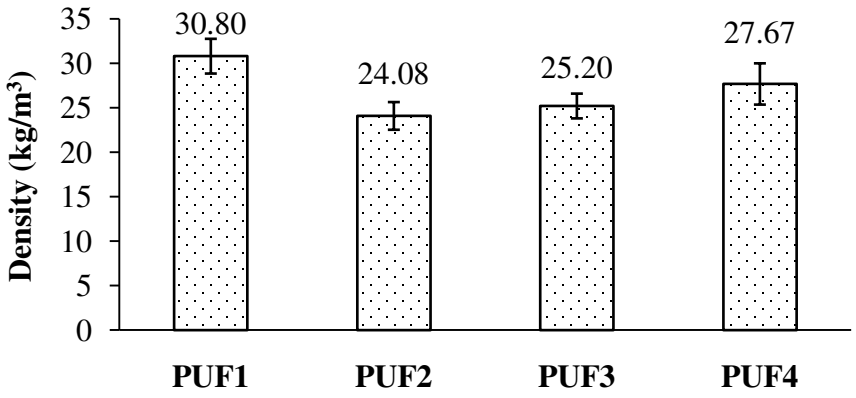

Figure 4.8 Density of PUFs from HTNR and PCL.

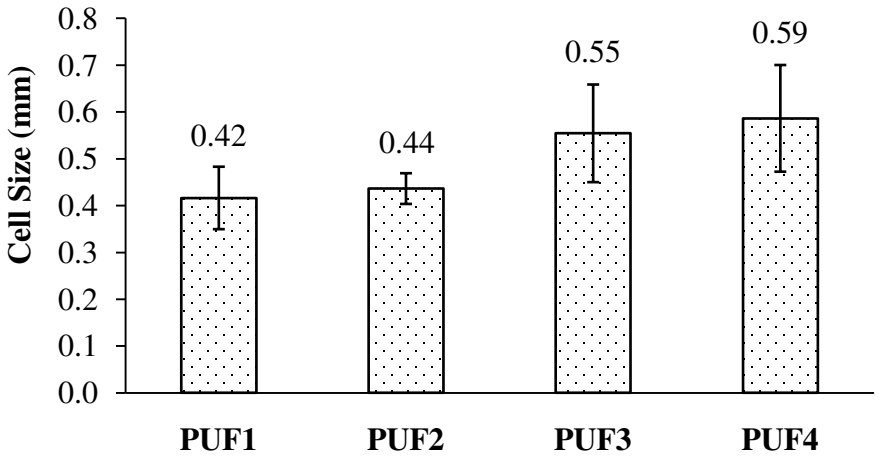

Figure 4.9 Cell size of PUFs from HTNR and PCL.

The density and cell size of PUF are listed in Table 4.7 and shown in Figure 4.8 and 4.9, respectively. The density and average cell diameter were in the range of 24-30 kg/m^3 and 0.42-0.59 mm, respectively. The NR-PUF (PUF1) showed the highest density. The molar ratio of HTNR/PCL showed slight effect on the foam density, but it tended to increase the cell size (the average diameter) when PCL content increased. There was no relationship among foam formation rate, foam density and cell size of the cellular structure.

4.1.5 Morphology of PUFs from HTNR and PCL

The cellular structure of PUF1-PUF4 was observed by SEM (Figure 4.10). All PUFs consisted of spherical and polyhedral cells and most of them were semi-closed cells. The NR-PUF (PUF1) showed almost smooth surface and well defined cell wall. In contrast, the mixture of HTNR and PCL resulted in heterogeneous surface and irregular cell shape. This was due to poor miscibility of PCL with water and high surface tension during the formation of foam [25].

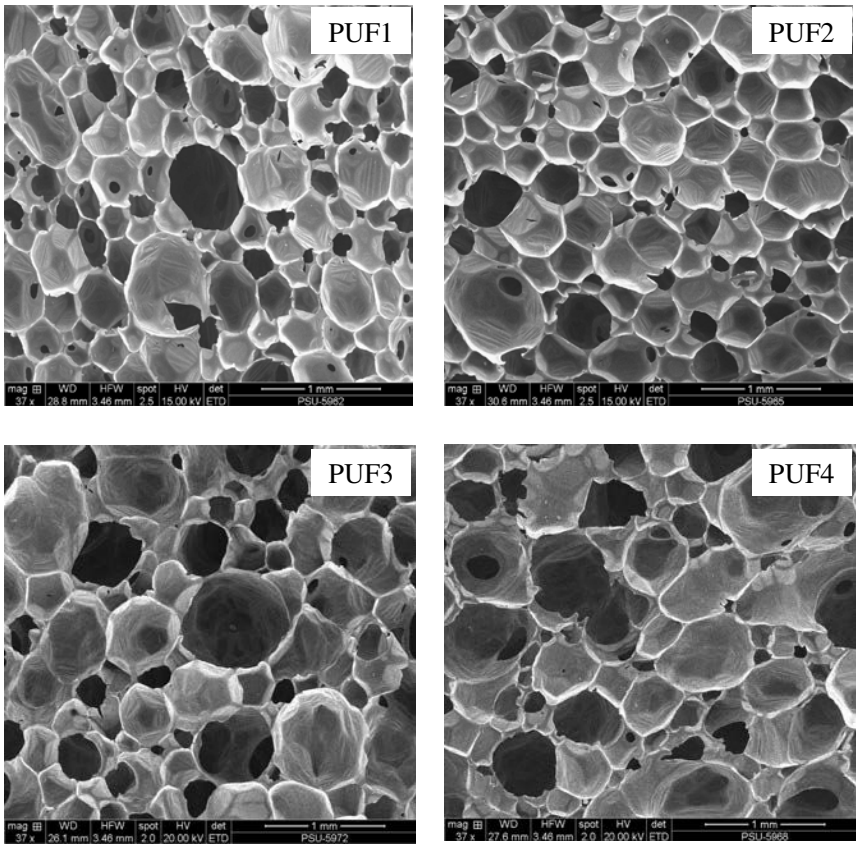

Figure 4.10 SEM micrographs of PUFs from HTNR and PCL.

4.1.6 Thermal properties of PUFs from HTNR and PCL

The effect of various molar ratio of HTNR/PCL on thermal properties of PUFs is given in Table 4.8 and Figure 4.11 - 4.12. Figure 4.11 shows the TGA curves of PUFs derived from a HTNR and HTNR/PCL polyol. Table 4.8 shows the resulting temperatures (T_{d5}, T_{d10} and T_{d50}) corresponding to 5, 10 and 50% weight loss of PUF. It was found that the PCL improved the thermal stability of the PUF. The best thermal stability was found in PUF3, for which T_{d5}, T_{d10} and T_{d50} were higher than those of PUF1 of approximately 26, 10 and 14 °C, respectively. Figure 4.12 shows the DTG curves of PUFs. A two step thermal degradation was observed for PUF1 and a three step thermal degradation was observed for PUF2-PUF4. Weight loss and characteristic temperature determined from the maximum of the derivative curve (T_{max}) were analyzed. The first stage degradation at 326 – 333 °C corresponded to urethane bond breaking, the second stage at 352 – 370 °C corresponded to a decomposition of precursors (HTNR) [13,14], the third stage at 437 – 465 °C corresponded to a decomposition of precursors (PCL) [26]. The maximum degradation temperature at the second and third stages was dependent on the PCL diol content.

Table 4.8 Thermal properties of PUFs from HTNR and PCL

Sample	HTNR /PCL	T_{d5} (°C)	T_{d10} (°C)	T_{d50} (°C)	1st Step		2nd Step		3rd Step	
					T_{max} (°C)	weight loss(%)	T_{max} (°C)	weight loss(%)	T_{max} (°C)	weight loss(%)
PUF1	1/0	239	289	368	332.9	27.22	357.9	15.59	-	-
PUF2	1/0.5	247	290	373	328.5	24.58	352.4	13.02	437.7	32.47
PUF3	1/1	265	299	382	326.4	20.46	366.3	20.68	450.9	30.03
PUF4	0.5/1	253	293	381	327.8	22.16	370.6	21.1	465	32.69

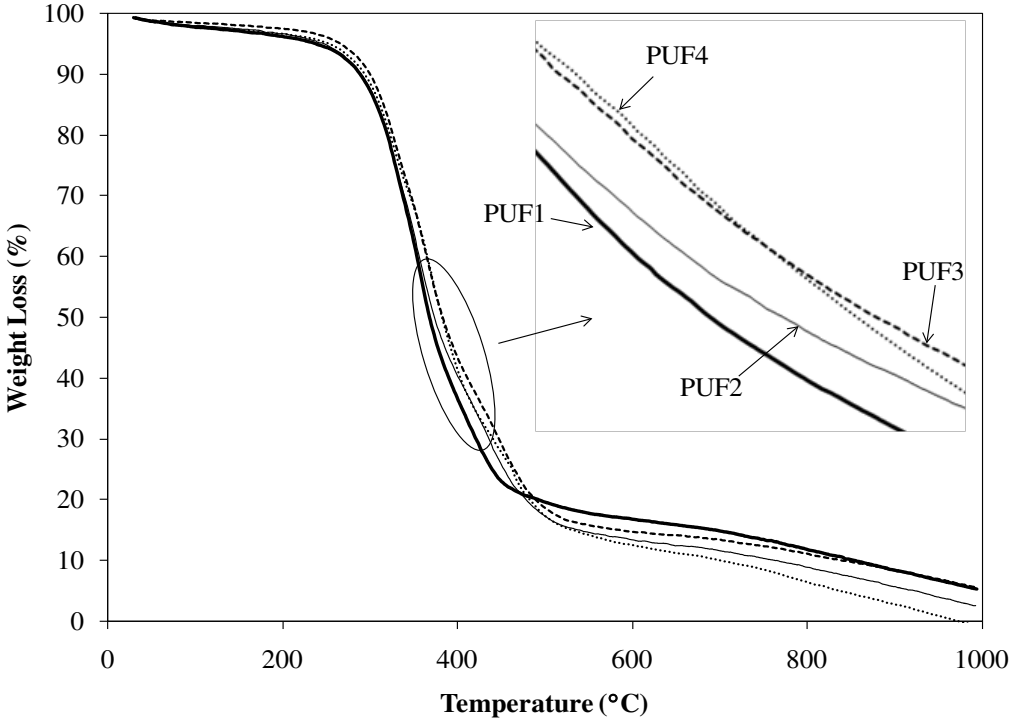

Figure 4.11 TGA curves of PUFs from HTNR and PCL.

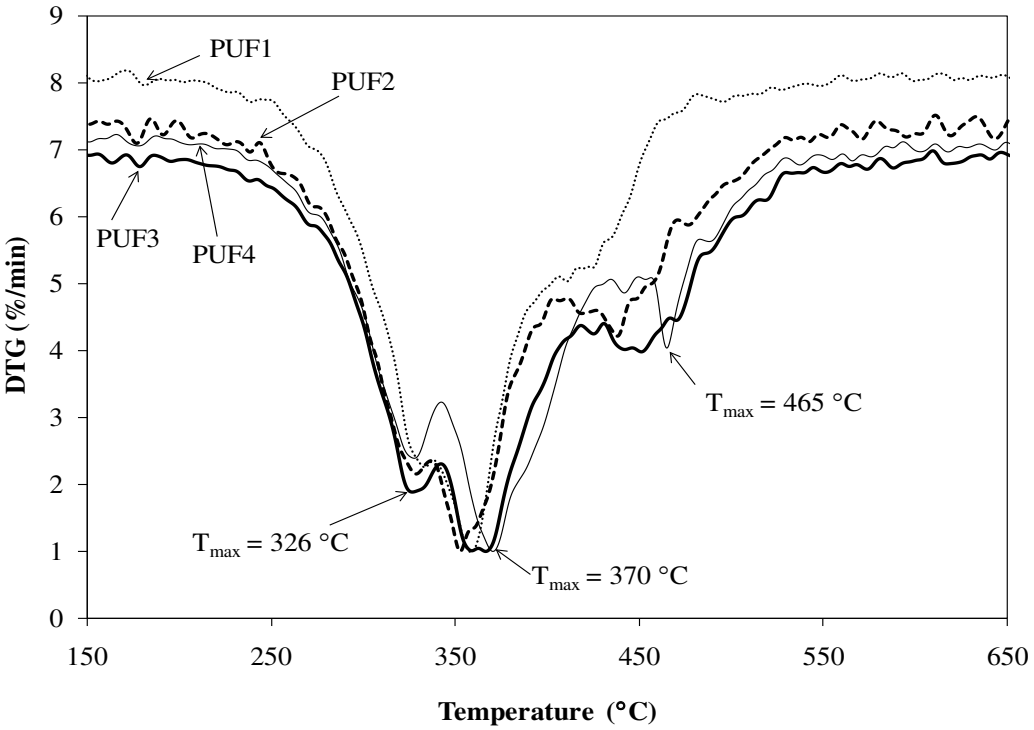

Figure 4.12 DTG curves of PUFs from HTNR and PCL.

4.1.7 Mechanical properties of PUFs from HTNR and PCL

In this part, the effect of ratio between HTNR and PCL on the mechanical properties of PUFs was studied in comparison with HTNR foam following the formulations in Table 3.3. These results are shown in Table 4.9 - 4.10 and Figure 4.13 - 4.19.

4.1.7.1 Tensile properties

The effect of various molar ratio of HTNR/PCL on tensile strength and Elongation at break of PUFs is given in Table 4.9 and Figure 4.13 - 4.15. The tensile properties of PUFs are listed in Table 4.9. The tensile strength of PUF1, PUF2, PUF3 and PUF4 were 114.66, 81.44, 86.20 and 103.62 kPa, respectively. The corresponding elongation at break was 65, 50, 48.33 and 51.25 %, respectively. It was found that PUF1 showed the highest tensile strength and elongation at break. The addition of PCL to the NR-PUF caused a decrease in the tensile strength and elongation at break. In general the tensile strength of foam strongly depends on the foam density; therefore, the density of each tested sample should be considered. In this point of view, the tensile strength was normalized with the density and the derived value was referred to as a specific tensile strength. All PUFs showed the specific tensile strength in the same range, 3.37-3.84 kN.m/kg.

Table 4.9 Tensile properties of PUFs from HTNR and PCL

Code	HTNR/ PCL	Tensile Strength (kPa)	Specific Tensile Strength (kN.m/kg)	Elongation at Break (%)
PUF1	1/0	114.66±2.00	3.84	65.00±8.66
PUF2	1/0.5	81.44±6.50	3.37	50.00±8.16
PUF3	1/1	86.20±9.58	3.41	48.33±2.89
PUF4	0.5/1	103.62±3.13	3.82	51.25±4.79

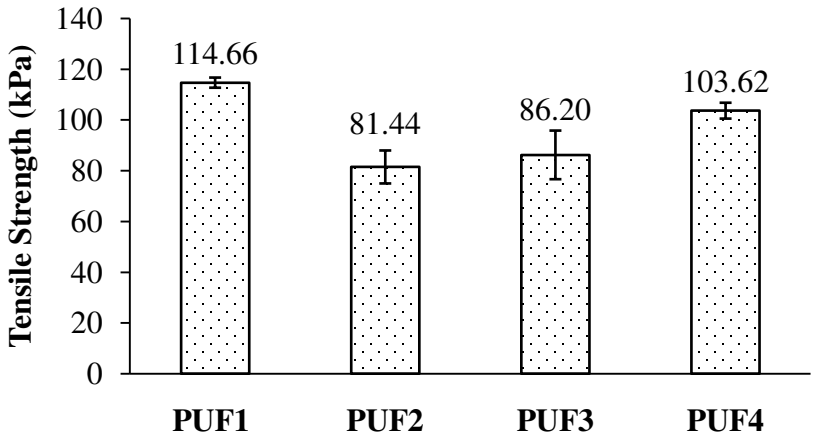

Figure 4.13 Tensile Strength of PUFs from HTNR and PCL.

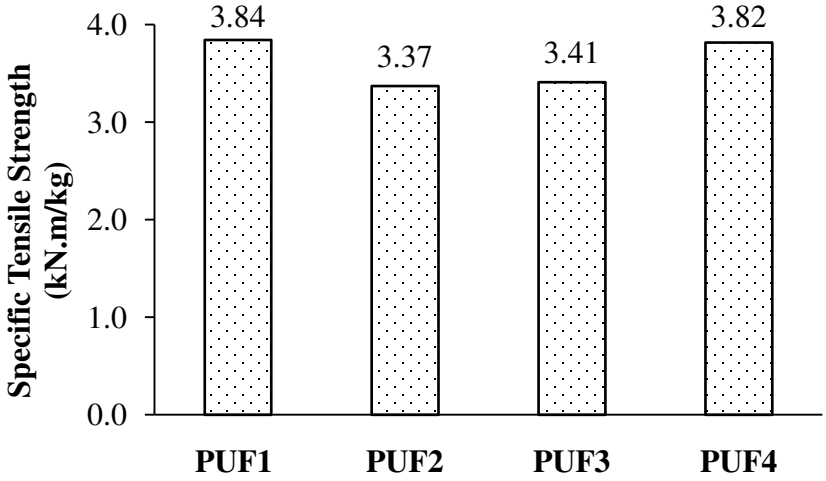

Figure 4.14 Specific tensile strength of PUFs from HTNR and PCL.

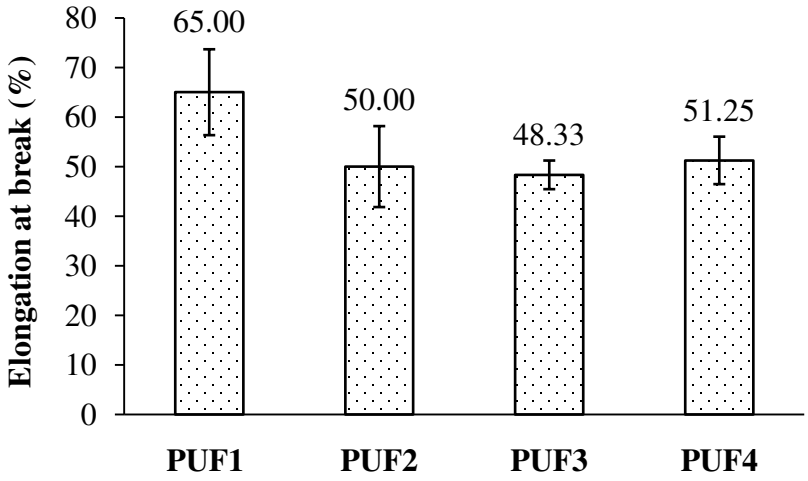

Figure 4.15 Elongation at break of PUFs from HTNR and PCL.

4.1.7.2 Compression properties

The effect of molar ratio of HTNR/PCL on compressive strength and compression set of PUFs is given in Table 4.10 and Figure 4.16 - 4.19. The compressive strength of PUF decreased when PCL increased. This phenomenon was also observed in the specific compressive strength, which was obtained by normalization of the compressive strength with the density of the sample. HTNR has an isoprenic structure which has a stronger tensile and compressive strength than that of ether or ester structure of commercial polyols [14].

Table 4.10 Compression properties of PUF from HTNR and PCL

Code	HTNR/ PCL	Compressive Strength (kPa)	Specific Compressive Strength (kN.m/kg)	Compression Set (%)	Specific Compression Set (%.m^3/kg)
PUF1	1/0	25.08±0.41	0.72	45.41±1.07	1.51
PUF2	1/0.5	20.36±0.93	0.61	40.57±0.58	1.34
PUF3	1/1	15.13±2.96	0.56	46.98±1.94	1.35
PUF4	0.5/1	14.49±1.36	0.46	48.76±1.82	1.69

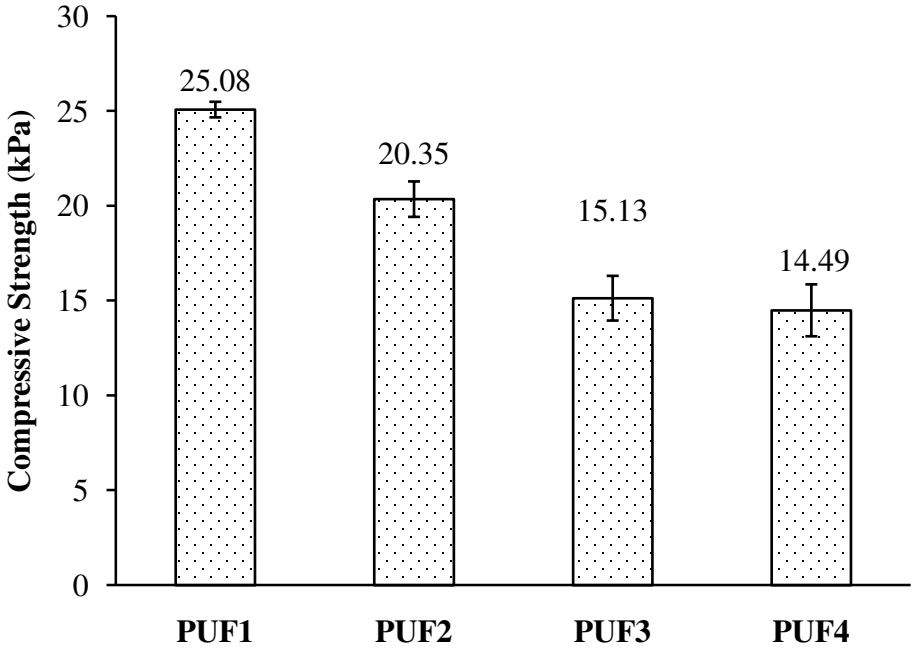

Figure 4.16 Compressive strength of PUFs from HTNR and PCL.

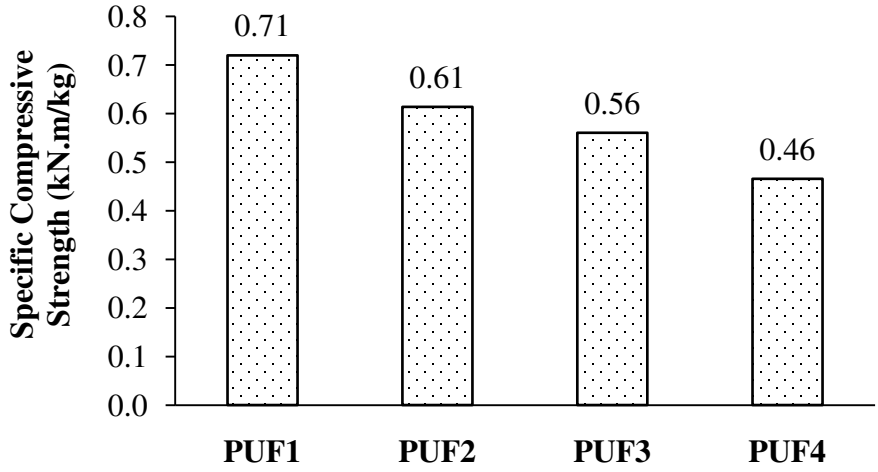

Figure 4.17 Specific compressive strength of PUFs from HTNR and PCL.

The compression set was performed to study the dimensional durability of foam under stress [27]. A low compression set indicates that the foam is more flexible or has a high elasticity, i.e., it can recover better its original shape after deformation. The addition of PCL could influence the compression set of PUF. PUF2 showed the lowest value (40%) whereas PUF3 and PUF4 showed higher value than PUF1. However, the compression set value of all PUFs was relatively high. This might be due to the effect of cellular structure which contained lots of semi-closed cells making it more rigid. It should be noted that the mechanical properties (tensile strength, elongation at break and compressive strength) of HTNR foam (PUF1) obtained in this study were higher than that reported previously [7,14].

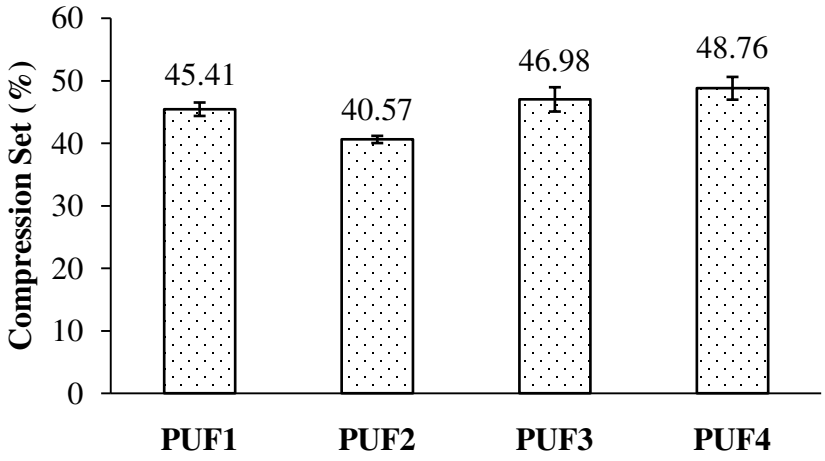

Figure 4.18 Compression set of PUFs from HTNR and PCL.

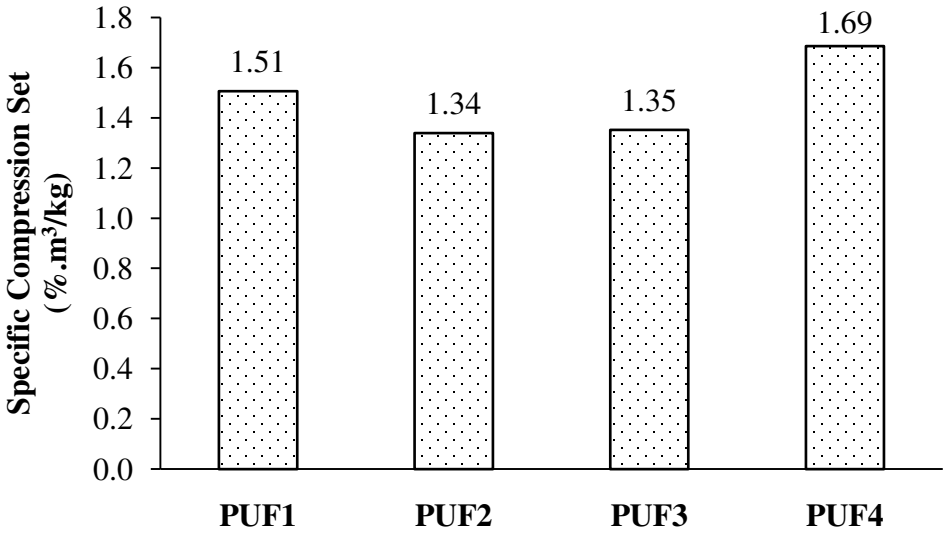

Figure 4.19 Specific compression set of PUFs from HTNR and PCL.

4.1.8 Biodegradation of PUFs from HTNR and PCL

The effect of various molar ratio of HTNR/PCL on biodegradation of PUF are given in Table 4.11 and Figure 4.20.

Table 4.11 Percentage of biodegradation of PUFs from HTNR and PCL

Time	Samples / percentage biodegradation					
(day)	PUF1	PUF2	PUF3	PUF4	Sodium benzoate	LDPE
2	1.03	1.03	0.90	1.03	12.51	0.34
5	2.06	1.89	1.45	1.54	21.60	0.34
7	3.09	3.09	2.95	3.60	28.97	0.34
9	3.77	3.77	4.14	5.14	32.23	0.34
12	4.46	5.31	6.02	6.17	33.60	0.34
14	4.80	6.69	6.34	6.51	34.29	0.69
16	5.31	7.71	6.45	6.51	34.46	1.03
19	5.83	8.74	6.52	6.51	35.49	1.20
21	6.51	9.77	6.59	6.69	36.52	1.37
23	7.37	10.80	7.31	7.20	37.54	1.54
26	7.89	10.97	7.72	7.20	37.89	2.23
28	8.40	11.31	7.76	7.54	38.92	2.23
30	8.74	11.66	7.95	7.54	39.94	2.23

Table 4.11 (cont.)

Time (day)	Samples / percentage biodegradation					
	PUF1	PUF2	PUF3	PUF4	Sodium benzoate	LDPE
33	8.91	12.86	8.12	7.89	40.63	2.23
35	9.43	14.91	9.11	9.26	41.66	2.23
37	10.63	19.54	11.95	12.51	44.40	2.23
40	12.86	25.71	14.52	17.14	48.17	2.23
42	15.09	30.17	18.02	20.74	50.06	2.23
44	16.80	33.26	20.22	24.00	52.63	2.23
47	20.74	36.00	25.12	25.54	56.57	2.74
49	25.54	38.92	28.12	28.29	60.00	2.92
51	28.46	40.63	29.76	30.00	61.89	3.09
54	29.49	41.83	31.97	31.37	62.92	3.09
56	30.69	42.86	33.00	32.92	64.29	3.25
58	31.37	43.54	35.12	33.77	64.80	3.25
60	31.89	45.60	37.12	35.49	64.97	3.25

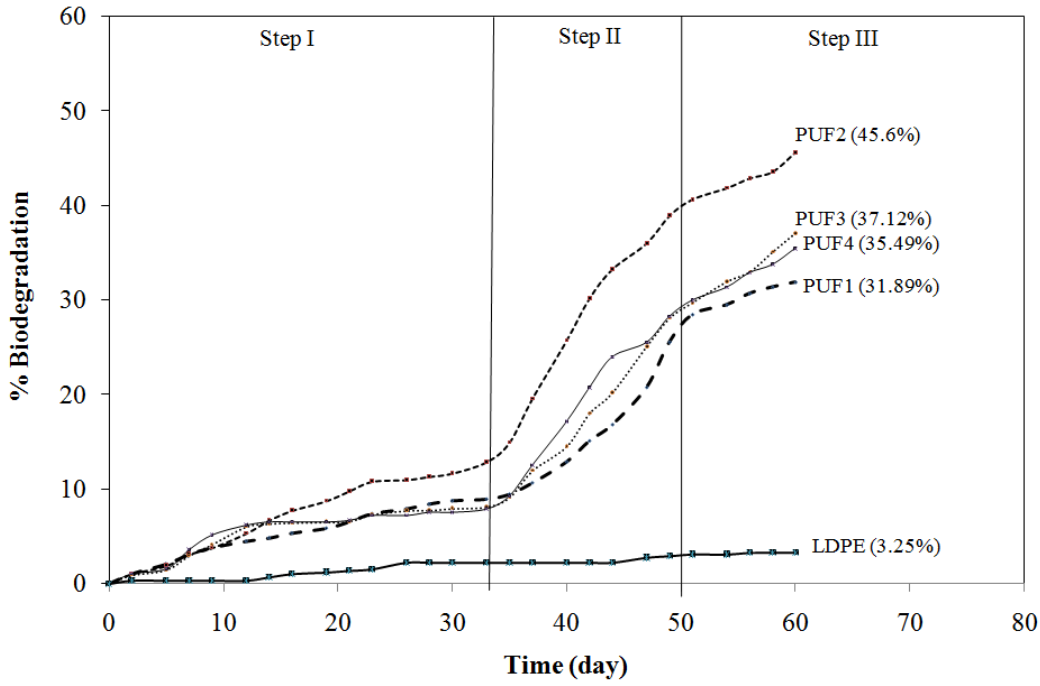

Figure 4.20 Percentage biodegradation of PUFs from HTNR and PCL.

The Sturm test is a common test to measure biodegradation. It is simple and low cost. Heterotrophs bacteria are a class of microorganisms that obtain carbon by ingesting organic molecules, need oxygen for the respiration and consequent production of the energy required to move, build cells, transport materials through the body, etc. The by-products of their metabolism are mainly water and carbon dioxide. Therefore, to follow the growth of such bacteria, two possibilities are available: (1) measure oxygen consumption or (2) carbon dioxide production. The principle of the Sturm test is based on that CO_2 is produced by the bacteria which generate it when they are alive and using the organic compounds contained in the hermetic systems as feed. Consequently, given a certain number of bacterial cells, for a biodegradable compound such sodium benzoate the amount of produced CO_2 should be the maximum; for a non-biodegradable material such as low density polyethylene should be zero, and it should be intermediate for a biodegradable compound. In this study, the Sturm test was adapted to the foams and it was carried out for 28 days to calculate the percentage of biodegradation of PUFs (Table 4.11 and Figure 4.20). PUF1, 2, 3 and 4 were cubes cut from the relative foams and LDPE sample was cut from a LDPE bottle. It was found that the percentage biodegradation of PUF1, PUF2, PUF3, PUF4 and LDPE was 8.4, 11.3, 7.7, 7.5 and 2.2%, respectively. Typically, an initial phase of very slow degradation (induction time) is observed in the biodegradability tests. This period can take several weeks based on the adaptation/selection of the microorganisms that metabolize the substrate (the sample) efficiently. A value of 10% degradation is universally used to describe the end of the induction time. Therefore, the test was continued for 60 days. A significant difference of biodegradability among the samples was observed; the percentage biodegradation is ranked in the following order: PUF2 (45.6%) > PUF3 (37.1%) > PUF4 (35.5%) > PUF1 (31.9%) > LDPE (3.3%). The percentage of biodegradation value of sodium benzoate (the positive control sample) was 39 and 65% at 28 and 60 days, respectively. It is known that biodegradation of the biodegradable polymers depends on type of microorganisms. It has been reported that percentage of biodegradation of the NR latex gloves was 10% when using Streptomyces coelicolor CH13 for 30 days [28], whereas the PUF1 showed 8.74 % for 30 days. We found that the colony numbers of PUF2 increased from $8x10^4$ CFU/mL at the beginning of the biodegradation test to $54x10^4$ CFU/mL at 60 days, indicating

the growth of bacteria (Figure 4.21). It was beyond our research scope to identify the type of bacteria. It is common to use the microorganisms from the waste water from certain sources for the biodegradation test; thus, we used the microorganisms as presented in the wasted water (sewage water) from the concentrated latex factory. It was assumed that some microorganisms in this waste water could consume NR as their carbon source.

We believed that foam density also played a role on the biodegradability. PUF2 had lower density than PUF4, leading to higher percentage of biodegradation, even though PUF2 had lower PCL diol content. Kinetics rate of degradation of PUF taken from the slope of curves in Figure 4.20 can be classified into 3 steps. Step I was the induction time as described earlier. This period took approximately 33 days. After the induction time (STEP II), the microorganisms acted more efficiently and produced more CO_2. This period occurred until the 50th day, and then the rate of degradation seemed to decrease. The 3 steps of degradation rate were also observed in LDPE and sodium benzoate. This should be due to the behavior of the microorganisms because all samples were tested with the same source of waste water (sewage water in the latex rubber factory). Although LDPE showed 3.3 % biodegradation, this value was very low and insignificant. There might have a few carbon sources for the microorganisms. Previous publications showed biodegradation of LDPE in a wide range, i.e. 8.5% [29] and 0.56% [30].

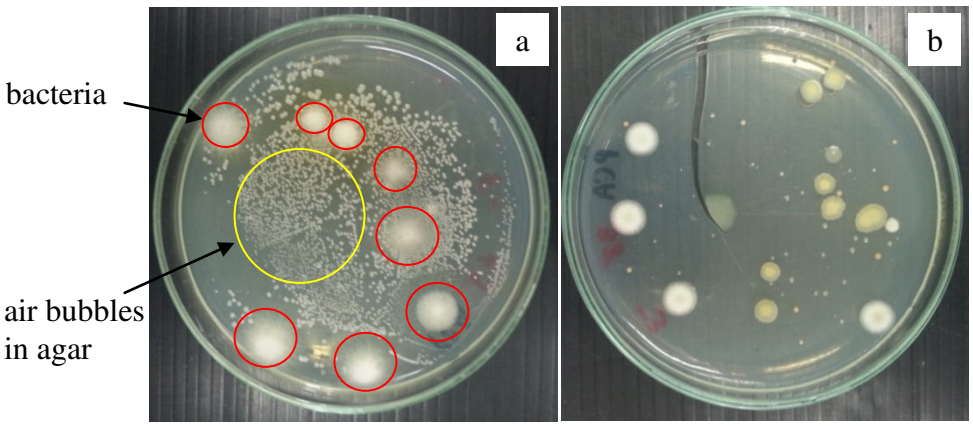

Figure 4.21 Colonies of total bacteria grown on Plate Count Agar of PUFs from HTNR/PCL (1/0.5 molar ratio) dilution 10^{-3}: before (a) and after (b) 60 days of biodegradation test

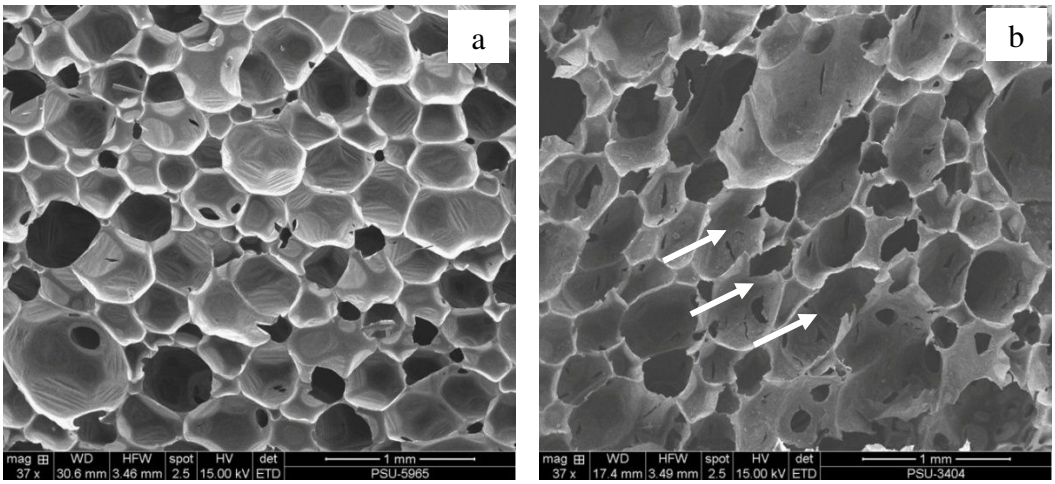

Figure 4.22 SEM micrographs of PUFs from HTNR/PCL (1/0.5 molar ratio) before (a) and after (b) 60 days of biodegradation test

As biodegradation is a phenomenon that begins at the surface of the materials, the foam morphology has been analyzed before and after the Sturm test through SEM. The micrographs of the tested samples treated with microorganisms for 60 days showed widespread tiny cracks on the cell wall (Figure 4.22). The hydrophilicity of NR and PCL could be compared in terms of water contact angle, 106° and 77° for NR and PCL, respectively [31,32]. The addition of PCL may increase hydrophilicity of PUF leading to higher biodegradation in PUF2 and PUF4. Furthermore, the effect of cell size was observed in PUF consisted of HTNR and PCL. The smaller cell size (PUF2) showed higher biodegradation than the larger one (PUF4) although PUF2 had lower PCL content than PUF4. Higher surface areas in the smaller cell sizes may attribute to this result. The smallest cell size of PUF1 did not play the role in the biodegradation.

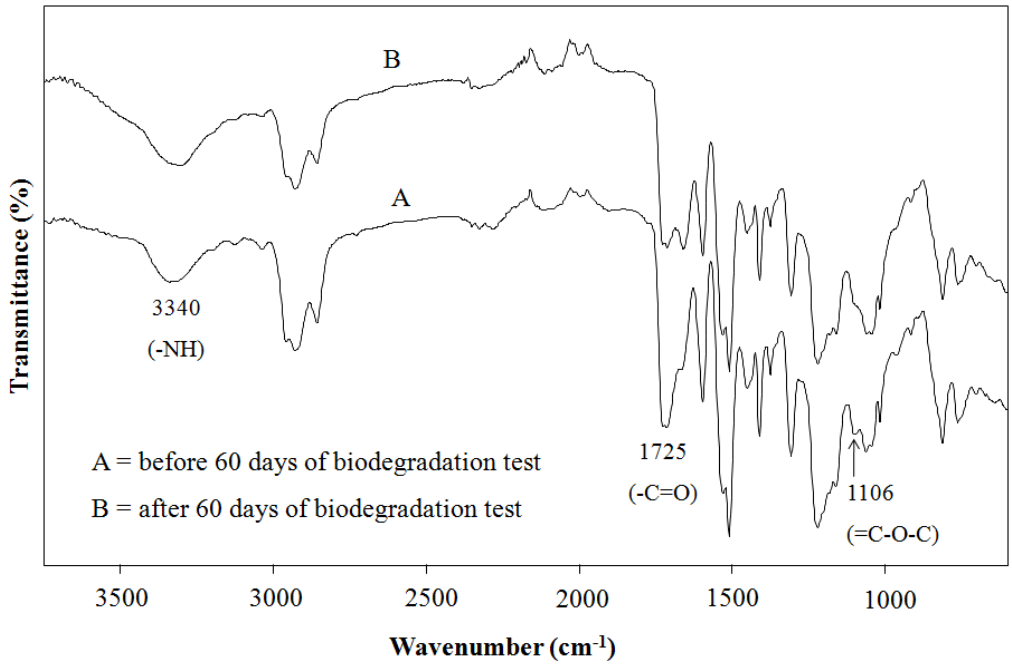

Figure 4.23 FTIR spectra of PUFs from HTNR/PCL (1/0.5 molar ratio)

An investigation was carried out by FTIR to check if a change had occurred in the chemical structure of the surface. The peak at 1725 cm^{-1} representing a carbonyl group of esters almost disappeared in the FTIR spectrum of tested sample after 60 days of incubation (Figure 4.23). The peak at 1106 cm^{-1} represents =C–O-C stretching in poly(ester urethane) [33] and it also disappeared in the tested samples. These results indicated that an ester hydrolysis took place as a result of the microbial treatment.

4.2 Preparation and properties of bio-based polyurethane foam (PUF) from polycaprolactone diol (PCL) and waste tires (WT)

4.2.1 Composition of WT

The thermogravimetric analysis (TGA) was used to quantify the composition of WT. This method permits in a shorter experimental time the separation of tire main components (oil, polymer, carbon black and other chemical). TGA-DTG results obtained from one tire sample rubber are shown in Figure 4.24. The waste tire crumbs used in this study came from the same source as that used by Sadaka *et al.* [6] and Tran *et al.* [7]; in the previous study they have been fully characterized. Therefore, in the present study only the thermogravimetric analysis was executed again to verify the rubber composition. Sadaka *et al.* [6] reported that processed oil or any other low boiling-point components degraded between 200-300°C, and NR and BR degraded with a maximum rate at 350°C and 410°C, respectively. The residue at 410-560°C was attributed to carbon black and the residue at the higher temperature was assigned to the inorganic fillers. The result obtained in the present study (Figure 4.24) agreed with that reported by Sadaka *et al.* [6]. The waste tire crumbs consisted of approximately 32% NR and 18% BR.

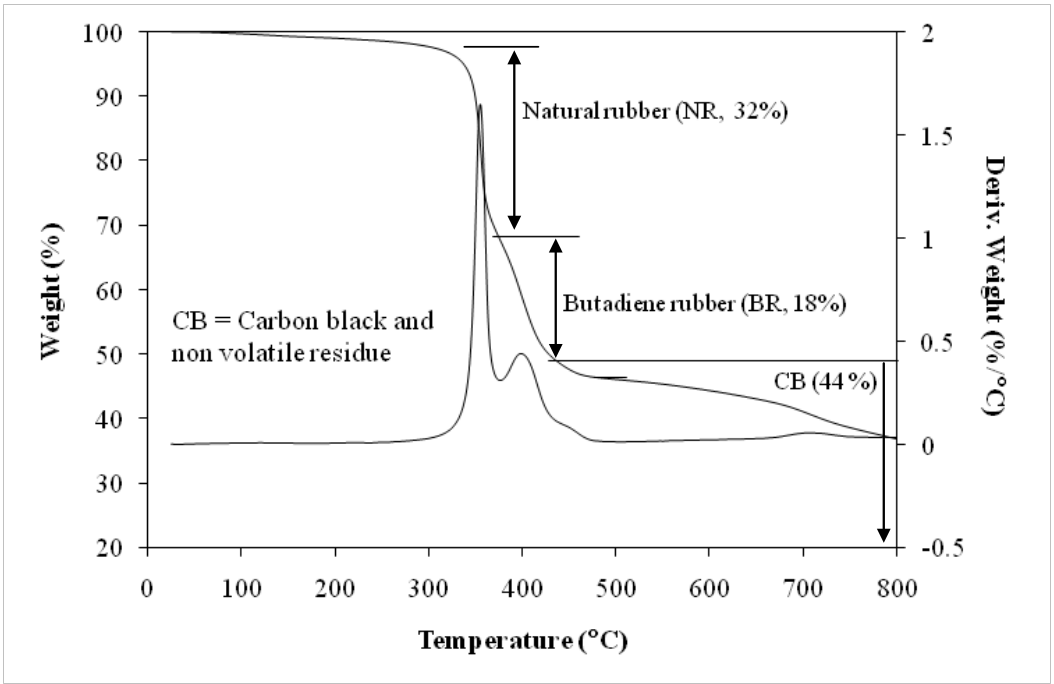

Figure 4.24 TGA and DTG curves of waste tires.

4.2.2 Synthesis of carbonyl telechelic oligomer from waste tires (CTWT)

The chemical structure of CTWT was characterized using ^{1}H-NMR data and all the chemical shifts as shown in Figure 4.25 and Table 4.12, respectively. The originality of the approach of this research work is that the polyisoprene (PI) and polybutadiene (PB) chains in the waste tire crumbs are reduced and functionalized to small oligomers. New signals appeared at 2.1, 2.15-2.6 and 9.8 ppm in the CTWT. The CTWT consisted of carbonyl telechelic natural rubber (CTNR) and carbonyl telechelic butadiene rubber (CTBR). These signals were assigned to the protons adjacent to carbonyl functional groups: 2.49 ppm ($H_{6+6'}$, **-C*H₂***CHO), 2.43 ppm (H_9, CH_3COC***H₂***CH_2-), 2.34 ppm (H_7, **-C*H₂***CH_2CHO), 2.25 ppm (H_8, CH_3COCH_2C***H₂***-), 2.10 ppm (H_{10}, **C*H₃***$COCH_2CH_2$**-)** and 9.8 ppm ($H_{5+5'}$, **-**CH_2C***H***O). The results confirm the presence of ketone and aldehyde groups at the chain ends of CTWT [6].

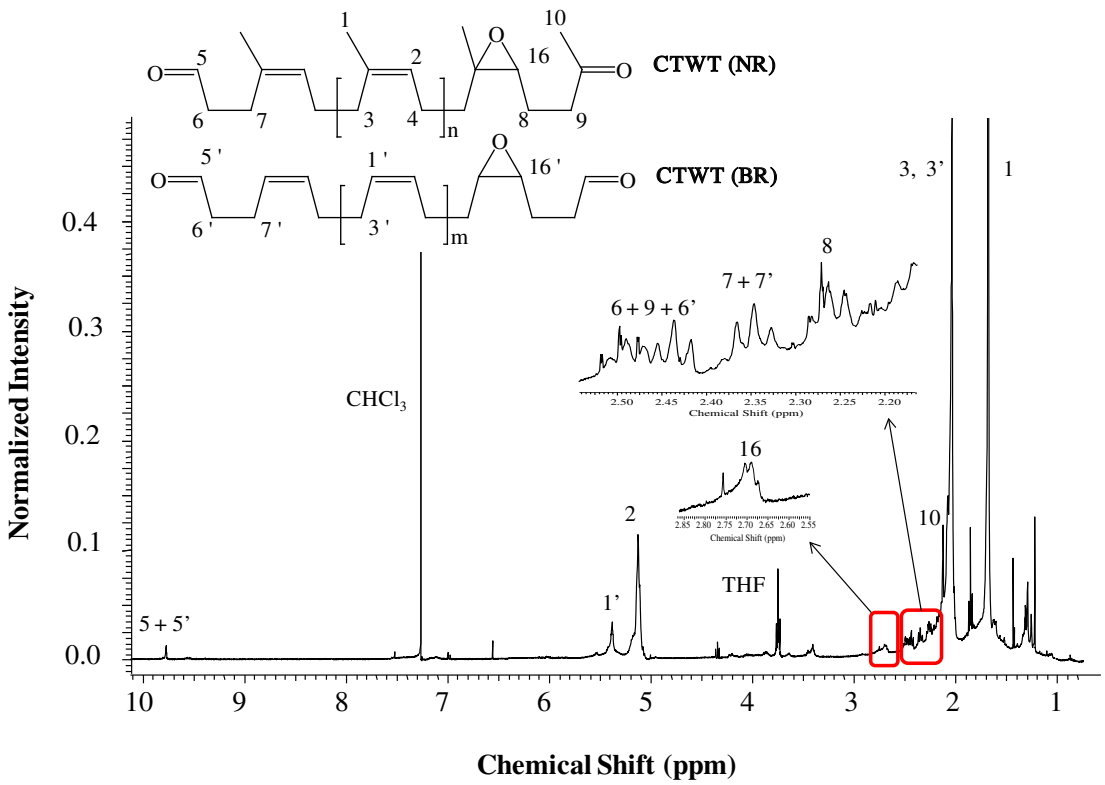

Figure 4.25 ^{1}H-NMR spectrum of CTWT.

Table 4.12 Chemical shift assignment of CTWT [7].

CTWT (NR)		CTWT (BR)	
Functional group	Chemical shift (ppm)	Functional group	Chemical shift (ppm)
–C(O)H	9.77 (H_5)	–C(O)H	9.77 ($H_{5'}$)
–C=CH–	5.12 (H_2)	–C=CH–	5.38 ($H_{1'}$)
$–CH_2C(O)H$	2.49 (H_6)	$–CH_2C(O)H$	2.49 ($H_{6'}$)
$CH_3C(O)CH_2–$	2.43 (H_9)	$–CH_2CH_2C(O)H$	2.34 ($H_{7'}$)
$–CH_2CH_2C(O)H$	2.34 (H_7)	$– CH_2CH_2CH=CH–$	2.00 ($H_{3'}$)
$CH_3C(O)CH_2CH_2$ –	2.25 (H_8)		
$CH_3C(O)CH_2–$	2.13 (H_{10})		
$–CH_2–$	2.00 (H_3)		
$–CH_3$	1.67 (H_1)		
–C(O)–CH–	2.7 (H_{16})	–HC(O)–C–	2.7 ($H_{16'}$)

When performing the synthesis of carbonyl oligomers, some epoxide units remain intact and can be detected from the signal of the proton in the 16 or 16′ positions; the degree of epoxidation and the molecular weight of oligoisoprene and oligobutadiene chains were determined directly from the ^{1}H-NMR spectra of the hydroxyl oligomers and calculated according to equation (1) – (6), respectively. "I" refers to the value of the integration of the relative protons as shown in Figure 4.25 and Figure 4.27 [7].

The proportion of epoxidation of HTNR $= \tau_{epox\ -HTNR} = \frac{I_{16}}{I_{16} + 2(I_2)}$ (1)

The ratio between oligobutadiene and oligoisoprene $= \tau_{OB/OI} = \frac{I_{1'}}{I_{1'} + 2(I_2)}$ (2)

The proportion of epoxidation of oligobutadiene

$$= \tau_{epox\ -OB} = \frac{\tau_{OB\ /OI}\ x\ (I_{16} + I_{16'})}{[\tau_{OB\ /OI}\ x\ (I_{16} + I_{16'})]\ + I_{1'}} \quad (3)$$

The proportion of epoxidation of oligoisoprene

$$= \tau_{epox\text{-}OI} = \frac{(1-\tau_{OB/OI}) \times (I_{16}+I_{16'})}{[(1-\tau_{OB/OI}) \times (I_{16}+I_{16'})] + I_2} \quad (4)$$

The molecular weight of oligobutadiene

$$= M_{n,NMR\text{-}HTWT\text{-}OB} = \left\{\frac{2I_{1'} \times 54.09}{I_{6,9,6'} \times (\tau_{OB/OI}) \times (1-\tau_{epox\text{-}OB})}\right\} + 86 \quad (5)$$

The molecular weight of oligoisoprene

$$= M_{n,NMR\text{-}HTWT\text{-}OI} = \left\{\frac{4I_2 \times 68.12}{I_{6,9,6'} \times (1-\tau_{OB/OI}) \times (1-\tau_{epox\text{-}OI})}\right\} + 128 \quad (6)$$

FTIR spectrum and assignment of functional group of CTWT are shown in Figure 4.26 and Table 4.13. Being the CTWT made of PI and PB, their main peaks can be found in the FTIR spectrum. Characteristic peaks in PI were found at 1665 cm^{-1} representing symmetric –C=CH stretching. The band at 837 cm^{-1} was attributed to –C=CH bending. The peaks of CH_2 and CH_3 stretching appeared at 2973 and 2850 cm^{-1}, respectively. The band at 1450 and 1377 cm^{-1} were assigned to C–H bending of CH_2 and CH_3, respectively [34,35]. FTIR spectrum of CTWT showed very strong absorption peak at 1720 and 1775 cm^{-1} corresponding to the carbonyl group.

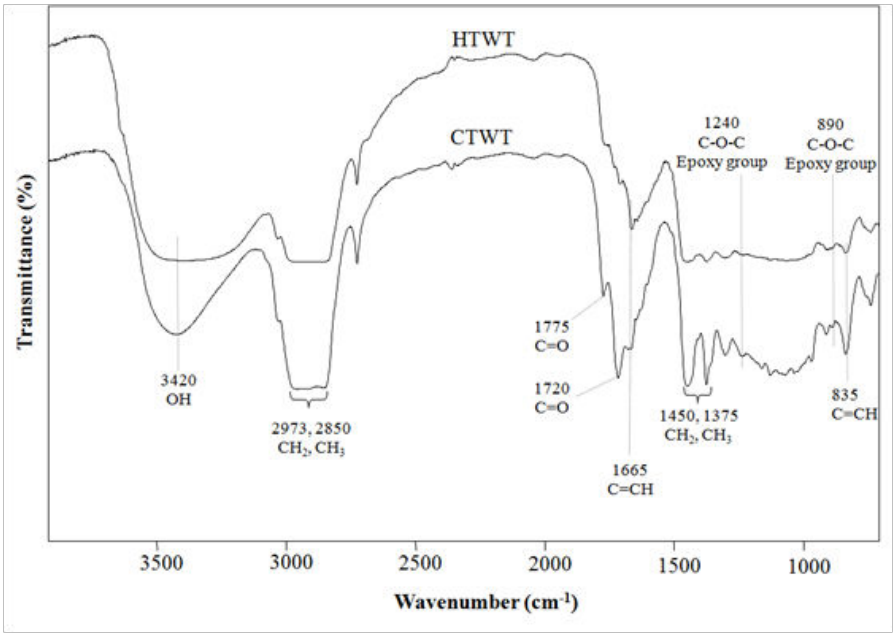

Figure 4.26 FTIR spectra of CTWT and HTWT.

Table 4.13 Wavenumber and functional groups of CTWT and HTWT

Wavenumber (cm^{-1})	Functional group
3400	ν (O-H)
2850 - 2990	ν (CH_2, CH_3)
1775	ν (C=O) in carbonyl compounds
1720	ν (C=O)
1665	ν (C=C)
1451, 1375	δ (CH_2, CH_3)
835	δ (C=C−H)

ν = Stretching, δ = bending

The average molecular weights ($\overline{M}n$ and $\overline{M}w$) and polydispersity instead of polydispersity index (Đ) of CTWT are shown in Table 4.14. This characterization was determined by GPC calibrated with polystyrene standards. The various molecular weights of CTWT were obtained by varying the amount of periodic acid (H_5IO_6). The targeted molecular weight of CTWT in this work was 1,500 g/mol. In the result, the molecular weight of the obtained CTWT did not correspond to the targeted molecular weight, which allows the calculation of the amount of periodic acid to use. Thus only in the synthesis of CTWT3, the amount of periodic acid was calculated by multiplying by the required number of mole by the factor 2, to obtain a molecular weight of CTWT close to the target one. It was found that, the molecular weight of CTWT and HTWT depended on ratio of periodic acid and WT: i.e. the molecular weight decreased with increasing ratio between periodic acid and WT. The optimum reaction time for periodic acid to cut WT chain was 24 h based on the preliminary studies [7].

Table 4.14 Characteristics of carbonyl telechelic oligomers from waste tires (CTWT)

Code	$m(H_5IO_6)$ /m(WT)	Y_1 (%)	Y_2 (%)	$\bar{M}n$-NMR -OB (g/mol)	$\bar{M}n$-NMR -OI (g/mol)	$\bar{M}n$-GPC (g/mol)	$\bar{M}w$-GPC (g/mol)	Đ
CTWT1	0.27	9	18	1,900	2,500	2,900	7,300	2.49
CTWT2	0.40	12	24	1,600	2,100	2,400	6,900	2.83
CTWT3	0.53	26	52	900	1,200	1,000	3,100	3.11

$\bar{M}n$-GPC = determined with GPC using polystyrene standards and corrected with Benoit factor (0.67 for polyisoprene), Y_1 = Yield1 is by % mass of waste tires crumbs (WT); Y_2 = Yield2 is by % mass of rubber (PI = Poly isoprene and PB = Polybutadiene; 50.67% of WT)

4.2.3 Synthesis of hydroxyl telechelic oligomer from waste tires (HTWT)

The ketone and aldehyde end-group of CTWT were reduced to hydroxyl end-groups using sodium borohydride. The ^{1}H-NMR spectrum of HTWT is displayed in Figure 4.27 and the chemical shifts of HTWT are listed in Table 4.15. The HTWT spectrum did not show the signal at 9.8 ppm for the aldehyde group but the signal of the CH_2 and CH proton in α position of hydroxyl end group appeared at 3.65 and 3.80 ppm, respectively.

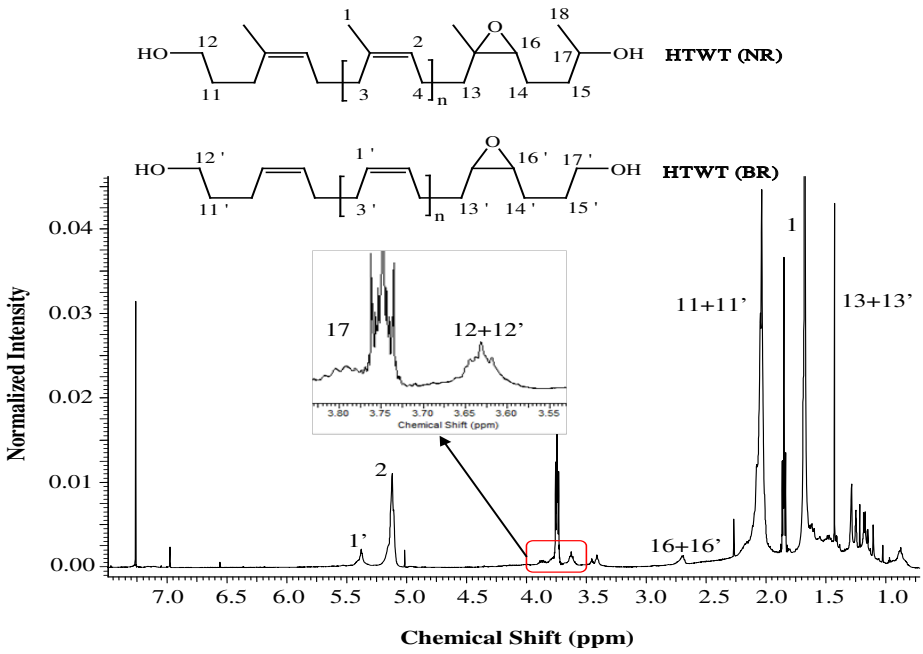

Figure 4.27 ^{1}H-NMR spectrum of HTWT.

Table 4.15 Chemical shift assignment of HTWT [7]

HTWT (NR)		HTWT (BR)	
Functional group	Chemical shift (ppm)	Functional group	Chemical shift (ppm)
–C=CH–	5.12 (H_2)	–CH=C–	5.38 ($H_{1'}$)
–CH(OH)	3.80 (H_{17})	–CH_2(OH)	3.65 ($H_{12'}$)
–CH_2(OH)	3.65 (H_{12})	–CH_2–	2.00 ($H_{11'}$)
–CH_2–	2.00 (H_{11})		
–CH_3	1.67 (H_1)		
–CH_3CH(OH)	1.20 (H_{18})		
	2.7 (H_{16})		2.7 ($H_{16'}$)

The FTIR spectrum of HTWT is shown in Figure 4.26 and the assignment of their functional groups is listed in Table 4.13. The peak at 3420 cm^{-1} for O-H stretching from the hydroxyl group was showed in the HTWT while the absorption band of carbonyl group at 1720 cm^{-1} was not found. This result confirmed that the carbonyl group in the CTWT was changed to the hydroxyl group in the HTWT. In the case of HTWT, the calculation was more complicated because of the presence of two types of oligomers (OI and OB). Thus, the ratio between OB and OI ($\tau_{OB/OI}$) had to be first calculated from the ratio of the integration values of the characteristic peaks of protons as shown in equation (4). The molecular weight ($\overline{M}_n$) of HTWT was determined from the ^{1}H-NMR spectrum of CTWT (Figure 2.25). The ^{1}H-NMR spectrum of CTWT showed two types of oligomers: oligobutadiene and oligoisoprene; using equations (7) and (8). The proportion of epoxidation of HTWT [$\tau_{epox\text{-}OB}$ for oligobutadiene (5.3 mol% epoxidation) and $\tau_{epox\text{-}OI}$ for oligoisoprene (10% mole epoxide) as shown in equation (5) and (6), respectively] were determined from the ^{1}H-NMR spectra (Figure 2.27).

The average molecular weights ($\overline{M}$n and $\overline{M}$w) and polydispersity instead of polydispersity index (Đ) of HTWT are listed in Table 4.16 and 4.17. The characterization and calculation were similar to those of CTWT. For this work, the targeted molecular weight of HTWT was 1,500 g/mol, and the obtained a molecular

weight of HTWT3 were 1,000 g/mol and 1,400 g/mol for the OB and OI, respectively. Therefore, HTWT3 was used as a precursor to synthesize PUFs from PCL and HTWT.

Table 4.16 Characteristics of hydroxyl telechelic oligomers from waste tires (HTWT)

Code	Starting material	Yield(%)	$\tau_{OB/OI}$	$\tau_{epoxy\text{-}OB}$	$\tau_{epoxy\text{-}OI}$
HTWT1	CTWT1	78	0.07	0.04	0.08
HTWT2	CTWT2	37	0.15	0.04	0.07
HTWT3	CTWT3	70	0.09	0.08	0.15

OB = Oligomer from butadiene; OI = Oligomer from isoprene

Table 4.17 Molecular weight of HTWT

Code	Starting material	$\overline{M}$n-NMR-OB (g/mol)	$\overline{M}$n-NMR-OI (g/mol)	$\overline{M}$n-GPC (g/mol)	$\overline{M}$w-GPC (g/mol)	Đ
HTWT1	CTWT1	1,400	2,700	2,400	7,200	2.93
HTWT2	CTWT2	1,700	2,100	2,700	7,800	2.85
HTWT3	CTWT3	1,000	1,400	1,600	3,600	2.34

$\overline{M}$n-GPC = determined with GPC using polystyrene standards and corrected with Benoit factor (0.67 for polyisoprene)

4.2.4 Synthesis and characterization of PUFs from HTWT and PCL

The PUFs were synthesized by varying the molar ratio between HTWT and PCL. The molar ratios of HTWT/PCL were 1/0 (PUF5), 1/0.5 (PUF6), 1/1 (PUF7) and 0.5/1 (PUF8). The expected chemical structure of PUF from HTWT and PCL is shown in Figure 4.28. Figure 4.29 represents the FTIR spectra of PUFs prepared from HTWT, PCL and PMDI. FTIR spectra confirmed the existence of the urethane structure. The broad absorption band at 3335 cm^{-1} represents stretching vibration of hydrogen bonded N–H urethane. The bands at 1532 cm^{-1} was attributed to the bending vibration of N–H and the stretching vibration of C–N which confirmed that urethane linkages were formed between -OH in HTWT and -NCO. The band at 1710-1725 cm^{-1} observed in PUF5-PUF8 was assigned to the carbonyl stretching of C=O that was hydrogen bonded with the N-H group of polyurethane [8,10-12,36]. The bands at 1510 and 1596 cm^{-1} were derived from the aromatic rings of PMDI [37]. The PCL-PUF also showed the same main characteristic frequencies as HTWT-PUF,

except there was no peak at 2277 cm^{-1} which belonged to the free -NCO. This result indicated that the reaction between -NCO and -OH in this foam was complete. The carbonyl stretching of PCL-based PUF appeared at 1725 cm^{-1} which overlapped to the carbonyl stretching of PCL [38].

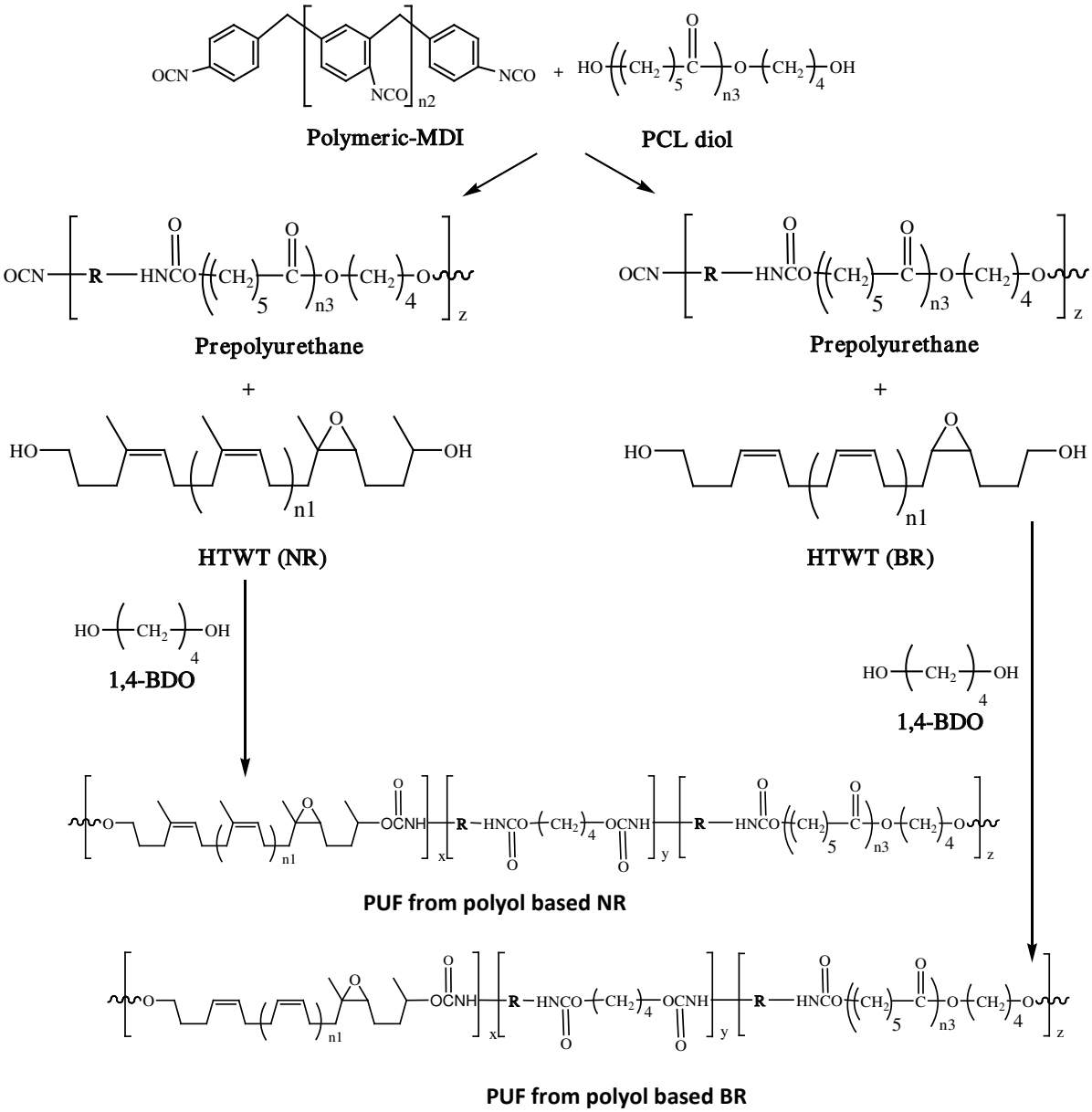

Figure 4.28 Chemical structure and reaction route of the PUFs from HTWT and PCL.

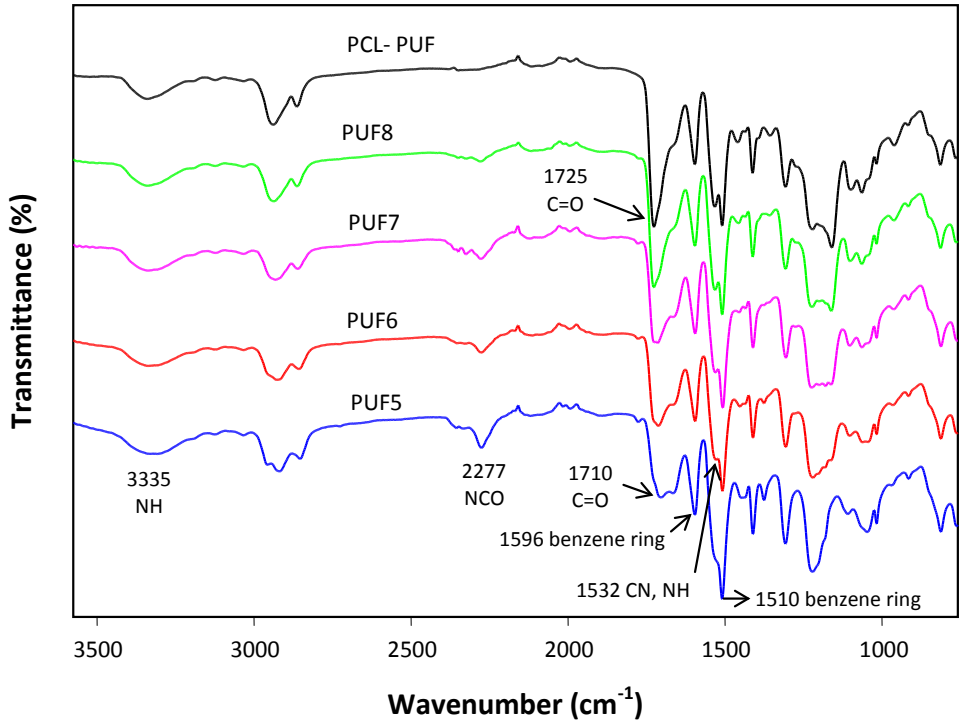

Figure 4.29 FTIR spectra of PUFs from HTWT and PCL.

4.2.5 Physical properties of PUFs from HTWT and PCL

In this part, the effect of molar ratio between HTWT and PCL (1/0, 1/0.5, 1/1 and 0.5/1) on the physical properties (foam formation rate, density and cell size) of PUFs were studied following the formulation in Table 3.4. These results are shown in Table 4.18 and Figure 4.30 - 4.32.

Table 4.18 Physical properties of PUFs from HTWT and PCL

Code	HTWT/ PCL	Creaming Time (s)	Rising Time (s)	Tack Free Time (s)	Density (kg/m^3)	Cell Size (mm)
PUF5	1/0	25	113	145	32.04±2.09	0.36±0.08
PUF6	1/0.5	27	127	300	61.16±6.62	0.26±0.10
PUF7	1/1	24	106	267	70.11±4.64	0.29±0.12
PUF8	0.5/1	18	98	223	38.10±1.08	0.52±0.21

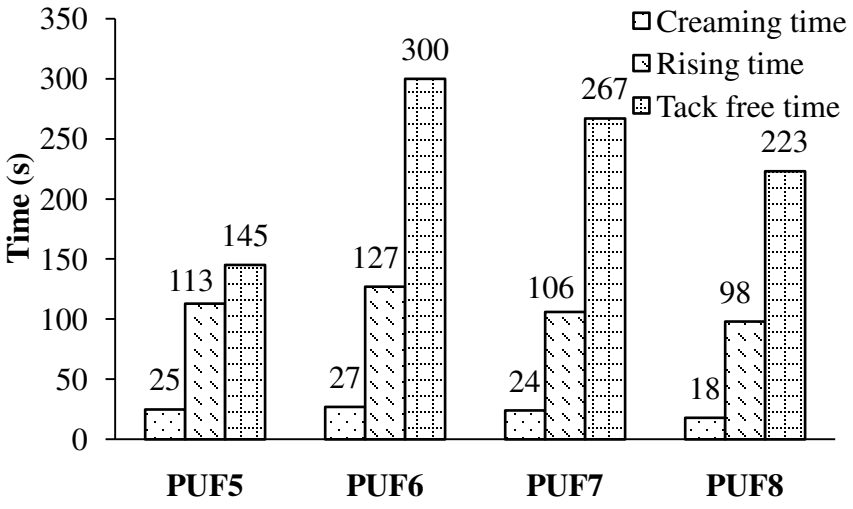

Figure 4.30 Kinetic characteristic of PUFs from HTWT and PCL.

Foam formation rate or the kinetic rate of PUF involved a creaming time, rising time and tack free time [39-41]. The creaming time started at the mixing step until the foam began to rise. The foam formation rate of HTWT and HTWT/PCL foam are given in Table 4.18 and Figure 4.30. Foam formation rate depended on diol compositions. The effect of PCL content on the foam formation rate of HTWT-based PUF was observed from PUF5 – PUF7. Their creaming time was in the same range, 24 – 27 sec and their rising time slightly different. In contrast, the addition of PCL strongly affected the tack free time because a significant increase in the tack free time was observed. The effect of HTWT/PCL ratio on the foam formation rate of PUF was observed from PUF6 – PUF8. Obviously, the foam formation rate increased with higher molar ratio of PCL. The creaming time, rising time and tack free time ranked in the following order: PUF6 > PUF7 > PUF8. Based on the preliminary study [24], PCL PUF showed higher foam formation rate than HTNR PUF. These results indicated that the hydroxyl groups from PCL are more reactive than the hydroxyl groups from HTWT leading to shorter tack free time in PUF6-PUF8.

The density and cell size of PUF are exhibited in Table 4.18 and Figure 4.31 - 4.32. The density and cell size of HTWT PUF (PUF5) and HTWT/PCL PUF (PUF6-PUF8) were in the range of 32-70 kg/m^3 and 0.26-0.52 mm, respectively. The effect of PCL content on the density and cell size of HTWT based PUF was observed from PUF5-PUF7. It was found that the addition of PCL increased the foam density.

In contrast, the cell size was decreased with increasing PCL content (PUF5 > PUF6, PUF7). The effect of HTWT/PCL ratio on the density and cell size of PUF was observed from PUF6-PUF8. The cell size increased with higher molar ratio of PCL. Based on the preliminary study [24], PUF from PCL alone showed higher cell size than PUF from hydroxyl telechelic natural rubber (HTNR). These results indicated that the hydroxyl groups from PCL are more reactive than the hydroxyl groups from HTNR leading to the highest cell size in PUF8. It was concluded that the increase of PCL content caused a faster reaction and the blowing efficiency increased.

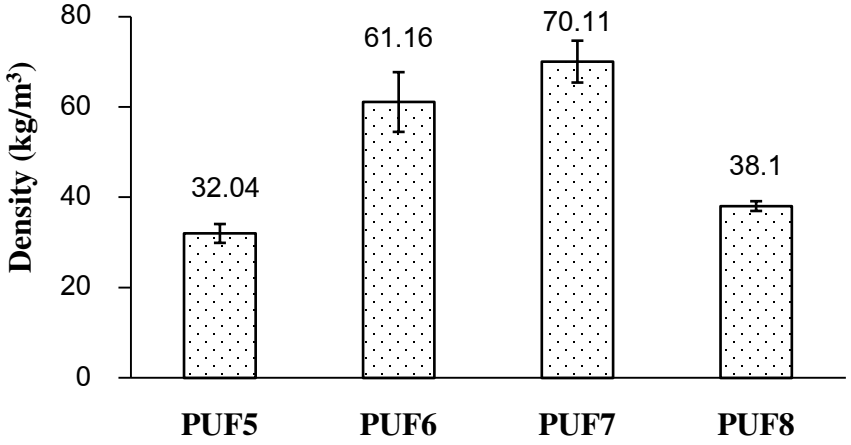

Figure 4.31 Density of PUFs from HTWT and PCL.

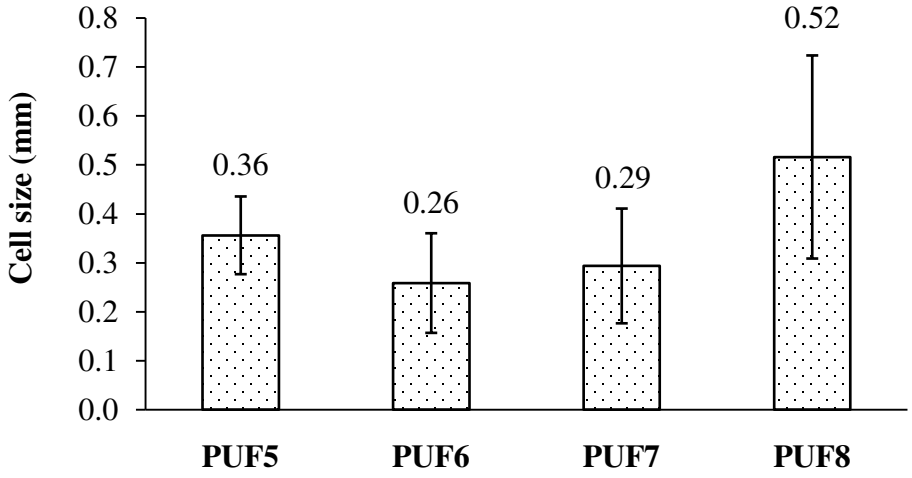

Figure 4.32 Cell size of FUFs from HTWT and PCL.

4.2.6 Morphology of PUFs from HTWT and PCL

SEM micrographs of PUFs with different molar ratio of HTWT/PCL are shown in Figure 4.33.

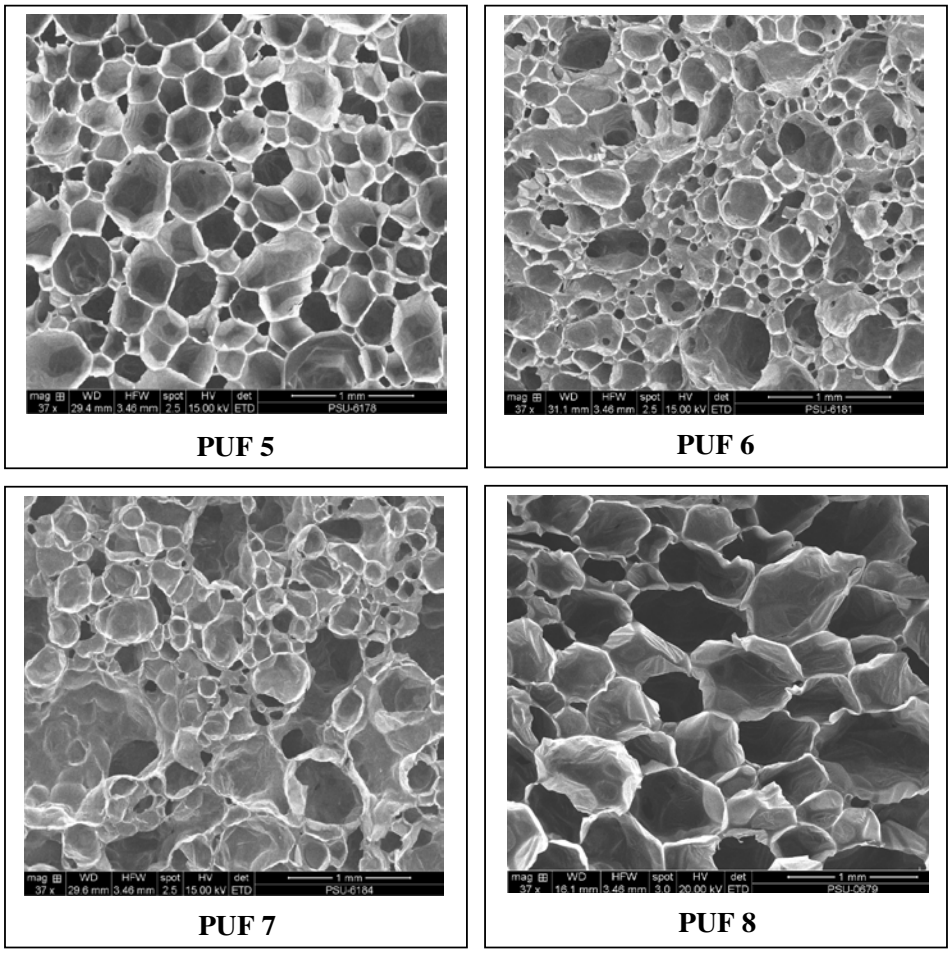

Figure 4.33 SEM micrographs of PUFs from HTWT and PCL.

Polyhedral, closed cells appeared in all the PUF and some semi-closed cells were also observed. The HTWT PUF (PUF5) showed almost smooth surface and well defined cell wall. In contrast, the mixture of HTWT and PCL resulted in heterogeneous surface and cell size distribution wider than PUF5. The variation of molar ratio between HTWT/PCL (higher concentration of PCL) causes more reactivity between the hydroxyl and isocyanate group, which results in foams with a small cell structure (PUF6 and PUF7), except PUF8.

4.2.7 Thermal properties of PUFs from HTWT and PCL

The thermal stability of PUF was investigated using the thermogravimetric analyses including both the analysis of the weight loss and the derivative of the weight loss curve. The results of thermogravimetric analyses are shown in Figure 4.34 - 4.35 and Table 4.19 for all PUFs

Table 4.19 Thermal properties of PUFs from HTWT and PCL

Sample	HTNR /PCL	T_{d5} (°C)	T_{d10} (°C)	T_{d50} (°C)	1st Step		2nd Step		3rd Step	
					Tmax (°C)	Weight loss (%)	Tmax (°C)	Weight loss (%)	Tmax (°C)	Weight loss (%)
PUF5	1/0	213	273	372	329	29	419	35	-	-
PUF6	1/0.5	251	295	392	346	31	432	31	451	6
PUF7	1/1	272	304	394	333	23	367	17	466	29
PUF8	0.5/1	276	309	399	333	18	372	18	451	29

Table 4.19 shows the resulting temperatures (T_{d5}, T_{d10} and T_{d50}) corresponding to 5, 10 and 50% weight loss of PUF. It was found that the PCL improves the thermal stability of the PUF. The best thermal stability was found in PUF8, for which T_{d5}, T_{d10} and T_{d50} were higher than those of PUF5 of approximately 63, 36 and 27 °C, respectively. The weight loss of PUF at T_{d5}, T_{d10} and T_{d50} were rising with the increasing PCL content. The increasing content of the PCL in the PUF resulted in the change of the thermal decomposition route of the PUF. The DTG curves of PUF5 presented a two step thermal decomposition and PUF6-PUF8 presented a three step thermal decomposition. A characteristic temperature was determined from the maximum of the derivative curve (T_{max}) and is listed in Table 4.19. The first stage of degradation at 330-346°C corresponded to breakage of the urethane bond. The second stage at 367-432°C corresponded to the decomposition of the HTWT [7], and the third stage at 451-466°C corresponded to the decomposition of the PCL diols [8,26].

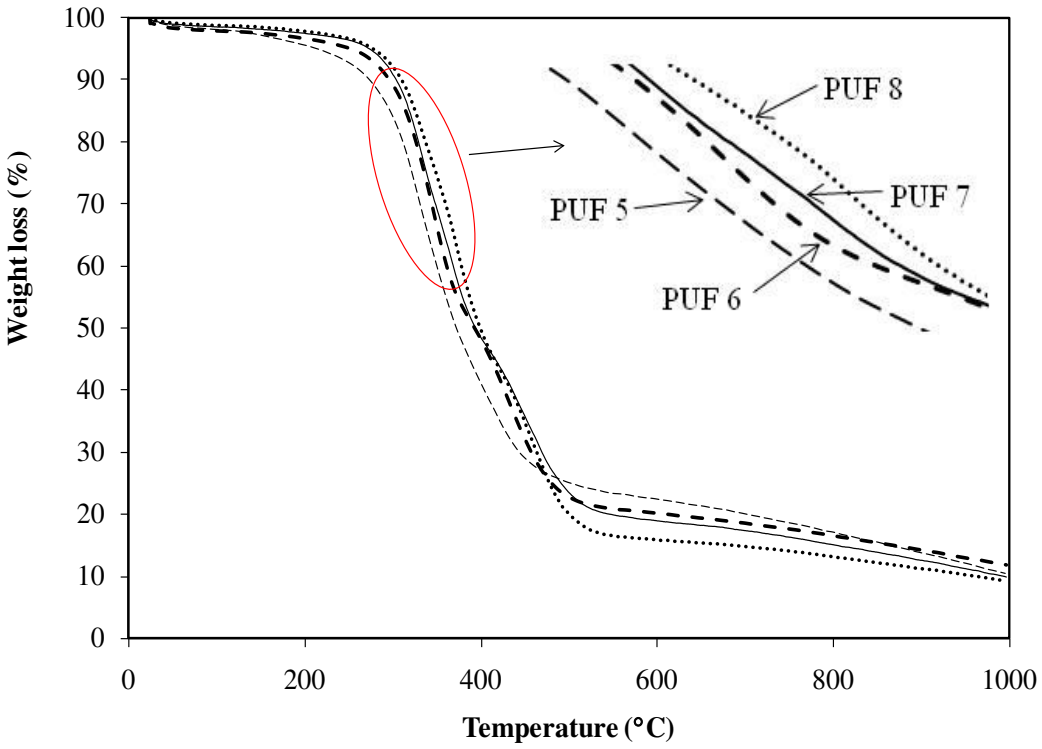

Figure 4.34 TGA thermograms of PUFs from HTWT and PCL.

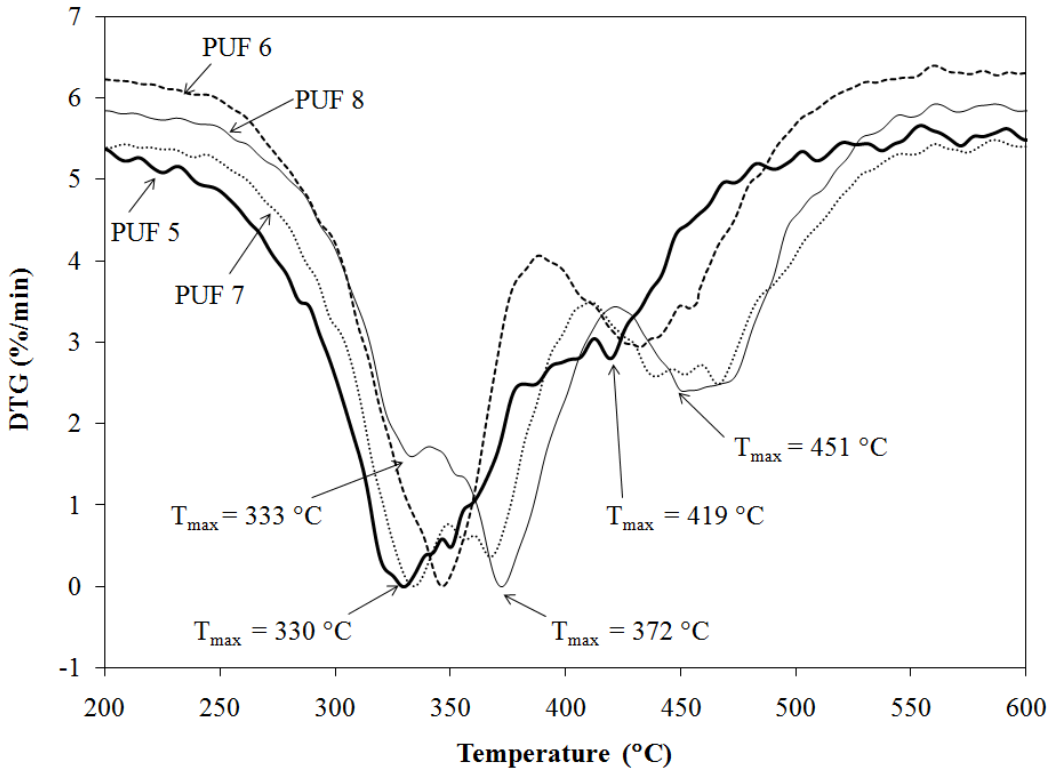

Figure 4.35 DTG thermograms of PUFs from HTWT and PCL.

4.2.8 Biodegradation of PUFs from HTWT and PCL

The effect of various molar ratio of HTWT/PCL on biodegradation of PUF are given in Table 4.20 and Figure 4.36.

Table 4.20 Percentage biodegradation of PUFs from HTWT and PCL

Time	Samples / % biodegradation					
(day)	PUF5	PUF6	PUF7	PUF8	Sodium benzoate	LDPE
2	0.00	0.00	0.00	0.34	12.69	0.00
5	2.06	2.74	0.00	2.06	22.11	0.00
7	5.14	5.83	1.54	4.46	29.14	0.00
9	6.86	7.71	3.26	5.14	32.57	0.00
12	6.86	8.40	4.29	5.83	34.46	0.00
14	10.11	13.71	7.20	9.26	37.37	0.86
16	12.69	17.66	8.91	11.83	39.60	1.03
19	18.00	22.97	14.91	18.17	46.63	2.06
21	24.34	29.32	19.20	21.60	50.40	2.06
23	28.12	34.29	21.77	23.49	52.97	2.06
26	30.34	37.54	23.49	25.03	54.86	2.06
28	31.20	39.09	23.66	25.54	55.37	2.06
30	31.89	40.46	23.66	26.06	56.06	2.06
33	33.43	42.52	24.00	26.91	57.94	2.06
35	35.66	45.94	25.54	28.12	60.86	2.06
37	36.69	47.66	25.89	28.46	62.06	2.06
40	38.06	50.40	26.74	29.49	64.63	2.06
42	39.09	51.77	27.26	30.00	65.14	2.06
44	40.63	53.14	28.29	30.69	65.66	2.06
47	42.52	55.54	29.83	31.72	66.86	2.06
49	44.92	58.80	31.72	33.09	68.06	2.06
51	46.46	60.52	32.74	33.94	69.09	2.06
54	47.49	61.54	33.43	34.80	69.94	2.06
56	48.34	62.23	34.12	35.49	70.46	2.06
58	48.86	62.74	34.46	35.66	70.97	2.06
60	51.26	64.29	35.83	38.06	71.66	2.06

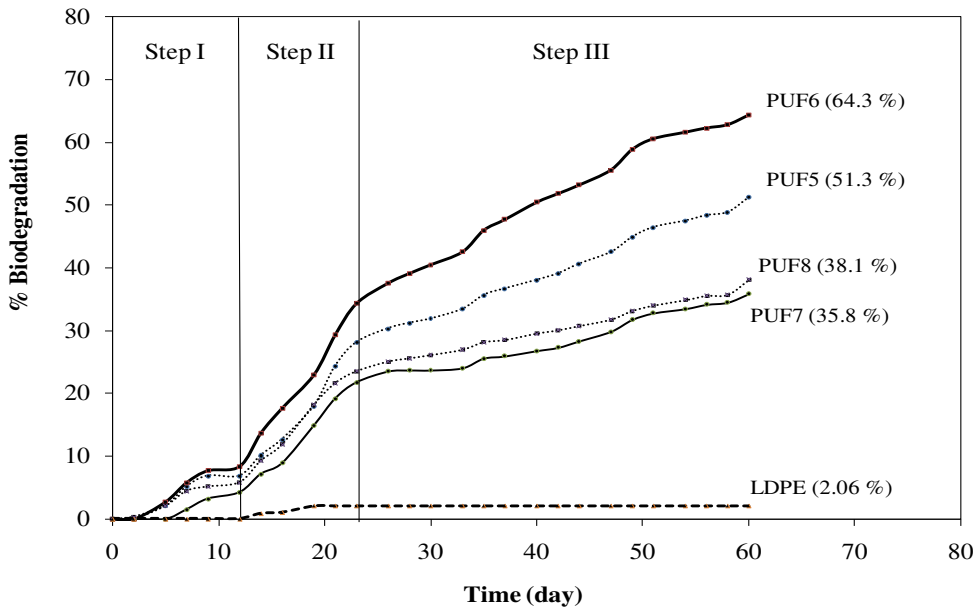

Figure 4.36 Percentage biodegradation of PUFs from HTWT and PCL.

The biodegradation tests of PUF was performed by the modified STURM test. This test is designated 301B by the Organisation for Economic Co-operation and Development (OECD). The test takes place in solution and is aerobic with the test sample as the only source of carbon. This test system is incubated at an ambient temperature with control for 60 days. The production of carbon dioxide is measured and used to calculate percentage biodegradation.

PUF5-PUF8 were cubes cut from the relative foams and LDPE sample was cut from a LDPE bottle. The Sturm test was adapted to the present study and the experimental results are shown in Figure 4.36. Generally the Sturm test was performed for 28 days and the data reported as %Biodegradation versus time, based on equation (13) and (14) reported in section 3.3.7 (in chapter 3). The results showed that after 28 days the percentage of biodegradation of samples could be ranked in the following order: PUF6 (39.1%) > PUF5 (31.2%) > PUF8 (25.5%) > PUF7 (23.7%). These results were very interesting because they showed a triple increase in the percentage of biodegradation compared to the PUF having a similar composition but constituted by the hydroxyl telechelic oligomers (HTNR) from the pure NR (STR CV60 grade) and PCL diols (these data have been obtained from previous experiments) as shown in Table 4.34. The test was continued and at the end (60 days),

the rank of %Biodegradation did not change and a high percentage of biodegradation was obtained for all samples. These values were also higher than those of the PUF prepared from the pure NR and they also showed the same ranking of %Biodegradation (Table 4.34).

The biodegradation rate was derived from the slope of the curves in Figure 4.36. All samples, except LDPE, showed a similar behavior that could be classified into 3 periods based on the biodegradation rate that was derived from a slope of the curve. The first period (I), of approximately 12 days, was an induction period in which the %Biodegradation was less than 10%. After the induction period the biodegradation rate increased remarkably. After 23 days the biodegradation rate decreased and biodegradation continued at a constant rate. The biodegradation rate for all the periods was in the following order: PUF6 > PUF5 > PUF8 > PUF7. We expected that the addition of PCL diols should increase the biodegradation of PUF because PCL is the biodegradable polymer and PCL diols would increase the hydrophilicity of PUFs. The water contact angle of NR and PCL is 106 and 77°, respectively [31,32]. However, this assumption proved to be right only for PUF6 which showed higher %Biodegradation than PUF5.

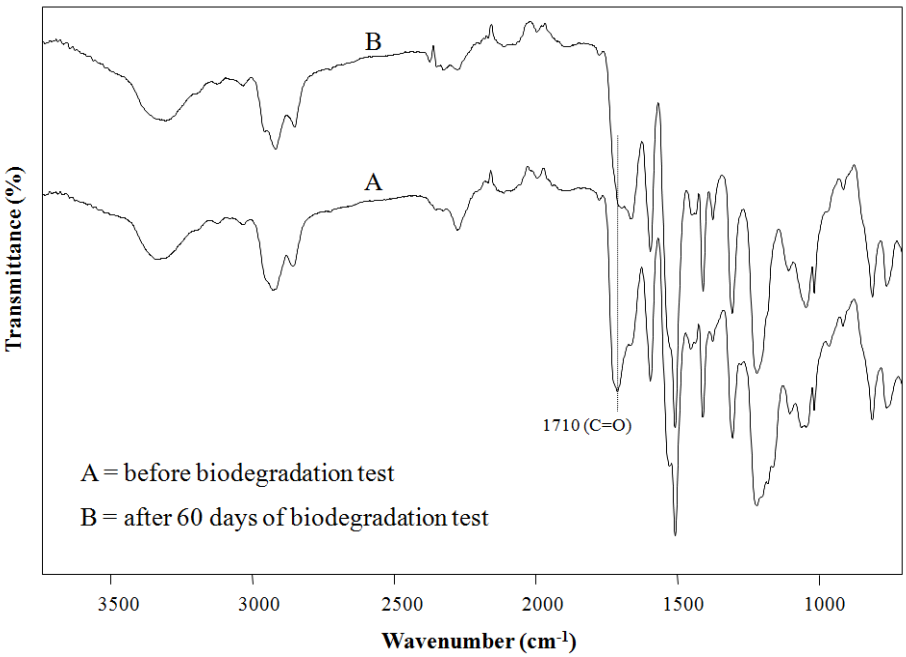

Figure 4.37 FTIR spectra of PUFs from HTWT/PCL (1/0.5 molar ratio): before and after biodegradation test

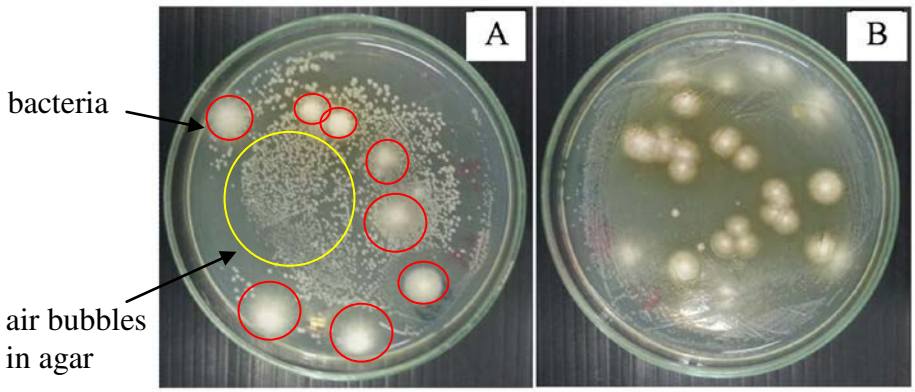

Figure 4.38 Colonies of total bacteria grown on Plate Count Agar of PUFs from HTWT/PCL (1/0.5 molar ratio) dilution 10^{-3}: before (a) and after (b) 60 days of biodegradation test

PUF6 was characterized by FTIR before and after testing for biodegradation to examine any changes in the functional groups. A decrease at wavelength 1,710 cm^{-1} was observed (Figure 4.37), and this implied a cleavage of the ester bonds of the urethane groups (H_2N-CO-OR) by the action of microbial esterases [42]. The colony numbers of PUF6 increased from 8 x 10^4 CFU/mL at the beginning of the biodegradation test to 31 x 10^4 CFU/mL at 60 days. These results indicated that there were effective bacteria in the waste water that could live and grow by using PUF as a carbon source (Figure 4.38).

4.3 References

1. Kébir, N., Morandi, G., Campistron, I., Laguerre, A. and Pilard, J.-F. 2005. Synthesis of well defined amino telechelic cis-1,4-oligoisoprenes from carbonyl telechelic oligomers; first studies of their potentialities as polyurethane or polyurea materials precursors. Polymer. 46(18): 6844-6854.
2. Morandi, G., Kebir, N., Campistron, I., Gohier, F., Laguerre, A. and Pilard, J.-F. 2007. Direct selective reductive amination of carbonyl telechelic oligoisoprenes: elaboration of promising tri- and tetrafunctionalized oligoisoprene intermediates. Tetrahedron Letters. 48(43): 7726-7730.

3. Saetung, A., Rungvichaniwat, A., Campistron, I., Klinpituksa, P., Laguerre, A., Phinyocheep, P. and Pilard, J.-F. 2010. Controlled degradation of natural rubber and modification of the obtained telechelic oligoisoprenes: Preliminary study of their potentiality as polyurethane foam precursors. Journal of Applied Polymer Science. 117: 1279-1289.
4. Panwiriyarat, W., Tanrattanakul, V., Pilard, J.-F. and Khaokong, C. 2011. Synthesis and characterization of block copolymer from natural rubber, toluene-2,4-diisocyanate and poly(ε-caprolactone) diol - based polyurethane. Materials Science Forum. 695: 316-319.
5. Chumeka, W., Pasetto, P., Pilard, J.-F. and Tanrattanakul, V. 2015. Bio-based diblock copolymers prepared from poly(lactic acid) and natural rubber. Journal of Applied Polymer Science. 132(6): 1-10.
6. Sadaka, F., Campistron, I., Laguerre, A. and Pilard, J.-F. 2012. Controlled chemical degradation of natural rubber using periodic acid: Application for recycling waste tyre rubber. Polymer Degradation and Stability. 97(5): 816-828.
7. Tran, T.K.N., Pilard, J.-F. and Pasetto, P. 2015. Recycling waste tires: Generation of functional oligomers and description of their use in the synthesis of polyurethane foams. Journal of Applied Polymer Science. 132(1): 1-11.
8. Güney, A. and Hasirci, N. 2014. Properties and phase segregation of crosslinked PCL-based polyurethanes. Journal of Applied Polymer Science. 131(1): 1-13.
9. Kébir, N., Campistron, I., Laguerre, A., Pilard, J.-F., Bunel, C., Couvercelle, J.-P. and Gondard, C. 2005. Use of hydroxytelechelic cis-1,4-polyisoprene (HTPI) in the synthesis of polyurethanes (PUs). Part 1. Influence of molecular weight and chemical modification of HTPI on the mechanical and thermal properties of PUs. Polymer. 46(18): 6869-6877.
10. Panwiriyarat, W., Tanrattanakul, V., Pilard, J.-F., Pasetto, P. and Khaokong, C. 2013. Physical and thermal properties of polyurethane from isophorone diisocyanate, natural rubber and poly(ε-caprolactone) with high NCO:OH content. Advanced Science Letters. 19(3): 1016-1020.

11. Panwiriyarat, W., Tanrattanakul, V., Pilard, J.-F., Pasetto, P. and Khaokong, C. 2013. Effect of the diisocyanate structure and the molecular weight of diols on bio-based polyurethanes. Journal of Applied Polymer Science. 130: 453-462.
12. Panwiriyarat, W., Tanrattanakul, V., Pilard, J.-F., Pasetto, P. and Khaokong, C. 2013. Preparation and properties of bio-based polyurethane containing polycaprolactone and natural rubber. J Polym Environ. 21(3): 807-815.
13. Saetung, A., Kaenhin, L., Klinpituksa, P., Rungvichaniwat, A., Tulyapitak, T., Munleh, S., Campistron, I. and Pilard, J.-F. 2012. Synthesis, characteristic, and properties of waterborne polyurethane based on natural rubber. Journal of Applied Polymer Science. 124(4): 2742-2752.
14. Saetung, A., Rungvichaniwat, A., Campistron, I., Klinpituksa, P., Laguerre, A., Phinyocheep, P., Doutres, O. and Pilard, J.-F. 2010. Preparation and physico-mechanical, thermal and acoustic properties of flexible polyurethane foams based on hydroxytelechelic natural rubber. Journal of Applied Polymer Science. 117(2): 828-837.
15. Gillier-Ritoit, S., Reyx, D.l., Campistron, I.n., Laguerre, A. and Pal Singh, R. 2003. Telecheliccis-1,4-oligoisoprenes through the selective oxidolysis of epoxidized monomer units and polyisoprenic monomer units incis-1,4-polyisoprenes. Journal of Applied Polymer Science. 87(1): 42-46.
16. Dworakowska, S., Bogdał, D., Zaccheria, F. and Ravasio, N. 2014. The role of catalysis in the synthesis of polyurethane foams based on renewable raw materials. Catalysis Today. 223: 148-156.
17. Mustafe, A.M.M. 2005. FTIR studies on 2K polyurethane paint. Degree of mastersin science department of physics, national university of singapore.
18. Cinelli, P., Anguillesi, I. and Lazzeri, A. 2013. Green synthesis of flexible polyurethane foams from liquefied lignin. European Polymer Journal. 49(6): 1174-1184.
19. Elzein, T., Nasser-Eddine, M., Delaite, C., Bistac, S. and Dumas, P. 2004. FTIR study of polycaprolactone chain organization at interfaces. J Colloid Interface Sci. 273(2): 381-387.

20. Kebir, N., Campistron, I., Laguerre, A., Pilard, J.F., Bunel, C. and Jouenne, T. 2007. Use of telechelic cis-1,4-polyisoprene cationomers in the synthesis of antibacterial ionic polyurethanes and copolyurethanes bearing ammonium groups. Biomaterials. 28(29): 4200-4208.

21. Wang, T.P., Li, D., Wang, L.J., Yin, J., Chen, X.D. and Mao, Z.H. 2008. Effects of CS/EC ratio on structure and properties of polyurethane foams prepared from untreated liquefied corn stover with PAPI. Chemical Engineering Research and Design. 86(4): 416-421.

22. Wong, C.S. and Badri, K.H. 2012. Chemical analyses of palm kernel oil-based polyurethane prepolymer. Materials Sciences and Applications. 3: 78-86.

23. Costal, M.R., Santos, M.T. and Diamantino, T.C. 2009. FTIR, a powerful technique in organic coatings failure diagnosis. In: Proceedings of the EUROCORR'2009. 17p.

24. Rattanapan, S., Pasetto, P., Pilard, J.-F. and Tanrattanakul, V. 2014. Preparation and Properties of Bio-based Polyurethane Foams from Polycaprolactone diol. Proceedings 2014 IUPAC World Polymer Congress (MACRO2014), Chiang Mai, Thailand. 81-83.

25. Gorna, K. and Gogolewski, S. 2003. Preparation, degradation, and calcification of biodegradable polyurethane foams for bone graft substitutes. Journal of biomedica materials research: Part A. 67: 813-827.

26. Askari, F., Barikani, M. and Barmar, M. 2013. Study on thermal stability of polyurethane-urea based on polysiloxane and polycaprolactone diols. Korean J Chem Eng. 30(11): 2093-2099.

27. Zhang, X.D., Bertsch, L.M. and Macosko, C.W. 1998. Effect of amine additives on flexible, molded foam properties. Cellular polymers. 17: 327-349.

28. Watcharakul, S., Umsakul, K., Hodgson, B., Chumeka, W. and Tanrattanakul, V. 2012. Biodegradation of a blended starch/natural rubber foam biopolymer and rubber gloves by Streptomyces coelicolor CH13. Electronic Journal of Biotechnology. 15(1): 1-13.

29. Calil, M.R., Gaboardi, F., Guedes, C.G.F. and Rosa, D.S. 2006. Comparison of the biodegradation of poly(caprolactone), cellulose acetate and their blends by the Sturm test and selected cultured fungi. Polymer Testing. 25(5): 597-604.

30. Leejarkpai, T., Suwanmanee, U., Rudeekit, Y. and Mungcharoen, T. 2011. Biodegradable kinetics of plastics under controlled composting conditions. Waste Management. 31(6): 1153-1161.

31. Noda, I. and Rubingh, D.N. 1992. Polymer Solutions, Blends, and Interfaces: Studes in polymer science. Amsterdam, Netherlands.

32. Bolbasov, E.N., Rybachuk, M., Golovkin, A.S., Antonova, L.V., Shesterikov, E.V., Malchikhina, A.I., Novikov, V.A., Anissimov, Y.G. and Tverdokhlebov, S.I. 2014. Surface modification of poly(L-lactide) and polycaprolactone bioresorbable polymers using RF plasma discharge with sputter deposition of a hydroxyapatite target. Materials Letters. 132: 281–284.

33. Shah, Z., Krumholz, L., Aktas, D., Hasan, F., Khattak, M. and Shah, A. 2013. Degradation of polyester polyurethane by a newly isolated soil bacterium, Bacillus subtilis strain MZA-75. Biodegradation. 24(6): 865-877.

34. Tanrattanakul, V. and Chumeka, W. 2010. Effect of potassium persulfate on graft copolymerization and mechanical properties of cassava starch/natural rubber foams. Journal of Applied Polymer Science. 116(1): 93-105.

35. Chumeka, W. 2013. Improvment of compatibility of poly(lactic acid) blended with natural rubber by modified natural rubber. Degree of Doctor of Philosophy Polymer (Science and Technology), Graduate School, Prince of Songkla University, Thailand and Chemistry and Physical Chemistry of Polymer, University of Maine, France.

36. Elwell, M.J., Ryan, A.J., Grünbauer, H.J.M. and Van Lieshout, H.C. 1996. An FT i.r. study of reaction kinetics and structure development in model flexible polyurethane foam systems. Polymer. 37(8): 1353-1361.

37. Hakim, A.A., Nassar, M., Emam, A. and Sultan, M. 2011. Preparation and characterization of rigid polyurethane foam prepared from sugar-cane bagasse polyol. Materials Chemistry and Physics. 129(1–2): 301-307.

38. Wu, C.-S. 2005. A comparison of the structure, thermal properties, and biodegradability of polycaprolactone/chitosan and acrylic acid grafted polycaprolactone/chitosan. Polymer. 46(1): 147-155.

39. Piszczyk, Ł., Strankowski, M., Danowska, M., Haponiuk, J.T. and Gazda, M. 2012. Preparation and characterization of rigid polyurethane–polyglycerol nanocomposite foams. European Polymer Journal. 48(10): 1726-1733.

40. Seo, W.J., Park, J.H., Sung, Y.T., Hwang, D.H., Kim, W.N. and Lee, H.S. 2004. Properties of water-blown rigid polyurethane foams with reactivity of raw materials. Journal of Applied Polymer Science. 93(5): 2334-2342.

41. Singh, H., Sharma, T.P. and Jain, A.K. 2007. Reactivity of the raw materials and their effects on the structure and properties of rigid polyurethane foams. Journal of Applied Polymer Science. 106(2): 1014-1023.

42. Shah, A., Hasan, F., Akhter, J., Hameed, A. and Ahmed, S. 2008. Degradation of polyurethane by novel bacterial consortium isolated from soil. Annals of Microbiology. 58(3): 381-386.

CHAPTER 5

CONCLUSIONS

5.1 Preparation and properties of bio-based PUFs from PCL and NR

A systematic study of preparation, characterization and testing of properties of bio-based PUF containing HTNR and PCL diol as the soft segment was performed. The effect of HTNR/PCL diol molar ratio on the foam formation rate and properties was investigated. The chemical structure of HTNR, PCL and HTNR based foams were confirmed by FTIR and ^{1}H-NMR. PCL diol provided faster reaction, thus higher PCL diol content showed higher foam formation rate. The HTNR foams observed by SEM micrographs showed almost closed cells. The molar ratio of HTNR/PCL influenced slightly the foam density, but tended to increase the cell size and provided irregular cell shape when PCL diol content increased. The thermal degradation stability depended on PCL diol content. Regarding to foam density, the tensile strength of all PUFs was in the same range. The addition of PCL diol decreased the elongation at break and compressive strength. The compression set of all PUFs was relatively high. The biodegradability was assessed according to a modified Sturm test. The biodegradation studies showed that the foams were partially decomposed by bacteria taken from sewage from the concentrated latex factory. PUF samples showed an induction time of 33 days in which the percentage of biodegradation was ~ 7-11%. At the end of testing (60 days), the highest degradation (45.6%) was found in the sample containing 1/0.5 of HTNR/PCL diol molar ratio.

5.2 Preparation and properties of bio-based PUFs from PCL and WT

Rubber crumbs from waste tires were used as a starting material for the synthesis of hydroxyl telechelic oligomers (HTWT), which have been used as diols in the polyurethane foam preparation (PUF). HTWT consisted of oligoisoprene and oligobutadiene chains, in a ratio that depended on the composition of the waste tire crumbs. HTWT were successfully synthesized in two steps, via carbonyl telechelic oligomers from waste tire crumbs (CTWT). Four PUF types were prepared with

different molar ratios between the HTWT and polycaprolactone (PCL) diols. ^{1}H-NMR and FTIR were performed on the obtained CTWT, HTWT and PUF to confirm the molecular structure. The kinetic rate of foam formation and foam morphology depended on the molar ratio between HTWT and PCL diol. The presence of the PCL diols decreased the kinetic rate by increasing the tack free time. The longer tack free time produced higher density foams with a smaller cell size. All foams showed a closed cell structure with a polyhedral shape. Addition of the PCL diols increased the thermal degradation stability of PUF. The biodegradation tests showed a promising result that all PUF samples were subjected to partial biodegradation. The biodegradation of PUF containing only HTWT was 31.2% and 51.3% at 28 days and 60 days of testing respectively whereas the PUF containing 1/0.5 HTWT/PCL diols (by mole) showed a higher biodegradation: 39.1% and 64.3% at 28 days and 60 days of testing respectively.

The foam formation rate of HTWT based PUF was higher than that of HTNR based PUF. All HTWT based PUF had a higher density than HTNR based PUF. The HTWT based PUF had smaller cell size in comparison to HTNR based PUF. The cellular structure of HTNR based and HTWT based PUF were different, but all PUFs showed almost closed cells. The HTWT based PUF had higher thermal degradation temperatures and were more biodegradable than HTNR based PUF.

PERSPECTIVES

In the present work, hydroxyl oligomers from natural rubber (HTNR), waste tire crumbs (HTWT) and polycaprolactone diols (PCL) were used as precursor to prepare biobased polyurethane foams (PUFs). Great emphasis has been placed on studies of the effect of HTNR/PCL and HTWT/PCL molar ratios on the properties of PUFs. As expected, these molar ratios have been shown to be an important factor in controlling the foam formation rate, physical and thermal properties, and biodegradation of PUFs. The thermal stability and biodegradation of PUFs were significantly improved by incorporation of PCL. However, the effect of molecular weight of PCL and amount of surfactant on the properties of PUFs has not been studied here and so would need to be further investigated in order to determine the optimum ratio.

The structure of the HTWT oligomers should be clarified, as it was shown that sulfur is still present in the oligomers and in the derived foams. The entity of the devulcanization should be assessed and the ability of periodic acid in cutting sulfur-sulfur bond should be proved in order to introduce the appropriate amount that allows obtaining the targeted molecular weight. As consequence, an increase of the reaction yield is expected, in terms of grams of obtained oligomers from initial amount of crumbs. The better knowledge of the oligomers molecular structure, which is probably branched and not linear, as depicted, will allow a deeper understanding of some of the foams properties, which could be tuned or improved.

Additionally, the biodegradation studies of the PUFs should be carried out using different types of microorganisms with the aim of understanding the exact mechanism of action and selecting the most appropriate strains in view of real application of biodegradation of the end of life products. The products of the biodegradation should be analyzed: if the polyisoprene/polybutadiene segments are intact, they could be reused; if they are cut, the exact structure must be known in order to study the toxicity of the fragments if they are released in the environment.

CURRICULUM VITAE

Name Mr.Suwat Rattanapan

Student ID 5410230011

Educational Attainment

Degree	Name of Institution	Year of Graduation
B.Sc. (Physics)	Prince of Songkla University	2000
M.Sc. (Polymer Technology)	Prince of Songkla University	2004

Scholarship Award during Enrolment

Grant of graduate school, Prince of Songkla University

Grant of Rajamangala University of Technology Srivijaya

List of Publications and Communications

Publications:

Suwat Rattanapan, Pamela Pasetto, Jean-François Pilard and Varaporn Tanrattanakul. 2014. Preparation and Properties of Bio-based Polyurethane Foams from Polycaprolactone diol. Proceedings 2014 IUPAC World Polymer Congress (MACRO2014). Chiang Mai, Thailand, July 6-11, 2014. pp. 81-83.

Suwat Rattanapan, Pamela Pasetto, Jean-François Pilard and Varaporn Tanrattanakul. 2015. Effect of the Molecular Weight of Natural Rubber based Diols on Bio-based Polyurethane Foams. Proceeding 2015 The second asia pacific rubber conference (APRC 2015). Phuket, Thailand, October 15-16, 2015. pp. 245-249.

Suwat Rattanapan, Pamela Pasetto, Jean-François Pilard and Varaporn Tanrattanakul. 2016. Polyurethane foams from oligomers derived from waste tire crumbs and polycaprolactone diols. Journal of Applied Polymer Science, p1-10, Accepted.

Suwat Rattanapan, Pamela Pasetto, Jean-François Pilard and Varaporn Tanrattanakul. 2016. Preparation and properties of bio-based polyurethane foams from natural rubber and polycaprolactone diol. Journal of Polymer Research, 23(9): p1-12, Accepted.

Communications:

Suwat Rattanapan, Pamela Pasetto, Jean-François Pilard and Varaporn Tanrattanakul. 2014. Preparation and Properties of Bio-based Polyurethane Foams from Polycaprolactone diol. IUPAC World Polymer Congress (MACRO2014), Chiang Mai, Thailand, July 6-11, 2014. (Oral)

Suwat Rattanapan, Pamela Pasetto, Jean-François Pilard and Varaporn Tanrattanakul. 2015. Effect of the Molecular Weight of Natural Rubber based Diols on Bio-based Polyurethane Foams. The second asia pacific rubber conference (APRC 2015), Phuket, Thailand, October 15-16, 2015. (Oral)

UNIVERSITE BRETAGNE LOIRE

Université du Maine

Thèse de Doctorat

Suwat RATTANAPAN

Préparation et Caractérisation des Propriétés de Mousses Polyuréthane Biobasées Synthétisées à Partir du Caoutchouc Naturel Modifié et de la Poly(ε-caprolactone)

Preparation and properties of bio-based polyurethane foam prepared from modified natural rubber and poly(ε-caprolactone

Résumé

L'objectif de ces travaux de recherche était de synthétiser de mousses polyuréthane (PUF) bio-basées à partir d'oligomères hydroxytéléchéliques issus du caoutchouc naturel (HTNR) ou à partir de poudrettes de pneus usagés (HTWT) et du diol de la polycaprolactone (PCL) comme segments soft. Les paramètres étudiés ont été le type de polyol et le rapport molaire entre HTNR/PCL et HTWT/PCL. La masse molaire de HTNR, HTWT et PCL étaient respectivement 1,800, 1400 et 2000 g/mol. L'effet du rapport molaire HTNR/PCL et HTWT/PCL (1/0, 1/0/5/, 1/1, et 0.5/1) sur la vitesse de formation des mousses et sur les propriétés chimiques et physiques a été étudié. Les structures chimiques de HTNR, HTWT et PUF ont été confirmées par FTIR et ^{1}H-RMN. Le diol de la PCL était le plus réactif donc augmentant le contenu de PCL-diol la vitesse de formation des mousses a augmenté. La densité des mousses a changé légèrement avec le rapport molaire cependant la résistance à la traction reste dans la même gamme. Le diamètre moyen des cellules a augmenté en fonction du contenu de PCL-diol et la tendance inverse a été observée pour l'allongement à la rupture et la résistance à la compression. L'observation au microscope électronique à balayage (MEB) a montré que les mousses basées sur les HTNR étaient alvéolées et fermées. La biodégradabilité a été évaluée selon le test de Sturm. Polyéthylène à baisse densité et benzoate de sodium ont été utilisés respectivement comme témoins négatif et positif. Les mousses ont montré une période d'induction de 33 jours dans lequel le pourcentage de dégradation était ~ 7-10%. La biodégradation de PUF contenant seulement HTNR a été 8.4% après 28 jours et 31.89% après 60 jours ; les PUF contenants 1/0.5 HTNR/PCL ont montré un pourcentage supérieure : 11.31% après 28 jours et 45.6% après 60 jours. Le rapport molaire HTWT/PCL a influencé beaucoup la vitesse de formation des mousses et leur morphologie. Cellules fermées de forme polyédrique ont été observé par microscopie électronique à balayage. Les résultats de l'analyse thermogravimétrique ont montré que l'addition du diol de la PCL a augmenté la température de dégradation. Il a été observé qu'une basse vitesse de réaction génère des mousses à haute densité, petit diamètre de cellule et haute distribution des diamètres. La biodégradation des PUF contenant seulement HTWT a été 31.2% après 28 jours et 51.3% après 60 jours, tandis que les PUF contenant 1/0.5 HTWT/PCL ont montré une dégradation plus élevée : 39.1% après 28 jours et 64.3% après 60 jours. La vitesse de formation des mousses basées sur les HTWT était supérieure à celle des mousses basées sur les HTNR. Toutes les mousses basées sur les HTWT ont une densité supérieure et une taille de cellule inférieure à celles basées sur HTNR. La structure des cellules des mousses basées sur les HTNR ou HTWT était différente cependant toutes les mousses ont montré des cellules quasi complètement fermées. Les mousses basées sur les HTWT ont montré des propriétés thermiques et de biodégradation meilleures par rapport aux mousses basées sur les HTNR.

Mots clés

polymères bio-basés, mousse polyuréthane bio-basée, polymères biodégradables, caoutchouc naturel, polycaprolactone, recyclage pneumatiques usagés, biodégradabilité

Abstract

The aim of this research was to prepare a bio-based polyurethane foam (PUF) containing hydroxyl telechelic oligomers from natural rubber (HTNR) and waste tire crumbs (HTWT) and polycaprolactone diol (PCL) as soft segments. The studied parameters included type of polyols and molar ratio between HTNR/PCL and HTWT/PCL. The molecular weight of HTNR and HTWT derived from ^{1}H-NMR spectra were 1,800 and 1,400 g/mol, respectively. The molecular weight of PCL diol was 2000 g/mol. The effect of HTNR/PCL and HTWT/PCL molar ratio (1/0, 1/0.5, 1/1 and 0.5/1) on the foam formation rate and physical and chemical properties of the resulting PUF was investigated. The chemical structure of HTNR, HTWT and PUF were confirmed by FTIR and ^{1}H-NMR. PCL diol provided faster reaction, thus higher PCL diol content showed higher foam formation rate. The foam density slightly changed with the molar ratio whereas the specific tensile strength of all samples was in the same range. The average diameter of cell increased with increasing contents of PCL diol. The addition of PCL diol resulted in reduced elongation at break and compressive strength. The cellular structure observed by SEM micrographs of HTNR based foams showed an almost closed cell. The biodegradability was assessed according to a modified Sturm test. Low density polyethylene and sodium benzoate were used as a negative and positive control sample, respectively. PUF samples showed an induction time of 33 days in which the percentage of biodegradation was ~ 7-11%. The biodegradation of PUF containing only HTNR was 8.4% and 31.89% at 28 days and 60 days of testing respectively whereas the PUF containing 1/0.5 HTNR/PCL (by mole) showed a higher biodegradation: 11.31% and 45.6% at 28 days and 60 days of testing respectively. The molar ratio of HTWT/PCL strongly affected the kinetic rate of foam formation and foam morphology. According to SEM micrographs, polyhedral closed cells were observed. The addition of the PCL diol increased the thermal degradation temperature of the PUF based on TGA results. A low kinetic rate provided PUF with a high density, small cell size and a broad cell size distribution. The biodegradation of PUF containing only HTWT was 31.2% and 51.3% at 28 days and 60 days of testing respectively whereas the PUF containing 1/0.5 HTWT/PCL diols (by mole) showed a higher biodegradation: 39.1% and 64.3% at 28 days and 60 days of testing respectively. The foam formation rate of HTWT based PUF was higher than the one of HTNR based PUF. All HTWT based PUF have a higher density than HTNR based PUF. The HTWT based PUF had an inferior cell size in comparison to HTNR based PUF. The cellular structure of HTNR based and HTWT based PUF were different, but all PUFs showed almost closed cells. The HTWT based PUF had a higher thermal degradation temperature and biodegradation properties than foams from HTNR.

Key Words

Bio-based polymer, bio-based polyurethane foam, biodegradable polymer, natural rubber, polycaprolactone, waste tire recycle, biodegradability

L'Université Bretagne Loire